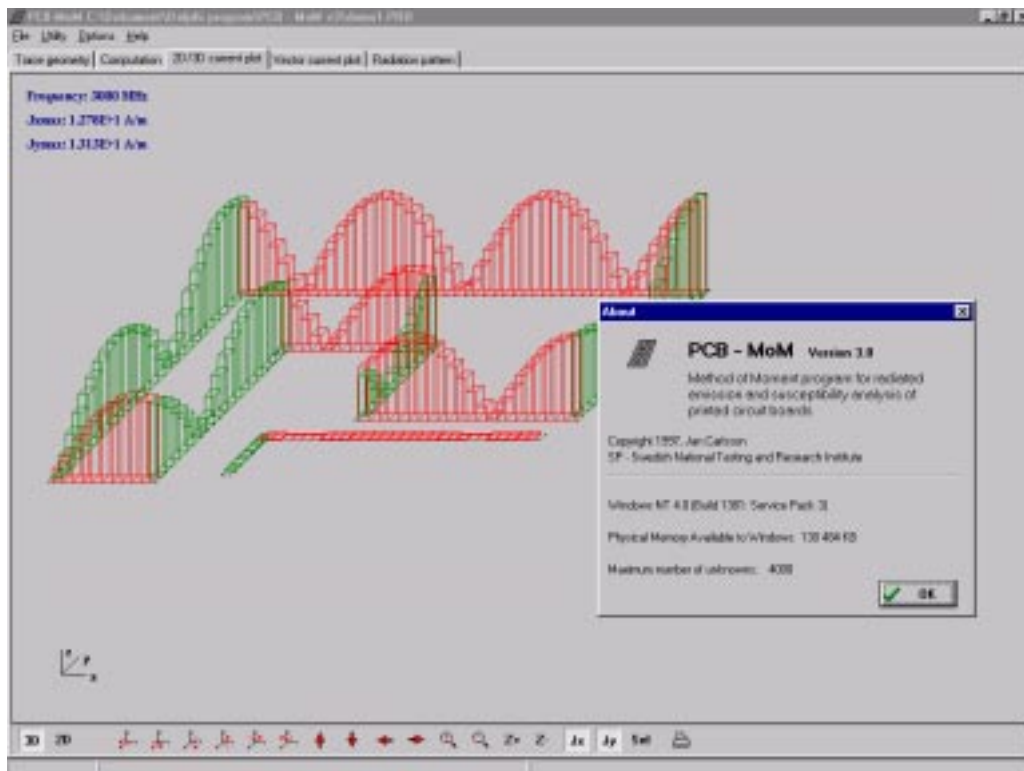


A method of moments program for radiated emission and susceptibility analysis of printed circuit boards

SP Swedish National Testing and Research Institute
Jan Carlsson



Abstract

This document gives a description of a frequency domain method of moments computer code that is intended for predicting radiated emission and susceptibility of printed circuit boards. The formulation is based on an electric field integral equation (EFIE) expressed in the frequency domain. The EFIE is solved by the method of moments using two-dimensional pulse basis functions and one-dimensional pulse testing functions. In order to incorporate dielectric material in the substrate a spectral domain formulation is used.

The program can be run under Windows 95/NT 4.0 or later.

Key words: Crosstalk, EFIE, Electric field integral equation, EMC analysis, MM, MoM, Method of moments, PCB, Printed circuit board, Radiated emission, Radiated susceptibility, Spectral domain.

Sveriges Provnings- och
Forskningsinstitut
SP Rapport 1998:03
ISBN 91-7848-707-2
ISSN 0284-5172
Borås 1998

Swedish National Testing and
Research Institute
SP Report 1998:03

Postal address:
Box 857, S-501 15 BORÅS,
Sweden
Telephone +46 33 16 50 00
Telex 36252 Testing S
Telefax +46 33 13 55 02

Contents

| | |
|---|----|
| <i>Abstract</i> | 2 |
| <i>Contents</i> | 3 |
| <i>Summary</i> | 5 |
| 1 Introduction | 7 |
| 2 Disposition | 9 |
| 3 Program overview | 10 |
| 3.1 Intended use | 10 |
| 3.2 Installation | 10 |
| 3.3 Description | 10 |
| 3.4 A quick look | 10 |
| 4 Defining the geometry | 14 |
| 4.1 General | 14 |
| 4.2 Segments | 15 |
| 4.2.1 Adding segments | 15 |
| 4.2.2 Editing segments | 15 |
| 4.2.3 Connecting segments..... | 16 |
| 4.2.4 Changing the default current element size | 17 |
| 4.3 Voltage sources | 17 |
| 4.3.1 Adding voltage sources | 18 |
| 4.3.2 Editing voltage sources | 18 |
| 4.4 Impedance elements | 18 |
| 4.4.1 Adding impedance elements | 18 |
| 4.4.2 Editing impedance elements..... | 18 |
| 4.5 Ground points | 19 |
| 4.5.1 Adding ground points..... | 19 |
| 4.6 Deleting items | 20 |
| 4.7 Show options | 20 |
| 5 Performing the computation | 22 |
| 5.1 Computing near- and far-fields | 23 |
| 5.2 Simulation time | 24 |
| 6 Visualising computed quantities | 26 |
| 6.1 Result lists | 26 |
| 6.2 3D current plot | 26 |
| 6.3 2D current plot | 28 |
| 6.4 Current vector plot | 28 |
| 6.5 Radiation pattern plot | 29 |
| 6.6 Extracting current in a point | 29 |
| 7 Validation | 31 |

| | |
|--|-----------|
| 7.1 Low frequencies | 31 |
| 7.1.1 Simple RLC circuit..... | 31 |
| 7.1.2 More complex RLC circuit..... | 32 |
| 7.2 Intermediate frequencies | 32 |
| 7.2.1 Comparison with transmission line theory - Open-ended transmission line | 32 |
| 7.2.2 Comparison with transmission line theory - Field induced current in transmission line..... | 34 |
| 7.2.3 Comparison with multiconductor transmission line theory - Crosstalk | 35 |
| 7.2.4 Comparison with measurements - Radiation from PCB..... | 36 |
| 7.2.5 Comparison with FDTD - Loaded loop | 37 |
| 7.3 High frequencies | 38 |
| 7.3.1 Near field - Square plate excited with incident plane wave | 38 |
| 7.3.2 Input impedance of printed dipole | 40 |
| 7.3.3 Radiation from patch antenna..... | 42 |
| 8 Theory..... | 45 |
| 8.1 Current distribution on a planar conducting structure in free space - Integral equation | 45 |
| 8.2 Solution by the method of moments..... | 47 |
| 8.2.1 Integration over self-terms | 53 |
| 8.2.2 Excitation with incident plane wave and voltage sources | 54 |
| 8.2.3 Determination of far-field radiation | 55 |
| 8.3 Extension to include a ground plane..... | 57 |
| 8.4 Extension to include connections to the ground plane | 59 |
| 8.5 Extension to include dielectric material | 62 |
| 8.5.1 Strategy | 62 |
| 8.5.2 Formulation in the spectral domain..... | 63 |
| 8.5.3 Solution of the harmonic 1D field problem..... | 64 |
| 8.5.3.1 Asymptotic solution..... | 64 |
| 8.5.3.2 Exact solution | 69 |
| 8.5.4 Modification of the method of moments matrix..... | 70 |
| 8.5.5 Computational details..... | 71 |
| 8.5.5.1 Fourier transform of the current basis and test functions | 71 |
| 8.5.5.2 Performing the integration..... | 72 |
| 8.5.5.3 Symmetry of the integrand | 74 |
| 8.5.5.4 Oscillation of the integrand | 75 |
| 8.5.5.5 Upper limit for integration..... | 76 |
| 8.5.5.6 Determination of far-field radiation..... | 78 |
| 8.5.5.7 Excitation with incident plane wave..... | 78 |
| 8.5.5.8 Symmetric matrix fill..... | 79 |
| 9 References | 81 |
| Appendix File formats | 82 |

Summary

This document describes a computer code, PCB-MoM, that is intended to be used in EMC applications for predicting radiated emission and susceptibility of printed circuit boards, PCB:s. The program can be used on an ordinary PC running Windows 95/NT 4.0 or later.

In using the PCB-MoM program, analysing a PCB is a three-step procedure: defining the geometry, performing a simulation and finally visualising the computed results. Each of these steps are devoted an own page in the program.

In order to define the geometry the conducting traces on the PCB are simply drawn on the screen using the built-in CAD-like interface. The subdivision of the traces into current and charge elements is done automatically, but can also be set manually by the user. Lumped, discrete voltage sources and impedance elements can easily be defined by pointing out the locations in the layout. In the same way ground points (i.e. metal connections to the underlying ground plane) can be defined.

When the geometry is defined a simulation can be performed. As excitation either the defined voltage sources or an incident plane wave can be used. The results from a simulation are primarily the current densities on the conducting traces. In addition the near-field in selected points and the far-field in selected angular ranges can be obtained.

The computed current densities can be viewed in different ways, as a 3D plot, as a 2D plot or as a vector plot. The computed radiation pattern in the far-field can be viewed as a polar plot.

1 Introduction

The analysis of radiated emission and susceptibility of printed circuit boards are important tasks in order to control the electromagnetic compatibility of an electronic device. The main advantage of analysis compared with measurements, is that the analysis can be done already during the design phase of the device. Thus, by analysis a costly redesign due to a failure in passing an EMC test can be avoided. However, it is important to realise that analysis is not a substitute to EMC tests but can very well be a complement. As a complement the analysis can give us insight into different coupling phenomena etc. on the circuit board, which can be very difficult to understand through measurements. It is also very easy to test different methods to reduce the radiated emission or increase the susceptibility level when an analysis is done. The evaluation of methods to reduce the radiated emission as e.g. re-routing of the clock signals on a printed circuit board can hardly be done by experiments.

The computer code described in this document can be used to analyse simple printed circuit boards regarding both radiated emission and susceptibility. Crosstalk between lands on a printed circuit board can also be computed. Even though the code in principle can be used for complicated circuit board layouts the large number of unknowns that are needed for the simulation results in a very long computation time. Therefore, it is not practical to analyse complicated circuit boards with many lands by this program. However, very often a priori knowledge and engineering judgements can be used in order to reduce the number of lands that are important for the analysis. For instance can, at least for a first approximation, the clock signal lands on a printed circuit board for a digital device be regarded as the main contributors to the radiated emission. In a similar way one often knows which circuits on the board that are the most susceptible, and therefore are the most important for the analysis of the radiated susceptibility. Of course, the same reasoning also holds for the crosstalk where one often only are interested in the crosstalk between certain lands.

The formulation used by the PCB-MoM program is based on an electric field integral equation (EFIE) expressed in the frequency domain. The EFIE is solved by the method of moments using two-dimensional basis functions and one-dimensional pulse testing functions. The choice and locations of the basis and the test functions are the same as used by Glisson & Wilton [1]. However, the formulation presented in [1] is extended to include structures that can be placed over and even connected to an infinite ground plane. The formulation is also extended to include lumped voltage sources and impedance elements placed at arbitrary positions on the structure. The impedance elements serve as models for discrete resistors, inductors and capacitors placed on the structure.

In order to take a dielectric material in-between the structure and the ground plane into account the formulation is further extended by using a spectral domain technique. By Fourier expanding the structure in two orthogonal directions the original three-dimensional problem is transformed to a spectrum of one-dimensional problems. Thus, we can solve a spectrum of simple one-dimensional problems in the spectral domain and then perform an inverse Fourier transform to obtain the wanted solution for the three-dimensional problem in the spatial domain. In the theory part of this document it is shown that the asymptotic part of the inverse Fourier integrals are equal to the elements in the method of moments (MoM) matrix computed in the spatial domain. This fact is used in the program so that the asymptotic part of the inverse Fourier integrals are computed as the MoM matrix elements in the spatial domain. The main advantage of using this technique is that the only thing we have to do to include a dielectric material is to modify the elements in the MoM matrix, computed in the spatial domain, with a correction factor.

The correction factor, which is an inverse Fourier integral, converge fast since the asymptotic part is extracted.

When using the method of moments the computation can be viewed as consisting of two parts: matrix filling and matrix inversion. When all current elements have the same size the MoM matrix will be symmetrical. Thus, only the elements on the diagonal and above have to be computed and consequently the matrix filling time can be reduced. The PCB-MoM program analyse the input data and if all current elements have the same size the symmetrical matrix is filled in an efficient way in order to reduce the computation time.

The results obtained by the PCB-MoM program have been tested against previously published results and against measurements. For low frequencies the results have been compared with ordinary circuit theory. Results for intermediate frequencies have been tested against ordinary transmission line theory and multiconductor transmission line theory. High frequency results and problems involving dielectric material have been compared with published results obtained by other methods and also with computations done with other programs.

2 Disposition

A brief overview of the PCB-MoM program and a description of the capabilities are given in chapter 3. The next following chapters describe how the program is used in order to analyse a printed circuit board, PCB.

In using PCB-MoM the analysis of a PCB is a three-step procedure. First the geometry has to be defined, i.e. the conducting traces on the PCB have to be drawn. How this is done and also how impedance elements and voltage sources are defined is described in chapter 4.

The second step is to perform the computation of the current density on the traces and, if desired, the radiated field in selected angular ranges. How this is done is described in chapter 5.

The last step which is to visualise the computed quantities, current density and radiated field, is described in chapter 6.

The PCB-MoM program has been extensively tested against previously published results and against measurements. A few comparisons are presented in chapter 7.

The last chapter describes the theory which PCB-MoM is based upon and the appendix describes the format for the files used by the program.

3 Program overview

3.1 Intended use

The PCB-MoM program is designed to be used in EMC applications where the interest is in determining the radiated emission and susceptibility of printed circuit boards. The intention has been to design a tool that can be of help to EMC engineers.

Since the program, in principle, can be used for analysing any planar structure it can e.g. also be used for analysing printed antennas.

3.2 Installation

The program can be installed on a PC running Windows 95 or Windows NT 4.0 or later. The installation is done by executing the "Setup.EXE" on the installation diskette. During the installation the following necessary files will be installed on the computer:

- PCBMOM.EXE, program file
- PCBMOM.HLP, help file
- PCBMOM.TES, text file containing constants necessary for time estimates (can be created by the program)
- DIEL.DLL, DLL-file containing routines for treating dielectric material
- CUREXTRACT.EXE, utility program for extracting current in a current element

3.3 Description

The PCB-MoM program is a method of moments program for analysing printed circuit boards with respect to radiated emission and radiated susceptibility in the frequency domain. The program can be used for analysing planar conducting structures placed either in free space or above a perfectly conducting infinitely large ground plane. For the case of a structure above a ground plane the region between the structure and the ground plane can be filled with a dielectric material, thus more closely simulating a real PCB. When the region between the structure and the ground plane is free space, connections between the structure and the ground plane can be defined (z-directed currents). The structure can be excited either by an incident plane wave with arbitrary incident direction and polarisation or an arbitrary number of voltage sources placed on the structure. The structure can be loaded by an arbitrary number of complex impedance elements simulating resistances, inductances and capacitances. The whole structure can also be defined to have a finite conductivity.

3.4 A quick look

In using PCB-MoM for analysing a PCB the first step is to define the geometry including impedance elements and voltage sources. The second step is to perform the computation for determining the currents and optionally the radiated field. When the computation is done the currents and the radiated field can be visualised in different ways. Each of these tasks are given an own page in the program. Switching between the pages is done by clicking on the corresponding page tab.

The geometry is defined on the "*Trace geometry*" page, Fig. 3:1.

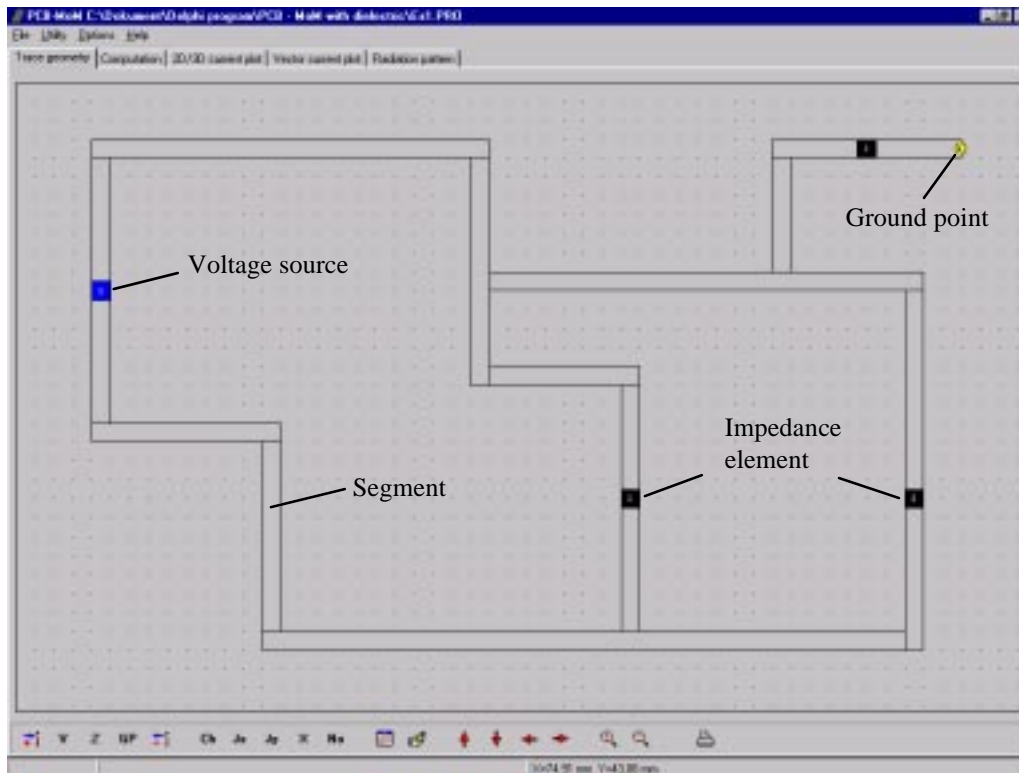


Fig. 3:1. The trace geometry page of the PCB-MoM program.

When the geometry, including impedance elements and voltage sources, is defined parameters for the computation can be set on the "Computation" page, Fig. 3:2.

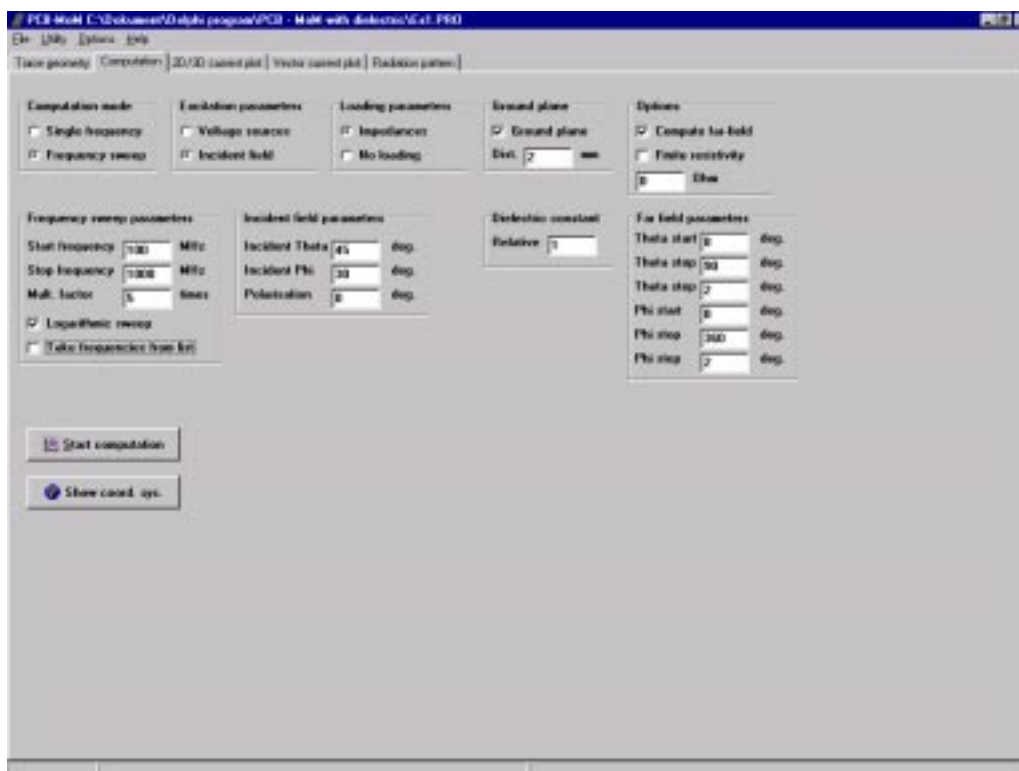


Fig. 3:2. The computation page where parameters for the computation are set.

After a simulation the computed current density on the conducting traces can be viewed either as a 2D/3D plot on the "2D/3D current plot" page, Fig. 3:3 and 3:4, or as a vector plot on the "Vector current plot" page, Fig. 3:5.

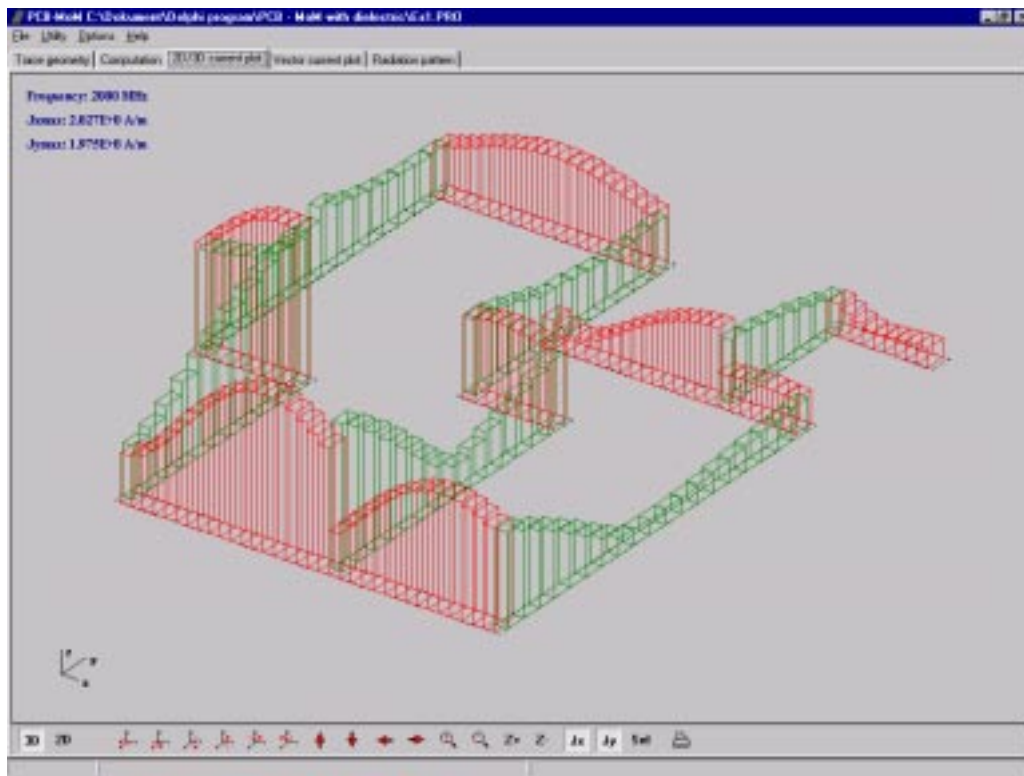


Fig. 3:3. Current density viewed as a 3D plot.

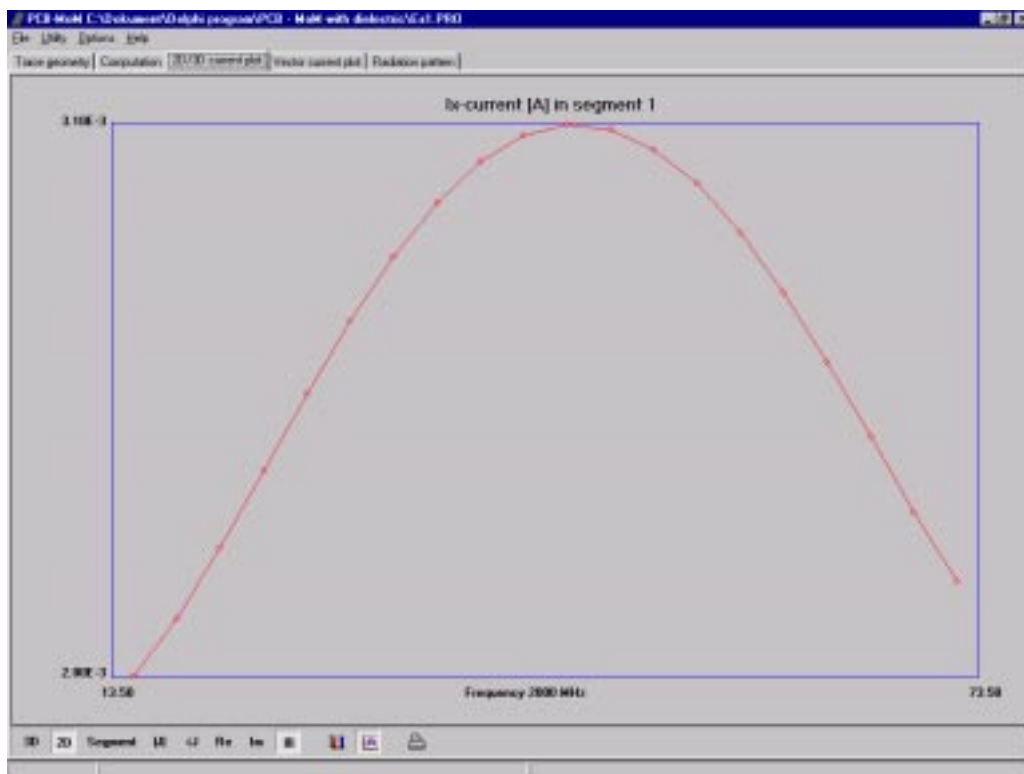


Fig. 3:4. Total current in a segment viewed as a 2D plot.

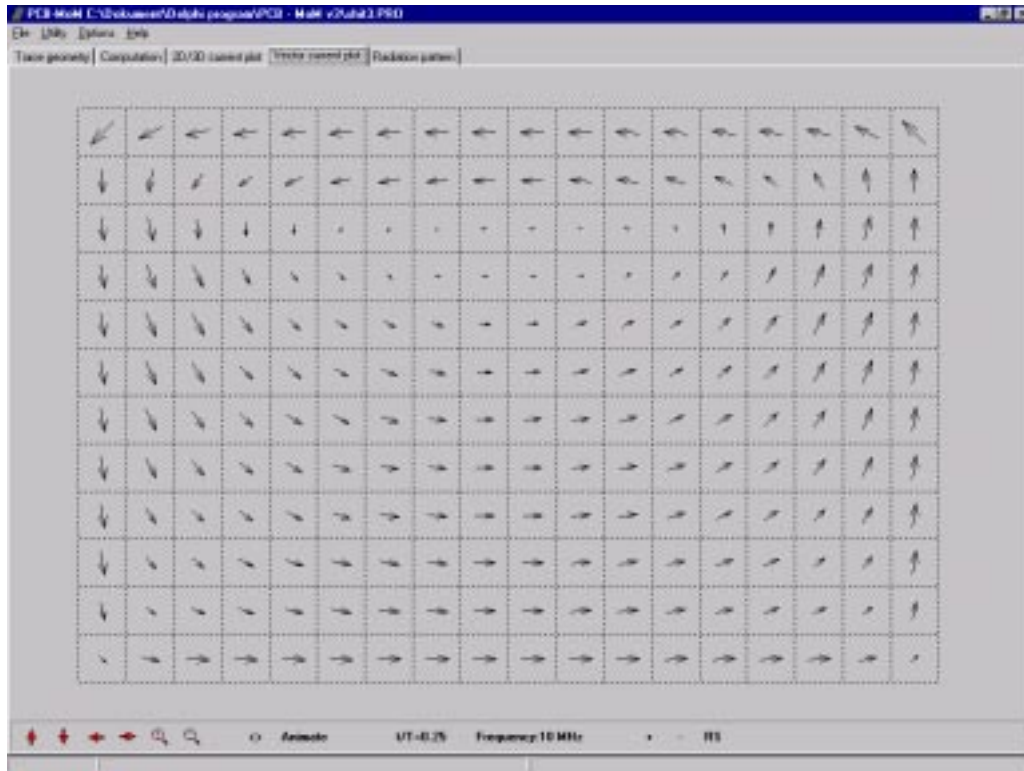


Fig. 3:5. Current density viewed as a vector plot.

If the radiated field is computed a cut can be shown as a polar plot on the "Radiation pattern" page, Fig. 3:6.

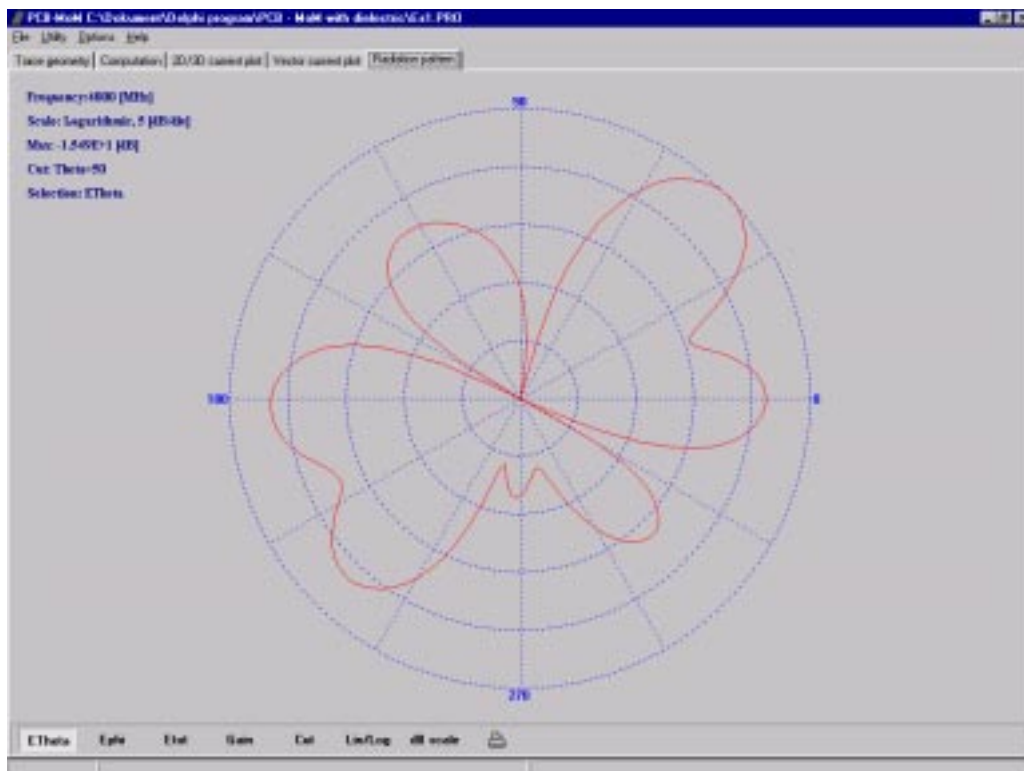


Fig. 3:6. Radiation pattern cut viewed as a polar plot.

4 Defining the geometry

4.1 General

The PCB-MoM program can be used for analysing planar conducting structures placed either in free space or above a ground plane. The structure consists of an arbitrary number of rectangular patches, so called segments, that can be connected to each other. The connected segments can e.g. model the conducting traces on a printed circuit board, PCB. Segments and elements placed on segments, such as impedance elements and voltage sources, are defined on the *"Trace geometry page"*. All geometrical input is done by using the mouse and the result is directly shown on the screen.

When the program is started an empty screen appears and the only options available are creating a new project or open an existing project. When choosing creating a new project the size of the PCB, or actually the size of the available area for the conducting structure, should be input. When this is done the screen will show an empty PCB where the conducting structure should be placed, Fig. 4:1. As a help when defining the structure the coordinates for the cursor can be seen at the bottom of the screen when it is moved over the layout area.

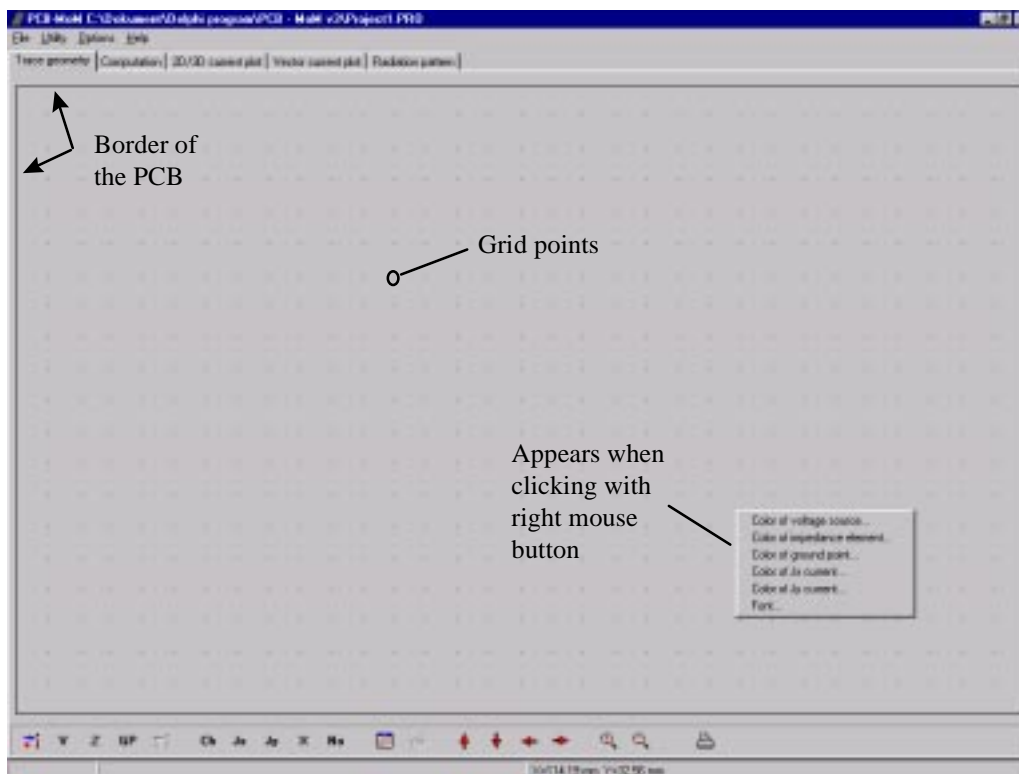


Fig. 4:1. Trace geometry page as it appears when a new project is created (no structure defined yet).

At the bottom of the screen, Fig. 4:1, a row with tools for creating the geometry is shown. Fig. 4:2 and the following chapters explain the meaning of the different tool buttons.

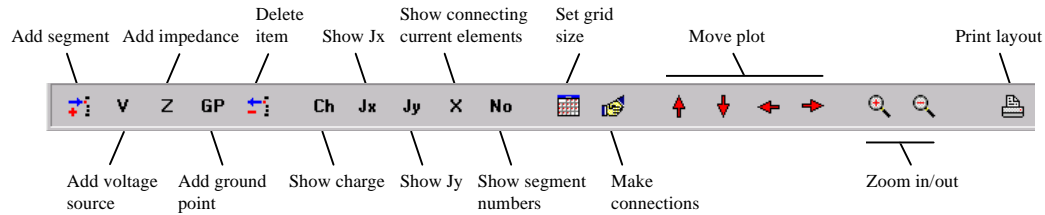


Fig. 4:2. Available tools for defining the geometry.

4.2 Segments

The conducting traces on a PCB is in the PCB-MoM program defined as a combination of connected rectangular conducting elements. These elements are called segments. Each segment is further divided into charge elements. Current elements are automatically set-up by the program based on the charge elements in the segment, Fig. 4:3.

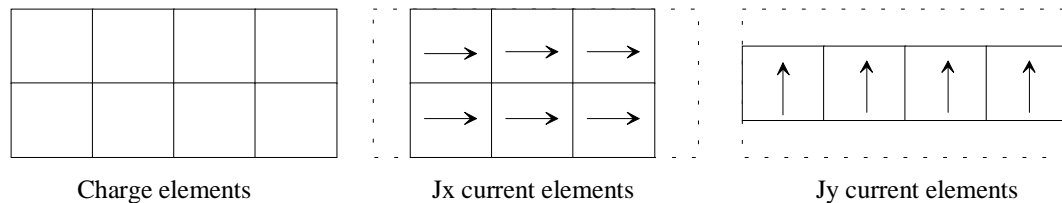


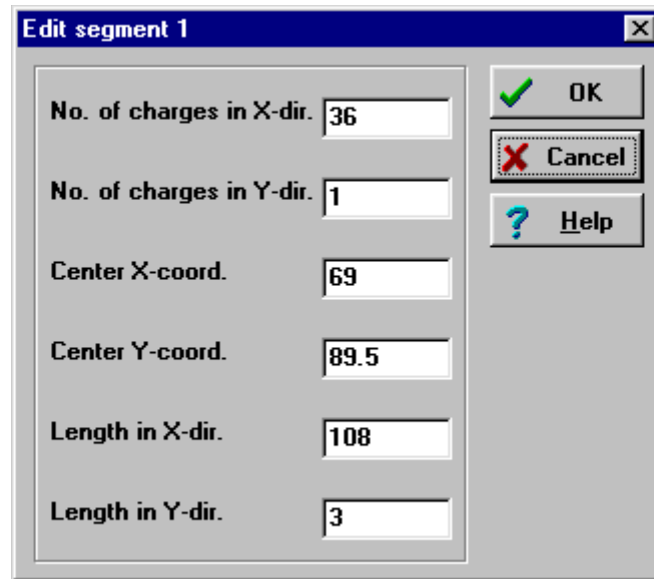
Fig. 4:3. Division of a segment into charge and current elements.

4.2.1 Adding segments

Segments can be added to the layout by pressing the "Add segment" button. When the button is pressed it will stay down until it is pressed again or another "Add" button is pressed. When the "Add segment" button is down the cursor will change shape to be a crosshair when it is over the layout area. Now a segment can be added to the layout by holding down the left mouse button and dragging out a rectangle. When drawn the rectangle will snap to the grid points and will also be divided into charge and current elements (see 4.2.4).

4.2.2 Editing segments

By clicking on a segment when the cursor is an arrow (all "Add" buttons are in their up state), a dialog box where the properties for the segment can be edited is shown, Fig. 4:4.



The dialog box titled "Edit segment 1" contains the following fields and buttons:

| | |
|--------------------------|------|
| No. of charges in X-dir. | 36 |
| No. of charges in Y-dir. | 1 |
| Center X-coord. | 69 |
| Center Y-coord. | 89.5 |
| Length in X-dir. | 108 |
| Length in Y-dir. | 3 |

Buttons on the right: OK (with a green checkmark), Cancel (with a red X), and Help (with a blue question mark).

Fig. 4:4. Edit segment dialog box.

By changing the values in the dialog box the segment size can be set precisely and the number of charge elements in the two orthogonal directions can be set. When the coordinates for the segment are changed in the dialog box the segment will not snap to the grid any more.

4.2.3 Connecting segments

When a segment is defined it will automatically be divided into charge elements and current elements as shown in Fig. 4:3. If two segments are placed next to each other so that the edges of charge elements in the two segments are touching each other there will from the beginning be missing current elements connecting the two segments, Fig. 4:5. These connecting current elements can be created by the program by clicking on the "Make connections" button.

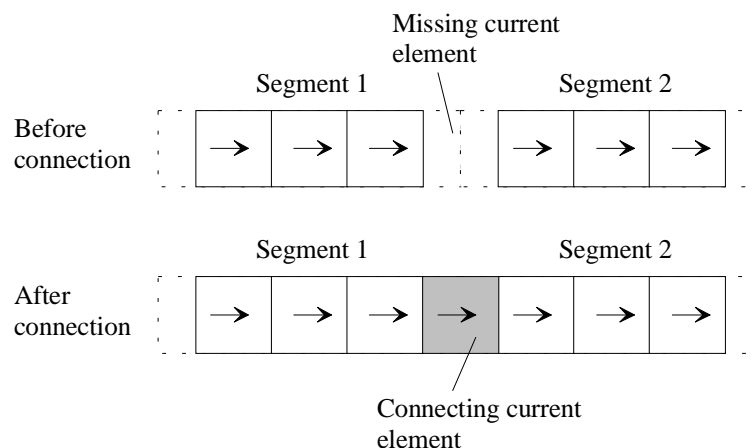


Fig. 4:5. Two adjacent segments before and after connection.

When connections have been made the created connecting current elements can be shown in the layout by pressing the "Show connecting current elements" button. It should be noted that the connections will also be made when a simulation is started, so it is not necessary to press the "Make connections" button.

For the connection process to be successful the sizes of the charge elements in the segments that are about to be connected must match. This means that the edges of the touching charge elements in the segments must be equally long. Therefore, when constructing a circuit with a ninety degree bend it can be wise to place a small segment containing only one charge element in the corner of the bend so that the number of charge elements (and therefore also their sizes) in the segments can be changed later without any problem, see Fig. 4:6.

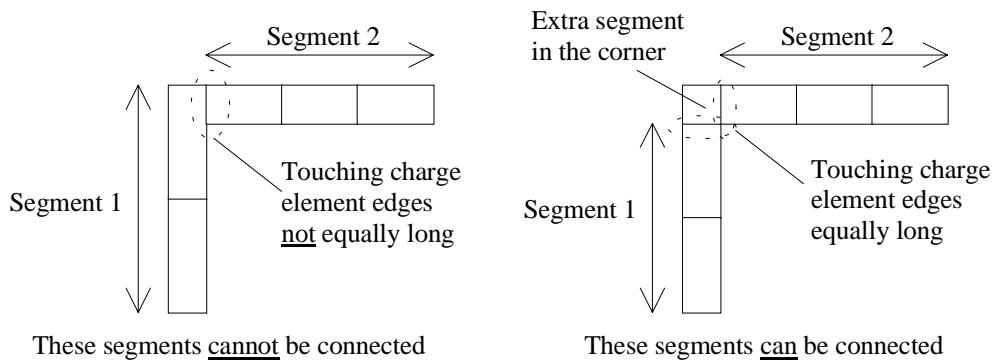


Fig. 4:6. Requirements for connections.

4.2.4 Changing the default current element size

When a segment is drawn on the layout page it will automatically be divided into charge and current elements. The number of charge elements a segment will get is based on the size of the segment, the grid size and a parameter controlling the number of charge elements per grid cell. These parameters can be set by pressing the "Set grid size" button whereby a dialog box will appear, Fig. 4:7.

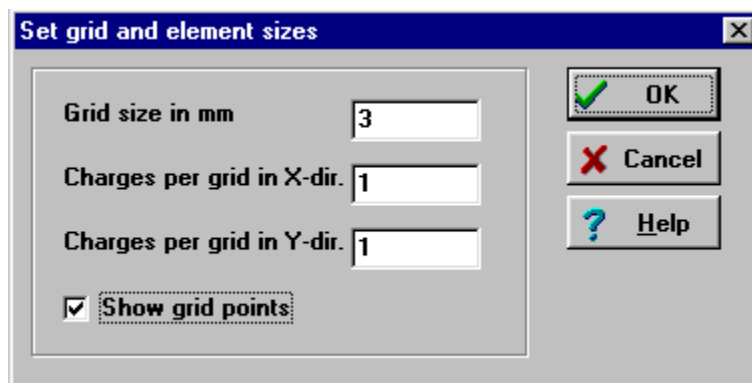


Fig. 4:7. Set grid size dialog box.

4.3 Voltage sources

An arbitrary number of voltage sources can be placed on the layout to serve as excitation of the structure. Voltage sources can be placed in either Jx or Jy current elements and will have a reference direction given by the direction of the current element.

Voltage sources are defined by the real and imaginary part of the voltage, thus making it possible to have sources with different phases.

4.3.1 Adding voltage sources

By pressing the "Add voltage source" button the program is ready to accept definition of voltage sources. When the button is pressed Jx current elements will be shown and a voltage source can be placed in a current element by placing the cursor over the element and pressing the left mouse button. If a voltage source should be placed in a Jy current element the "Show Jy" button must first be pressed. Note that sources can only be defined if either Jx or Jy is shown, not if both are shown at the same time.

4.3.2 Editing voltage sources

Voltage sources can be edited when the cursor is an arrow (all "Add" buttons are in their up state) simply by clicking on a source in the layout. When clicking on a source a dialog box where the complex voltage can be set will appear, Fig. 4:8. The title of the dialog box shows the identification number of the selected voltage source.

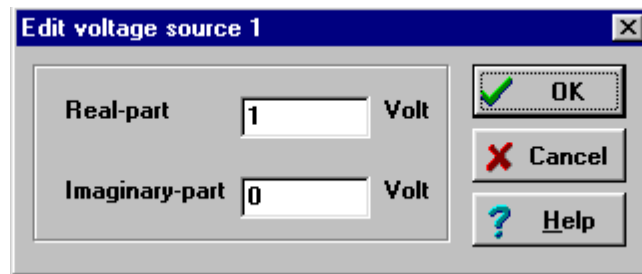


Fig. 4:8. Edit voltage source dialog box. Voltage source number one selected.

4.4 Impedance elements

An arbitrary number of impedance elements can be placed on the layout to serve as loading of the structure. Impedance elements can be placed in either Jx or Jy current elements and can represent a resistance, inductance or a capacitance.

4.4.1 Adding impedance elements

By pressing the "Add impedance" button the program is ready to accept definition of impedance elements. When the button is pressed Jx current elements will be shown and an impedance element can be placed in a current element by placing the cursor over the element and pressing the left mouse button. If an impedance element should be placed in a Jy current element the "Show Jy" button must first be pressed. Note that impedance elements can only be defined if either Jx or Jy is shown, not if both are shown at the same time.

4.4.2 Editing impedance elements

Impedance elements can be edited when the cursor is an arrow (all "Add" buttons are in their up state) simply by clicking on an impedance element in the layout. The title of the appearing dialog box will show the identification number of the selected impedance element.

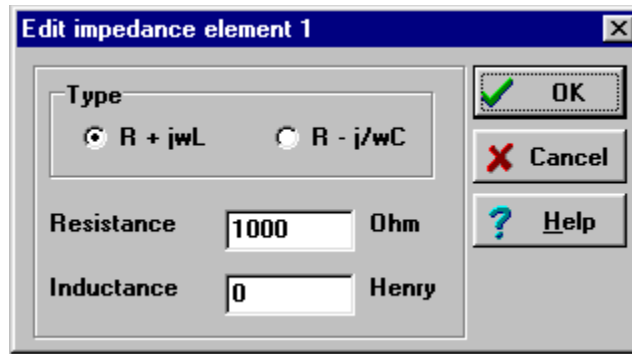


Fig. 4:9. Edit impedance element dialog box. Impedance element number one selected.

By selecting type of impedance an impedance element can either represent a resistance in series with an inductance or a resistance in series with a capacitance. By letting the value in one of the edit boxes in the edit impedance element dialog box be equal to zero a single resistance, inductance or capacitance can be defined.

4.5 Ground points

If the structure is placed over a ground plane and the region in-between is free space connections between the structure and the ground plane can be made. These connections are in the program called ground points.

4.5.1 Adding ground points

Ground points can be added to the layout by first pressing the "Add ground point" button and after that left clicking in the charge element where the ground point should be placed. When clicking in a charge element a dialog box asking for which edge the ground point should be placed on will appear, Fig. 4:10.

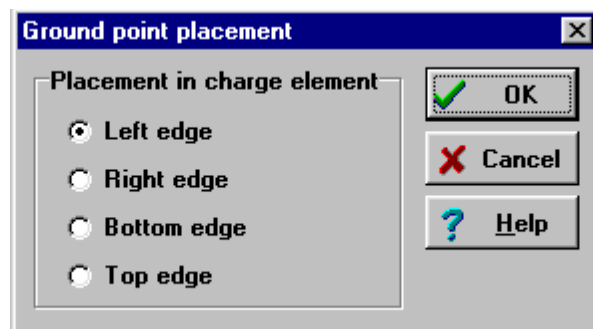


Fig. 4:10. Placement of ground point dialog box.

Ground points will support z-directed currents that must be connected to currents in the segment in which the ground point is defined. Therefore, certain restrictions must be followed when placing the ground points. The program does not check the validity of ground points so care should be utilised when using them. In using ground points the following rules should be followed:

- Place a ground point in a segment that supports only one type of currents (either J_x or J_y currents)

- Place the ground point on an edge of the segment, i.e. the leftmost or rightmost charge element in a segment that supports only J_x currents and the top or bottom charge element in a segment that supports only J_y currents

4.6 Deleting items

Items placed in the layout can be deleted by pressing the "Delete item" button. When the button is pressed a dialog box will appear where the type of item to delete can be chosen, Fig. 4:11. When an item is deleted all remaining items of the same type will get new numbers so that the items are numbered from one to the total number of items.

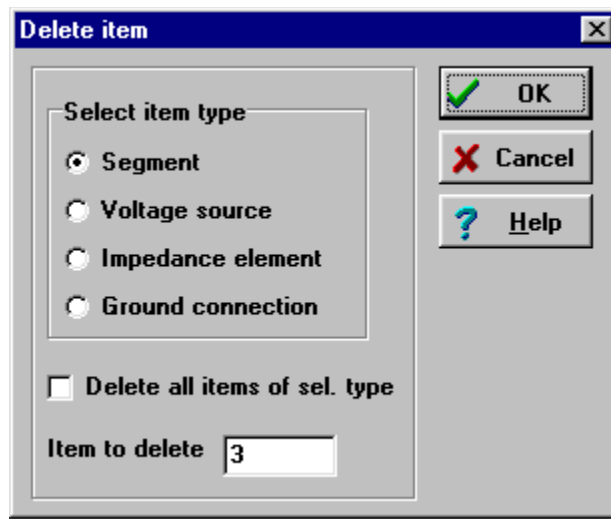


Fig. 4:11. Delete item dialog box.

4.7 Show options

In order to see small details in the layout the layout can be zoomed and moved by pressing the zoom and move buttons, respectively. The layout can also be moved on the screen by holding down the left mouse button, when the cursor is an arrow, and dragging the layout. When this is done the cursor change shape to be a hand. The layout can also be moved by using the arrow keys and zoomed by using the "+" and "-" keys. By clicking with the right mouse button in any part of the layout a pop-up menu, where colours and font for the details in the layout can be set, will be shown.

The charge and current elements in segments can be shown by pressing the "Show charge", "Show J_x " and "Show J_y " buttons, respectively. When connections have been made (by pressing the "Make connections" button) the connecting current elements can be shown by pressing the "Show connecting current elements" button. Connecting current elements are shown as filled coloured rectangles in order to distinguish them from other current elements.

Details for the project can be viewed by selecting "View project file" under "Utility" in the main menu, Fig. 4:12.

Details for Ex1.PRO [X]

| Last saved | Layout | |
|------------------|----------------|--------------|
| Date: 1997-10-18 | Length: 160 mm | Close |
| Time: 13:26:29 | Width: 100 mm | |

Details

| | |
|-----------------------------|---------------------------|
| No. of segments: 12 | Ground plane height: 2 mm |
| No. of charge elements: 160 | Resistivity not specified |
| No. of sources: 1 | No. of impedances: 3 |
| No. of ground points: 1 | Grid size: 3 mm |
| Charges per x-grid: 1 | Charges per y-grid: 1 |
| Free space environment | |

Notes:

Notes entered in this field will be saved in a separate text file that can be read and edited by a standard text editor.

Fig. 4:12. View project file dialog box.

5 Performing the computation

When the geometry is defined the program is ready to compute the currents on the segments and, optionally, the radiated field in desired directions. When a dielectric material is not defined also the near field in selected points can be computed.

All computation parameters are set on the "Computation" page, Fig. 5:1.

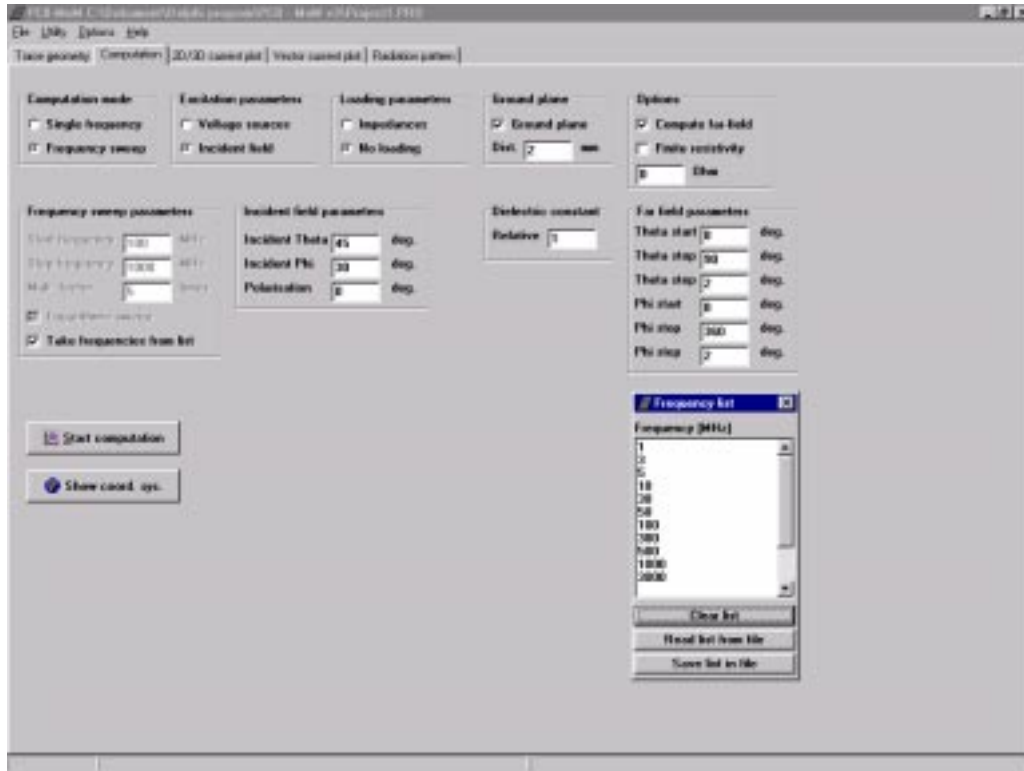


Fig. 5:1. The computation page where parameters for the computation are set.

The computation can either be performed for a single frequency or for a frequency sweep. If frequency sweep is selected it can either be a linear, logarithmic or a sweep of frequencies taken from a list. For linear and logarithmic frequency sweep the start, stop and the step or multiplication factor have to be defined. During a simulation the present frequency is shown on the screen and the computation can be aborted any time by pressing the "Abort computation" button (appears when a simulation is started).

Two different sets of excitation parameters can be chosen from, voltage sources or incident field. When choosing voltage sources as excitation the defined voltage sources on the layout (can be seen on the trace geometry page) will be used. If incident field is chosen an incident plane wave will be used as the excitation. For this case voltage sources, if any, on the layout will not be used. When incident field is chosen an additional box, where the incident direction and polarisation for the incident field can be set, will be shown. The amplitude of the incident field is 1 V/m.

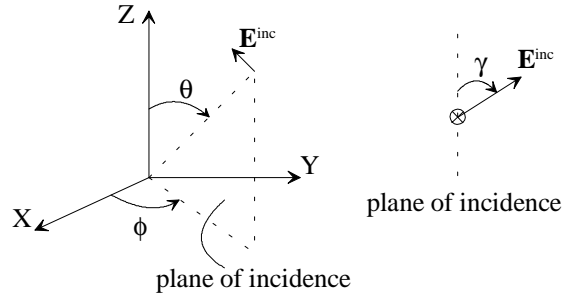


Fig. 5:2. Definition of direction and polarisation for incident field excitation.

If impedance elements for the structure have been defined and should be taken into account in the simulation "*Impedances*" must be checked in the loading parameters box. If "*No loading*" is checked impedance elements, if any, will not be taken into account.

If "*Ground plane*" is checked an infinitely large and perfectly conducting ground plane will be placed under the structure at the specified distance. When ground plane is chosen an additional box, where the relative permittivity for the region between the structure and the ground plane can be set, will be shown. For free space this constant should be equal to unity. Ground connections cannot not be used if the permittivity differs from unity.

If "*Compute far-field*" is chosen in the "*Options*" box the normalised E-field will be computed in the selected angular sector. The definition of the angles is the same as for the incident field excitation, Fig. 5:2. Also in the "*Options*" box the whole structure can be defined to have a finite conductivity. For perfectly conducting structures the finite resistivity should not be checked.

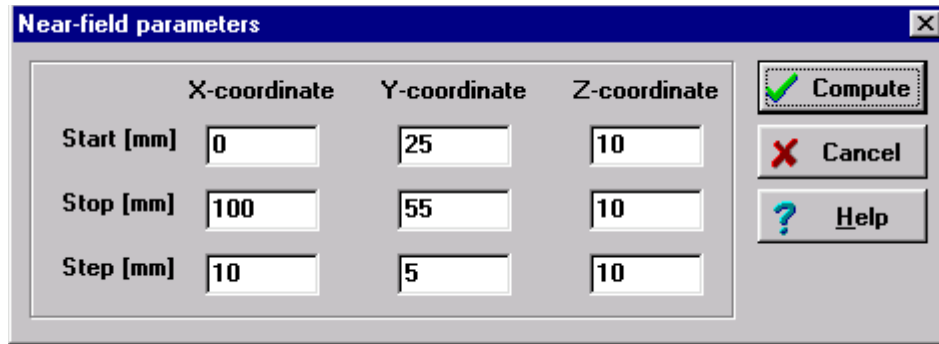
When a dielectric constant not equal to unity is defined it might happen that the program shows a warning when a simulation is started. The warning is "*Not sufficient number of points for spectral domain integration*". When this warning is shown it is recommended that the simulation is aborted and the number of integration points is increased. This can be done through the "*Options - Set accuracy for integration in spectral domain*" in the main menu. For details see the theory part of this document.

5.1 Computing near- and far-fields

The near- and far-fields can be computed when the current density on the structure has been computed. It should be noted that when the near- and far-fields are computed after a computation of the current density (i.e. outgoing from currents saved in files) the environment is free-space no matter if the currents were computed with a dielectric material present. If the far-field should be computed when a dielectric material is present the far-field computation should be requested when the current density is computed, as described in the previous chapter. The near-field cannot be computed when a dielectric material is present.

When the structure is excited by an incident plane wave the computed field, both near and far-field, is the scattered field from the structure. When the excitation is done by voltage sources the computed field is the total field.

The "Compute near-field" and "Compute far-field" can be found under "Utility" in the main menu. When selected a dialog box where the parameters can be input will appear, Fig. 5:3 and 5:4.

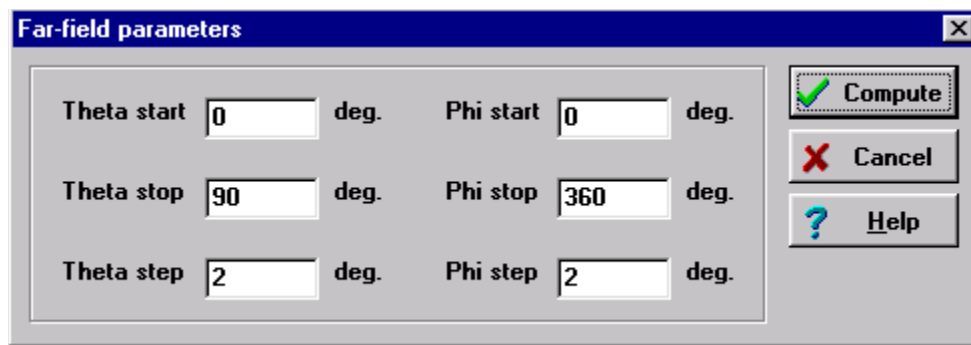


The "Near-field parameters" dialog box contains three columns for X-coordinate, Y-coordinate, and Z-coordinate. Each column has three input fields: Start [mm], Stop [mm], and Step [mm]. The values are: X (0, 100, 10), Y (25, 55, 5), and Z (10, 10, 10). On the right, there are three buttons: "Compute" (with a green checkmark icon), "Cancel" (with a red X icon), and "Help" (with a blue question mark icon).

| | X-coordinate | Y-coordinate | Z-coordinate |
|------------|--------------|--------------|--------------|
| Start [mm] | 0 | 25 | 10 |
| Stop [mm] | 100 | 55 | 10 |
| Step [mm] | 10 | 5 | 10 |

Fig. 5:3. Near-field parameter dialog box.

When selecting field points for the near-field computation the points should not be too close to the structure in order to obtain reliable results. As a rule of thumb the distance from any field point to any point on the radiating structure should be at least 1.5 times the current element size. If any field point is closer than one current element size the program will give a warning.



The "Far-field parameters" dialog box contains two columns for Theta and Phi. Each column has three input fields: start, stop, and step, followed by the unit "deg.". The values are: Theta (0, 90, 2) and Phi (0, 360, 2). On the right, there are three buttons: "Compute" (with a green checkmark icon), "Cancel" (with a red X icon), and "Help" (with a blue question mark icon).

| | Theta | Phi |
|------------|-------|-----|
| start deg. | 0 | 0 |
| stop deg. | 90 | 360 |
| step deg. | 2 | 2 |

Fig. 5:4. Far-field parameter dialog box.

5.2 Simulation time

Considering the total simulation time a simulation can be viewed as consisting of two parts, matrix filling and matrix inversion. Of course, both the fill and inversion time will depend on the size of the matrix which in turn is determined by the number of current elements. For a given number of current elements (unknowns) the only part we can have influence on is the fill time, the inversion time will remain the same. The fill time can be affected by choosing the sizes of the current elements. If all current elements have the same size the matrix is symmetrical and the matrix fill time can be reduced since the program doesn't have to compute all matrix elements. The fill time will also vary with frequency since the integrals associated with the matrix elements can be computed more efficiently when the distance between current elements is large in terms of the wavelength.

Figure 5:5 shows the matrix fill and inversion time as a function of the number of unknowns (the size of the matrix) for a structure in free space. As can be seen in Fig. 5:5 the time saving for a symmetrical matrix compared to a non-symmetric can be considerable, especially when the number of unknowns is not too large. When the

number of unknowns become large the inversion time will start to dominate over the fill time. For the example in the figure this happens, for the symmetrical matrix, around 1000 unknowns.

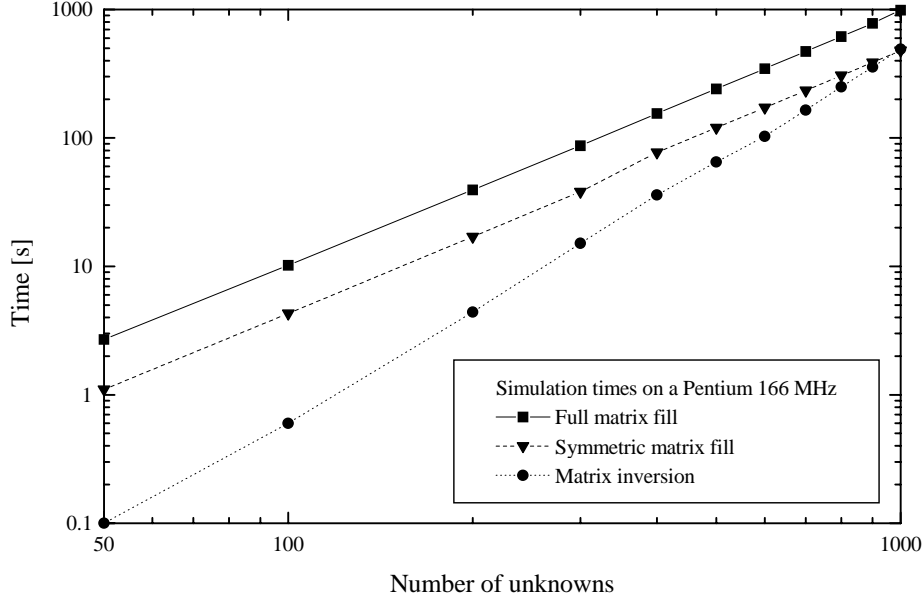


Fig. 5:5. Simulation time for a structure in free space.

Analysing the results in Fig. 5:5 the following approximate relations between the number of unknowns, N , and the fill and inversion times can be found:

$$\begin{cases} \text{Fill time} \propto C_1 \cdot N^2 \\ \text{Inversion} \propto C_2 \cdot N^3 \end{cases}$$

where C_1 and C_2 are constants.

It should be noted that the fill time is considerably longer if a dielectric material is defined since the matrix elements are more complicated to compute, see the theory part.

By choosing "Show time estimate before computation" under "Options" in the main menu the program will show an estimate of how long the requested simulation will take. Since the simulation time will vary from computer to computer first a calibration has to be done. During the calibration process the program will measure the fill and inversion times and save constants in a file (PCBMOM.TES). Once a calibration has been performed the constants in the calibration file will be used for determining the time estimate according to the above formulas.

6 Visualising computed quantities

When a simulation is completed the computed results can be viewed either as lists in text format or as graphs.

6.1 Result lists

Results can be listed by choosing some of the list options in the main menu, Fig. 6:1.

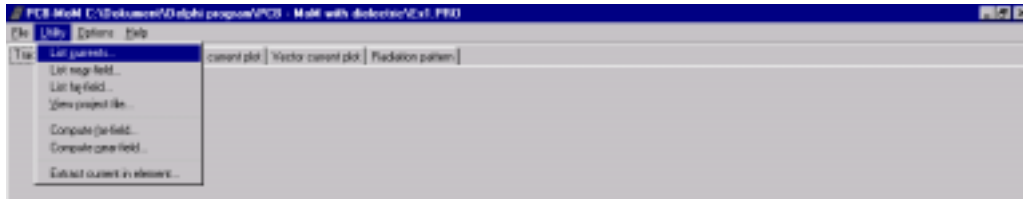


Fig. 6:1. List options in the main menu.

When one of the list options is selected a dialog box with a list of the selected quantities is shown. As an example the current list is shown in Fig. 6:2. In the list the current density and the size and location of the individual current elements can be seen.

| No. | Amp [A/m] | Phase [deg] | dx [mm] | dy [mm] | dz [mm] | xc [mm] | yc [mm] |
|-----|-----------|-------------|---------|---------|---------|---------|---------|
| 1 | 1.912E+00 | -1.60 | 3.00 | 3.00 | - | 15.00 | 89.50 |
| 2 | 1.926E+00 | -4.90 | 3.00 | 3.00 | - | 18.00 | 89.50 |
| 3 | 1.941E+00 | -8.30 | 3.00 | 3.00 | - | 21.00 | 89.50 |
| 4 | 1.955E+00 | -12.00 | 3.00 | 3.00 | - | 24.00 | 89.50 |
| 5 | 1.969E+00 | -15.00 | 3.00 | 3.00 | - | 27.00 | 89.50 |
| 6 | 1.981E+00 | -18.00 | 3.00 | 3.00 | - | 30.00 | 89.50 |
| 7 | 1.992E+00 | -22.00 | 3.00 | 3.00 | - | 33.00 | 89.50 |
| 8 | 2.002E+00 | -25.00 | 3.00 | 3.00 | - | 36.00 | 89.50 |
| 9 | 2.010E+00 | -28.00 | 3.00 | 3.00 | - | 39.00 | 89.50 |
| 10 | 2.017E+00 | -31.00 | 3.00 | 3.00 | - | 42.00 | 89.50 |
| 11 | 2.022E+00 | -34.00 | 3.00 | 3.00 | - | 45.00 | 89.50 |

Fig. 6:2. Jx current list dialog box.

6.2 3D current plot

By clicking on the "2D/3D current plot" page tab the computed current density on the structure will be shown as a 3D plot (for an example see Fig. 3:3 and 6:4). If the computation was performed for more than one frequency first a dialog box, where the frequency can be selected, will be shown. In order to change frequency for the 3D plot, click the page tab and the select frequency dialog box will be shown.

At the bottom of the screen a row with tool buttons is shown. With these tools the plot can be manipulated in different ways, Fig. 6:3.

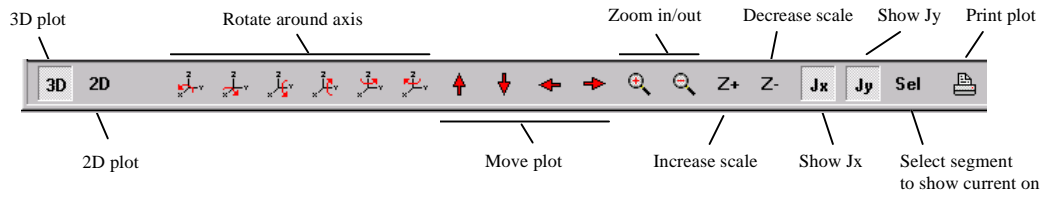


Fig. 6:3. Available tools for manipulating the 3D current plot.

In addition to using the tool buttons the plot can be moved either by using the mouse or by using the arrow keys. The plot can also be zoomed by using the "+" and "-" keys and rotated with the "x", "y" and "z" keys. By holding down the shift key the rotation will be in the reverse direction. By clicking with the right mouse button in the plot the colours for the Jx and Jy currents can be changed.

By pressing the "Select segment to show current on" the current density on individual segments can be turned on or off, Fig. 6:4. This can be helpful when the structure consists of many segments and the currents on some segments are blocked by the currents on some other segments.

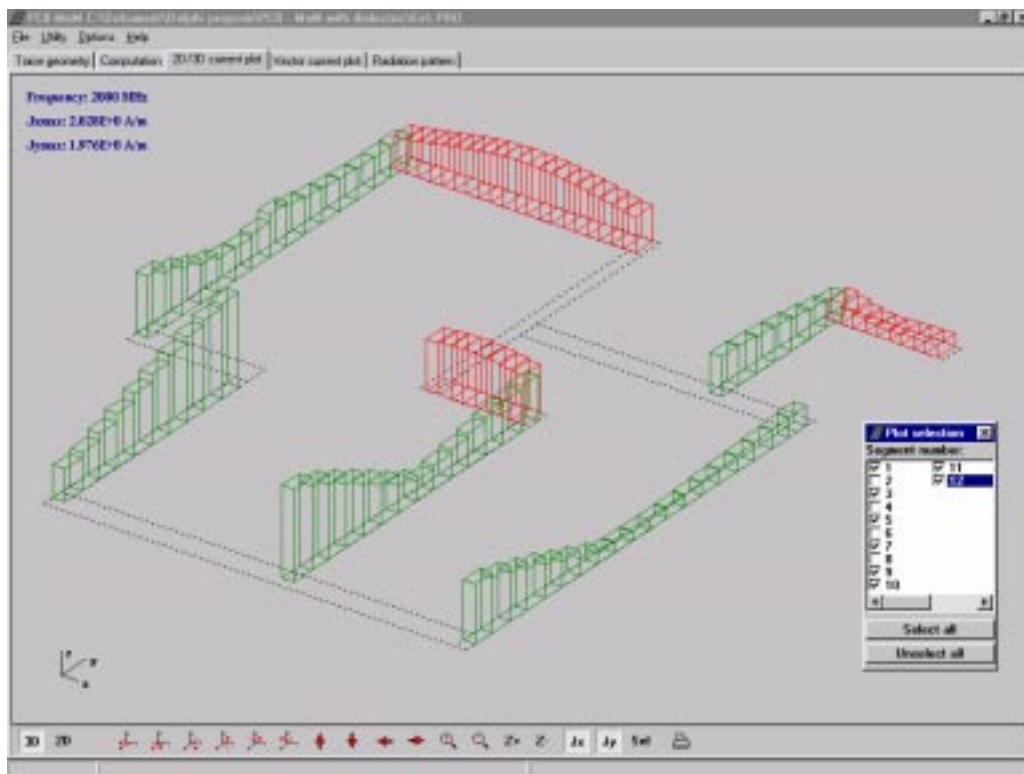


Fig. 6:4. Current density shown as a 3D current plot.

6.3 2D current plot

A 2D plot of the current in a particular segment can be shown by pressing the "2D" button when a 3D plot is shown (for an example see Fig. 3:4). When the button is pressed first a dialog box asking for the identification number of the segment will appear. If the segment contains both J_x and J_y current elements an additional dialog box asking for which type of current and which row or column to plot will also appear. Row numbers start from the top in a segment and column numbers start from the left.

At the bottom of the screen a row with tool buttons is shown. With these tools the parameter to plot can be chosen, Fig. 6:5. Also at the bottom of the screen the coordinates of the cursor when it is moved over the plot can be seen. Thus, making it possible to determine the values at points in the plot.

The unit for the current density is A/m and the phase plot is in degrees. The total current in a segment (or a row or column of currents) is defined as the current density multiplied with the transverse width of the particular current element. Thus, the total current can be expressed as:

$$\begin{cases} I_x^{tot} = \Delta y J_x \\ I_y^{tot} = \Delta x J_y \end{cases}$$

By clicking with the right mouse button in the plot the colours for the plot can be changed.

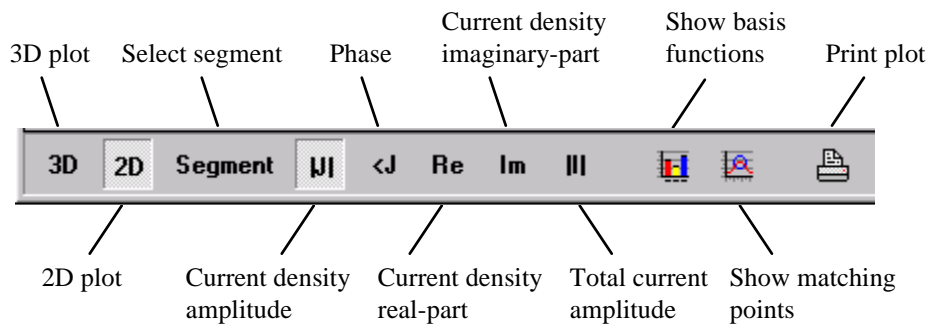


Fig. 6:5. Available tools for manipulating the 2D current plot.

6.4 Current vector plot

A vector plot of the current density can be shown by clicking on the "Vector current plot" page tab (for an example see Fig. 3:5). In the vector plot the currents are shown as arrows with a length that is proportional to the amplitude and a direction given by the current direction. An animation of how the current density changes through a period can be seen by clicking the "Animation" button. The relative phase can also be changed manually by clicking on the "<>" button.

At the bottom of the screen a row with tool buttons is shown. With these tools the plot can be manipulated in different ways, Fig. 6:6.

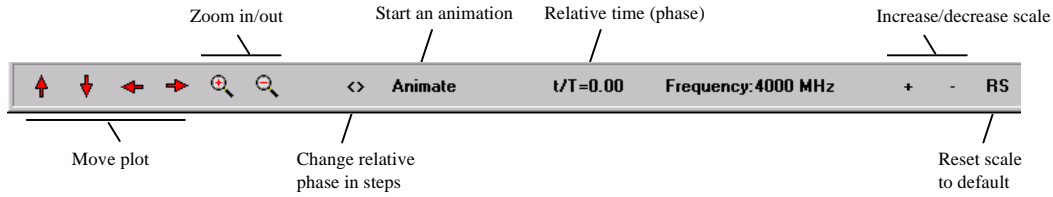


Fig. 6:6. Available tools for manipulating the vector current plot.

In addition to using the tool buttons the plot can be moved either by using the mouse or by using the arrow keys. The plot can also be zoomed by using the "+" and "-" keys.

6.5 Radiation pattern plot

If the far-field has been computed the normalised radiation pattern can be shown as a 2D polar plot by clicking on the "Radiation pattern" page tab (for an example see Fig. 3:6).

The E-field in the plot is normalised to the factor $\frac{e^{-jkr}}{r}$ so that the plotted results are in

Volts. If the computation was performed for a single frequency, besides the E-field, the power gain can also be plotted. At the bottom of the screen a row with tool buttons is shown. With these tools the cut and which field component to plot can be selected, Fig. 6:7.

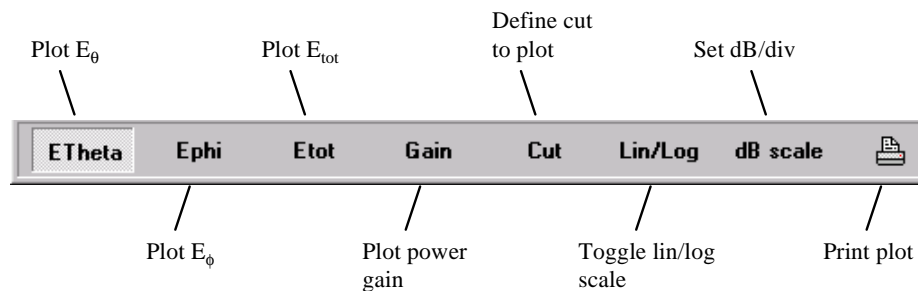


Fig. 6:7. Available tools for the radiation pattern plot.

By clicking with the right mouse button in the plot the colours for the plot can be changed.

6.6 Extracting current in a point

The current density in a particular current element can be extracted from the data files and saved in a text file by using the utility program "CurExtract.EXE". This program can either be used standalone or started from within PCB-MoM. The current extracting program is started from PCB-MoM by selecting "Extract current in element" under "Utility" in the main menu.

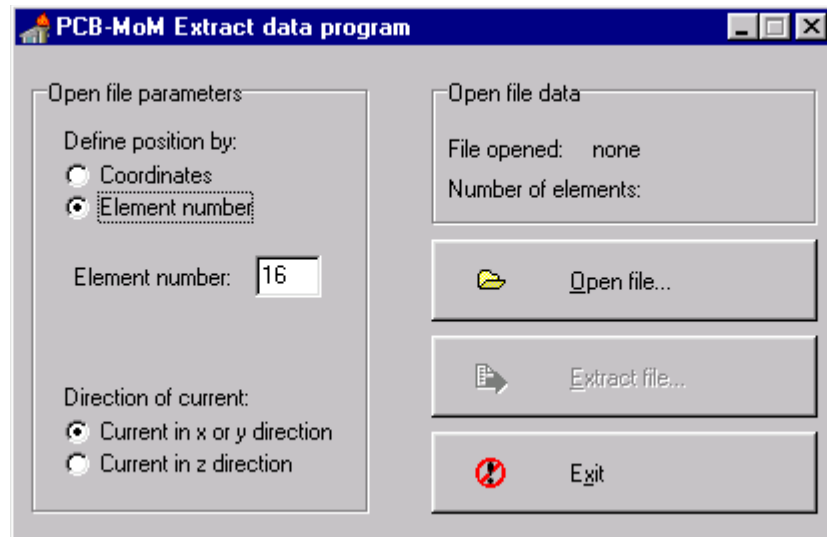


Fig. 6:8. The current extracting program.

When the extracting program has been run the resulting data file will contain the current density in the selected current element as a function of frequency. This file can then be plotted or further analysed in another program.

7 Validation

In order to test the validity of the results obtained by the PCB-MoM program several test cases have been run, some of which are presented in this chapter.

7.1 Low frequencies

For low frequencies, i.e. where the circuit is small compared to the wavelength, the results obtained by the program should agree with ordinary lumped parameter circuit analysis. Below two examples are given that shows that the agreement is excellent even at very low frequencies where the current element size is extremely small in terms of the wavelength.

7.1.1 Simple RLC circuit

Figure 7:1 shows the analysed RLC circuit. In the PCB-MoM program the loop was modelled as a 80 by 40 mm rectangular loop built of 5 mm wide segments. The current element size was 5 by 5 mm.

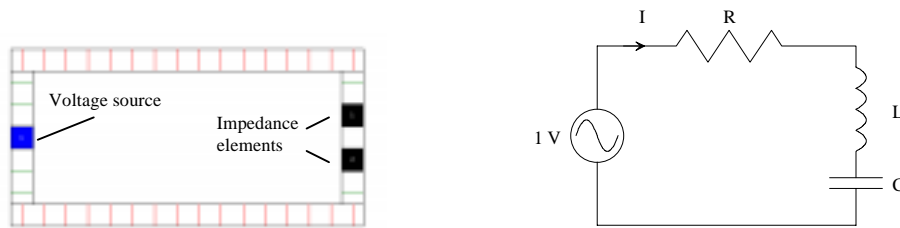


Fig. 7:1. RLC circuit in PCB-MoM and corresponding equivalent circuit.
R=1 kOhm, L=1 mH and C=1 μ F.

The current in the loop calculated with lumped circuit theory and the PCB-MoM program as a function of the frequency is shown in table 7:1. The agreement is found to be excellent. It could also be noted that the agreement is excellent even for as low frequencies as 1 Hz. At this frequency the current element size is only approx. $1.7 \cdot 10^{-11} \lambda$, where λ is the wavelength.

| Frequency [Hz] | Circuit theory | | PCB-MoM | |
|-------------------|----------------------|------------------|----------------------|------------------|
| | Abs(I) [A] | Arg(I) [deg.] | Abs(I) [A] | Arg(I) [deg.] |
| 1 | $6.28 \cdot 10^{-6}$ | 89.6 | $6.28 \cdot 10^{-6}$ | 89.6 |
| 10 | $6.27 \cdot 10^{-5}$ | 86.4 | $6.27 \cdot 10^{-5}$ | 86.4 |
| 100 | $5.32 \cdot 10^{-4}$ | 57.8 | $5.32 \cdot 10^{-4}$ | 57.8 |
| 1k | $9.89 \cdot 10^{-4}$ | 8.69 | $9.89 \cdot 10^{-4}$ | 8.69 |
| 10k | $9.99 \cdot 10^{-4}$ | -2.69 | $9.99 \cdot 10^{-4}$ | -2.69 |
| 100k | $8.47 \cdot 10^{-4}$ | -32.1 | $8.47 \cdot 10^{-4}$ | -32.1 |
| 1M | $1.57 \cdot 10^{-4}$ | -81.0 | $1.56 \cdot 10^{-4}$ | -80.9 |

Table 7:1. Current in the RLC circuit in Fig. 7:1 computed with circuit theory and the PCB-MoM program.

7.1.2 More complex RLC circuit

As another test of the low frequency performance of the program a more complicated circuit was analysed, Fig. 7:2. In the PCB-MoM program the loop was modelled as a 80 by 40 mm rectangular loop built of 5 mm wide segments. The current element size was 5 by 5 mm.

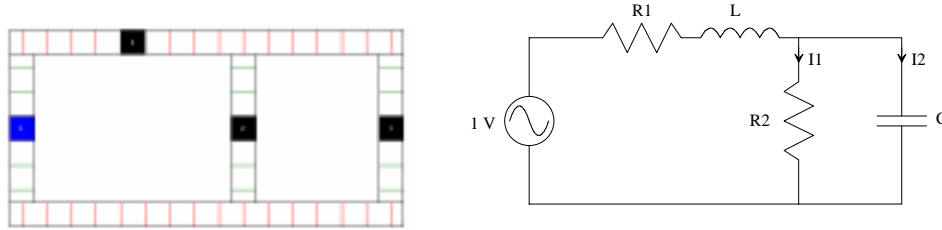


Fig. 7:2. More complex RLC circuit in PCB-MoM and corresponding equivalent circuit. $R1=1\text{ k}\Omega$, $R2=0.5\text{ k}\Omega$, $L=0.1\text{ mH}$ and $C=1\text{ }\mu\text{F}$.

As can be seen from the results in table 7:2 also for this case the agreement is excellent.

| Freq. [kHz] | Circuit theory | | | | PCB-MoM | | | |
|----------------|----------------------|------------------|----------------------|------------------|----------------------|------------------|----------------------|------------------|
| | I1 | | I2 | | I1 | | I2 | |
| | Abs(I) [A] | Arg(I) [deg.] | Abs(I) [A] | Arg(I) [deg.] | Abs(I) [A] | Arg(I) [deg.] | Abs(I) [A] | Arg(I) [deg.] |
| 1 | $2.87 \cdot 10^{-4}$ | -64.5 | $9.02 \cdot 10^{-4}$ | 25.5 | $2.87 \cdot 10^{-4}$ | -64.5 | $9.02 \cdot 10^{-4}$ | 25.5 |
| 10 | $3.18 \cdot 10^{-5}$ | -87.6 | $9.99 \cdot 10^{-4}$ | 2.37 | $3.18 \cdot 10^{-5}$ | -87.6 | $9.99 \cdot 10^{-4}$ | 2.37 |
| 100 | $3.18 \cdot 10^{-6}$ | -93.3 | $9.98 \cdot 10^{-4}$ | -3.32 | $3.12 \cdot 10^{-6}$ | -93.3 | $9.98 \cdot 10^{-4}$ | -3.32 |

Table 7:2. Current in the RLC circuit in Fig. 7:2 computed with circuit theory and the PCB-MoM program.

7.2 Intermediate frequencies

7.2.1 Comparison with transmission line theory - Open-ended transmission line

As a comparison with transmission line theory an open-ended transmission line, Fig. 7:3, was considered.

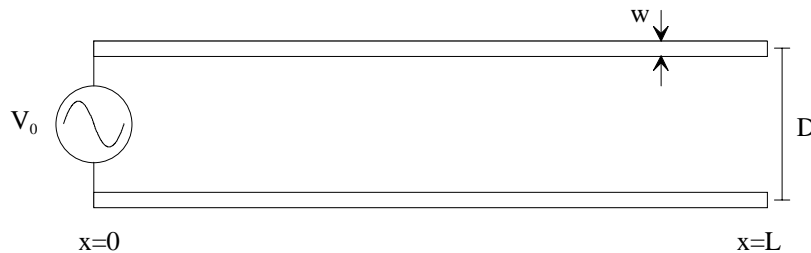


Fig. 7:3. Open-ended transmission line excited with a voltage source. For the test case: $L=500\text{ mm}$, $D=20\text{ mm}$, $w=2\text{ mm}$.

In the PCB-MoM program the transmission line in Fig. 7:3 was modelled as two parallel segments with a width of 2 mm and a centre to centre distance of 20 mm. The number of

current elements in each of the two parallel segments was 24 by 4, i.e. four parallel currents in each of the two conductors of the transmission line.

Using transmission line theory the current as a function of the distance from the source was computed with equation 7:1. The characteristic impedance for the transmission line was computed with equation 7:2 (collinear plates) and the voltage reflection coefficient at the open end, Γ_L , was set to unity.

$$I(x) = \frac{V_0}{Z_0(1 + \Gamma_L e^{-j2L\beta})} [e^{-jx\beta} - \Gamma_L e^{j\beta(x-2L)}] \quad (7:1)$$

$$Z_0 = 120 \cdot \ln\left(\frac{4D}{w}\right) \quad (7:2)$$

The current as a function of the position along the transmission line for a few frequencies is shown in Fig. 7:4. As can be seen the agreement between transmission line theory and the PCB-MoM program is good. It should be noted that in the PCB-MoM program the transmission line was modelled with four parallel currents in each of the conductors in order to model the transverse current distribution. With only one current element in the transverse direction the disagreement is slightly larger.

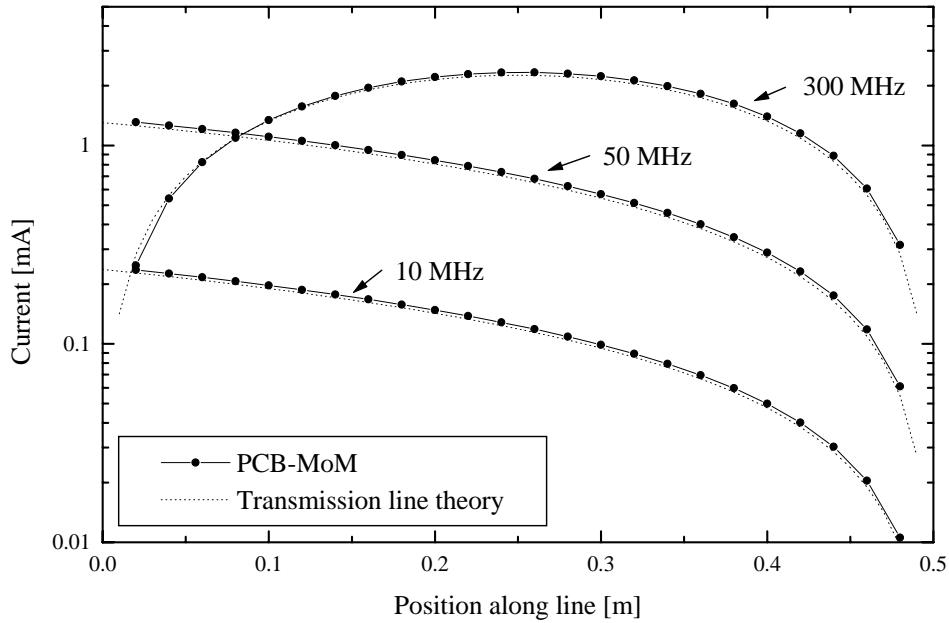


Fig. 7:4. Comparison between transmission line theory and the PCB-MoM program for the open-ended transmission line in Fig. 7:3.

7.2.2 Comparison with transmission line theory - Field induced current in transmission line

As another comparison with transmission line theory the conductor over a ground plane in Fig. 7:5 was considered. The conductor was excited with a plane wave coming from above and with the E-field polarised along the line. The computed quantity was the induced current through one of the terminating resistors.

Using the transmission line theory the per unit length parameters, inductance L and capacitance C , were first computed with LC-Calc [2] a finite difference program. The capacitance was found to be 21.0 pF/m and the inductance 0.53 $\mu\text{H}/\text{m}$. The per unit length parameters were then used in BMTL [3] a finite difference time domain program that solves the transmission line equations. In the BMTL program the conductor was divided into 50 elements and 4096 time steps were used for the computation. This gives a frequency resolution of approx. 3.66 MHz.

In the PCB-MoM program the conductor was divided into 28 current elements along the length and 4 in the transverse direction.

As can be seen from the results in Fig. 7:6 the agreement between the two approaches is good.

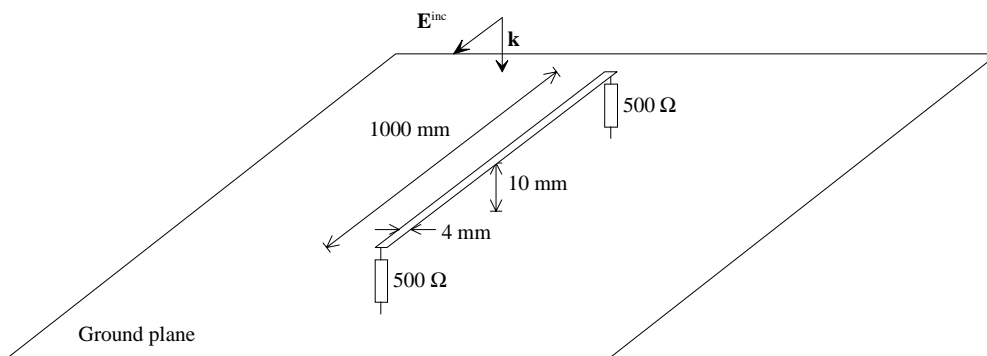


Fig. 7:5. Terminated conductor over ground plane. Excitation with incident plane wave from above with E-field polarised along the line.

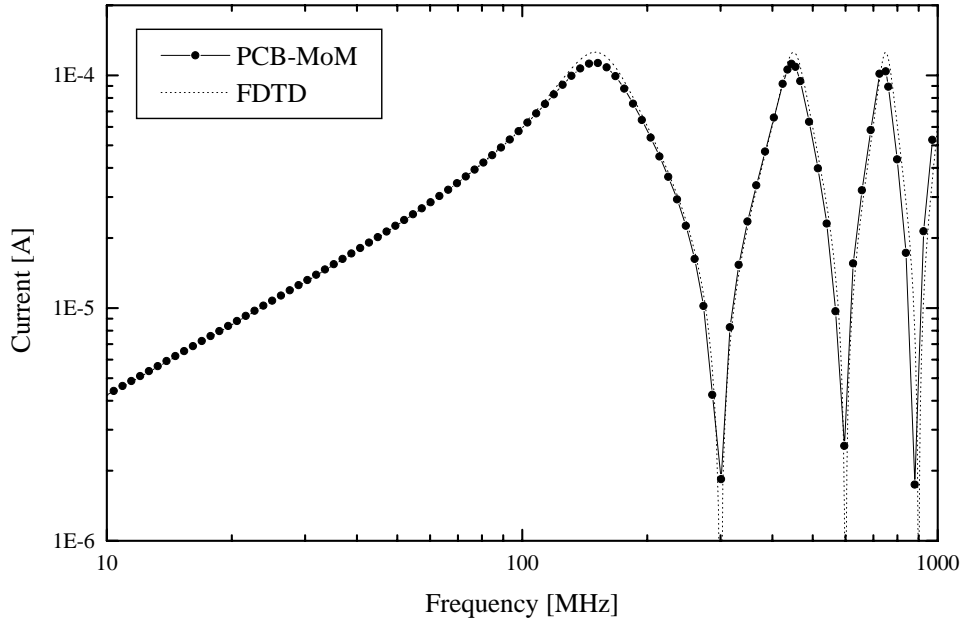


Fig. 7:6. Induced current through one of the load resistances in Fig. 7:5 computed with the PCB-MoM program and with transmission line theory implemented in a FDTD program.

7.2.3 Comparison with multiconductor transmission line theory - Crosstalk

As a comparison with transmission line theory for multiconductor lines the configuration in Fig. 7:7 was considered. One of the lines in Fig. 7:7 was excited with a 1V voltage source and the other ends of both lines were terminated with 1 kOhm resistors. The computed quantity was the current through the R_l resistor in line 2.

Using the multiconductor transmission line theory the per unit length parameters, inductance matrix L and capacitance matrix C , were first computed with LC-Calc [2] a finite difference program. The matrices were found to be:

$$\mathbf{L} = \begin{bmatrix} 0.383 & 0.067 \\ 0.067 & 0.383 \end{bmatrix} [\mu\text{H} / \text{m}], \quad \mathbf{C} = \begin{bmatrix} 30.0 & -5.25 \\ -5.25 & 30.0 \end{bmatrix} [\text{pF} / \text{m}]$$

The per unit length parameters were then used in BMTL [3] a finite difference time domain program that solves the multiconductor transmission lines equations. In the BMTL program the conductors were divided into 50 elements and 8192 time steps were used for the computation. This gives a frequency resolution of approx. 11.4 MHz.

In the PCB-MoM program the conductors were divided into 20 current elements along the length and 4 in the transverse direction.

As can be seen from the results in Fig. 7:8, the agreement is good also for this case.

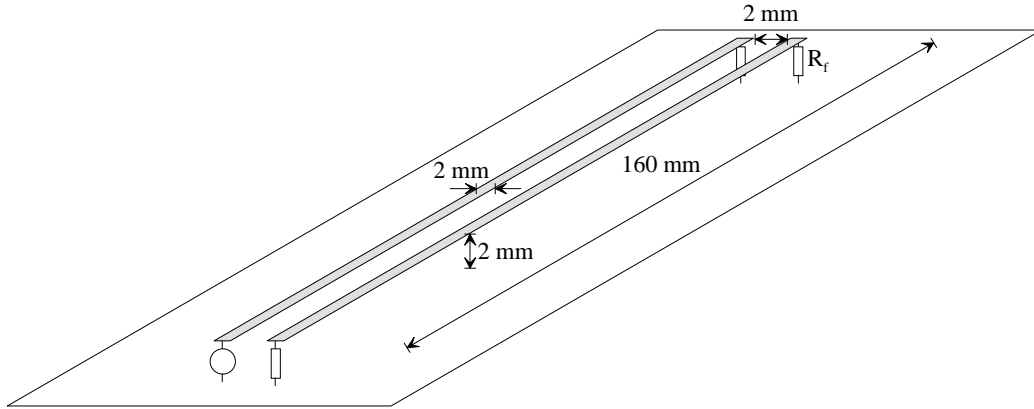


Fig. 7:7. Geometry for computation of crosstalk between two parallel lines that are terminated to a common ground plane. All resistors are 1 kOhm.

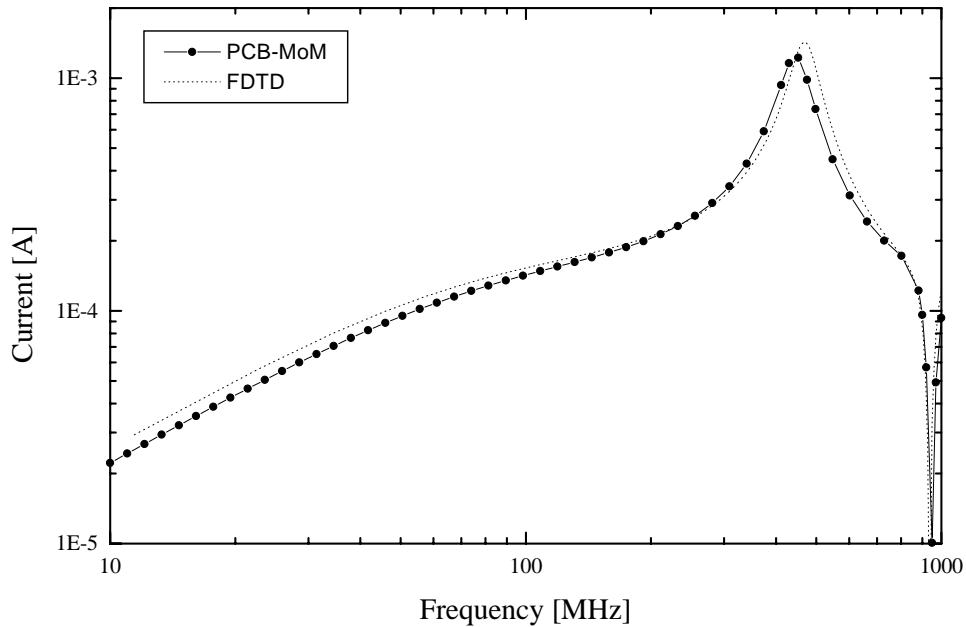


Fig. 7:8. Computed current through the R_f resistor in Fig. 7:7. Computation done with PCB-MoM and with multiconductor transmission line theory implemented in a FDTD program.

7.2.4 Comparison with measurements - Radiation from PCB

As a comparison with measurements a simple PCB with a single 10 MHz clock oscillator was constructed, Fig. 7:9. The radiation from the PCB was measured in a fully anechoic chamber and the result was compared with computations done with PCB-MoM.

For the computation it is necessary to know the output voltage from the clock oscillator at the desired frequencies. The voltage was measured with a spectrum analyzer. Since this measurement is not trivial the uncertainty is quite high and probably explains the disagreement between measurement and simulation. However, it is interesting to note that the overall behaviour of the radiated field is predicted well, Fig. 7:10.

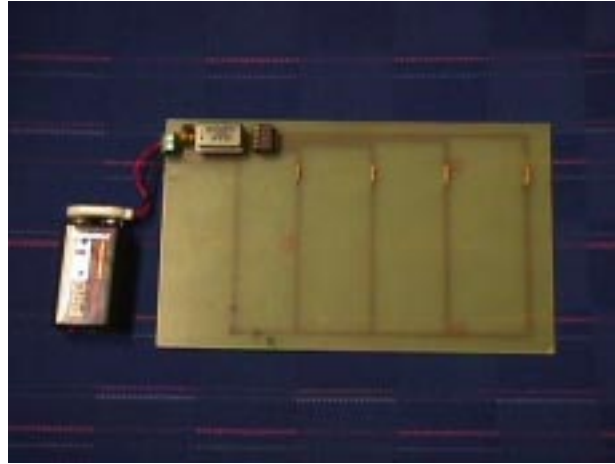


Fig. 7:9. Photograph of the tested PCB.

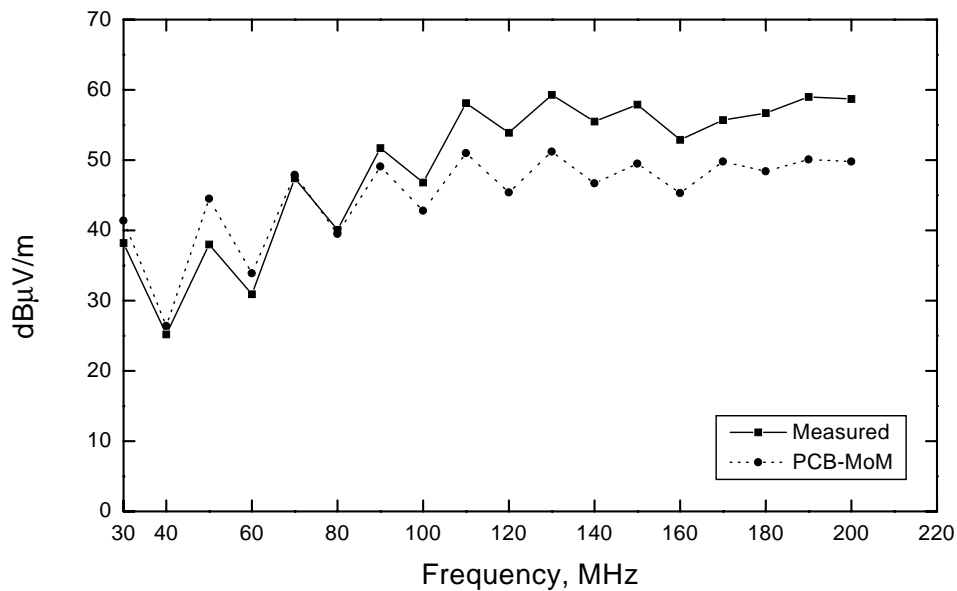


Fig. 7:10. Measured and computed radiation from the PCB in Fig. 7:9.

7.2.5 Comparison with FDTD - Loaded loop

For testing the capability of treating conducting structures on a dielectric substrate the loaded rectangular loop in Fig. 7:11 was analysed. The loop was fed by a voltage generator with an amplitude of 1 Volt and an internal resistance of 50 Ohm. The computed quantity was the current in the feed point and the result was compared with results obtained by the commercial FDTD program XFDTD. As can be seen in Fig. 7:12 the agreement between the two approaches is good. However, it can be noted that the current amplitude predicted by XFDTD around 700 MHz is slightly too large. It should not be higher than 20 mA due to the internal resistance of the source.

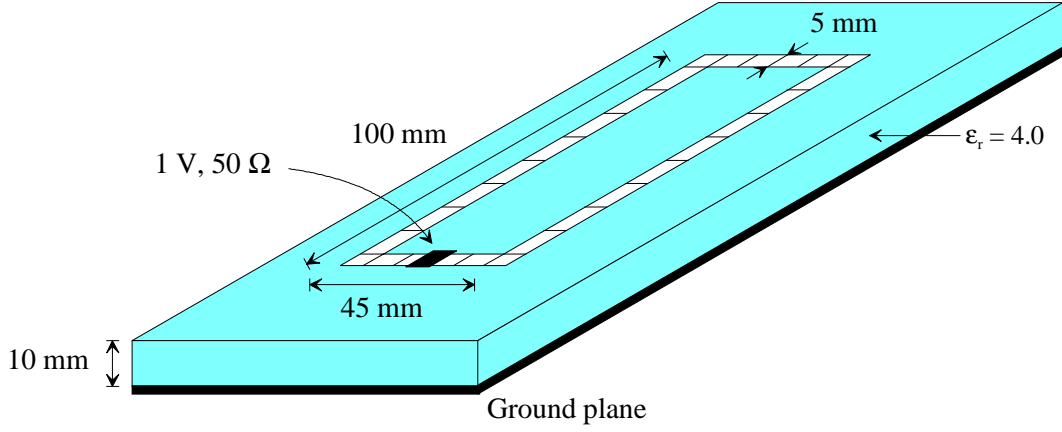


Fig. 7:11. Loaded rectangular loop.

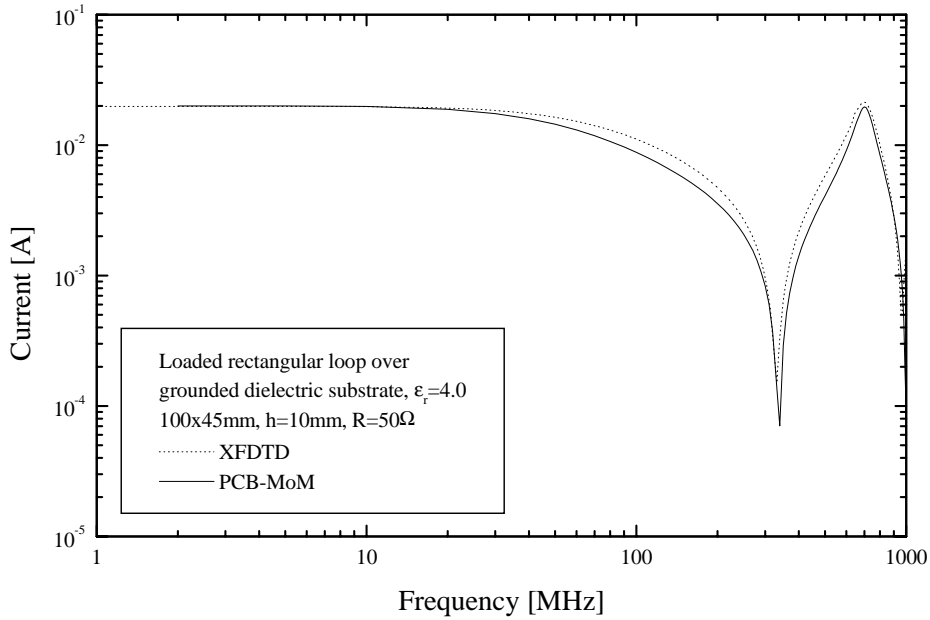


Fig. 7:12. Computed current amplitude at the feed point of the loaded loop in Fig. 7:11. Solid line represents PCB-MoM, dotted line the XFDTD program.

7.3 High frequencies

7.3.1 Near field - Square plate excited with incident plane wave

As a test of the capability of computing the near field the configuration in Fig. 7:13 was considered. The plate was excited with a normal incident plane wave with the E-field polarised along the x-axis. The computed quantities were the total field components E_x and E_z close to the surface of the plate. Since PCB-MoM gives the scattered field when the excitation is an incident field, the total field was computed as: $\mathbf{E}^{\text{tot}} = \mathbf{E}^{\text{scat}} + \mathbf{E}^{\text{inc}}$, where the incident field is given by: $\mathbf{E}^{\text{inc}} = \hat{x}e^{jkz}$. For the computation the plate was divided into 25 by 25 charge elements.

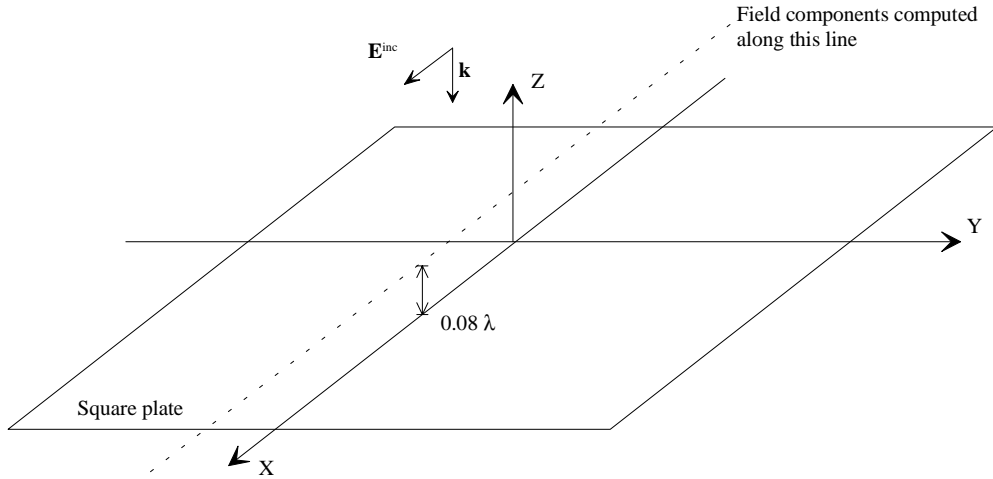


Fig. 7:13. Square plate excited with an incident plane wave. Plate dimension $\lambda \times \lambda$.

The results in Fig. 7:14 and 7:15 compare very well with the results reported in [4] and the results obtained with the FDTD program XFDTD. In [4] two different method of moments programs and a UTD program were used.

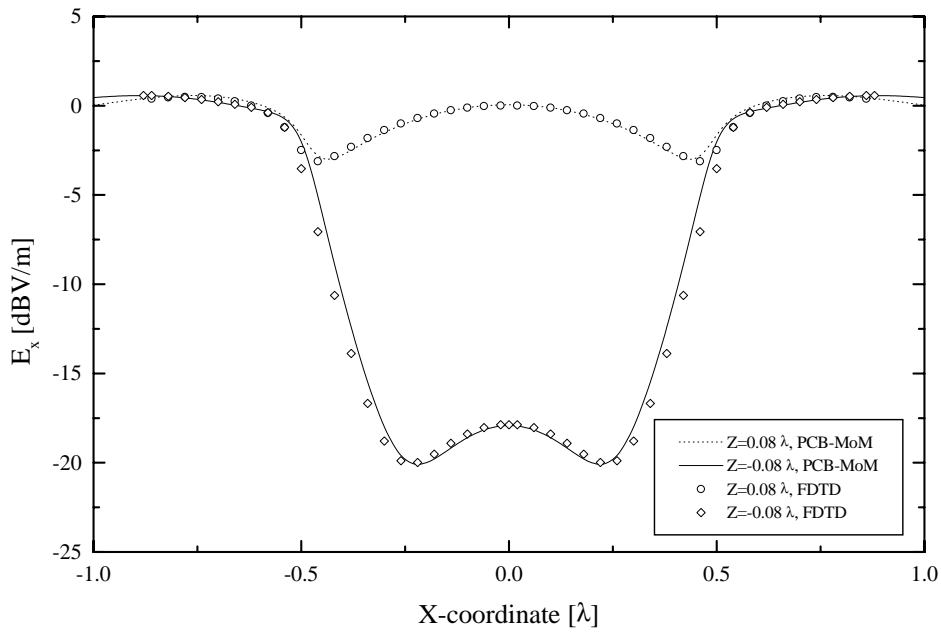


Fig. 7:14. Computed E_x along the lines: $-\lambda < x < \lambda$, $y = 0$, $z = \pm 0.08\lambda$.
Plate defined by: $-\lambda/2 < x, y < \lambda/2$, $z = 0$.

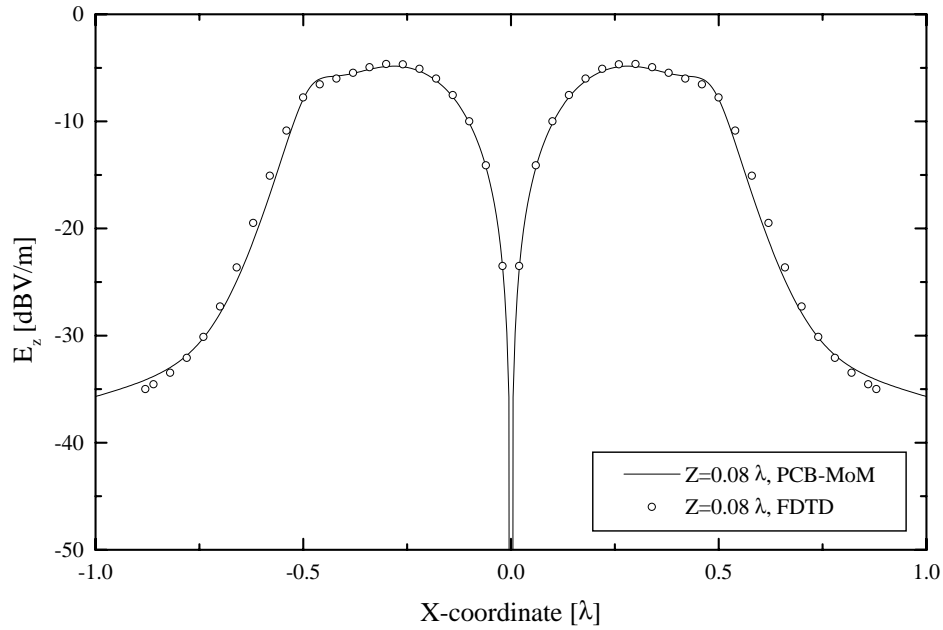


Fig. 7.15. Computed E_z along the line: $-\lambda < x < \lambda$, $y = 0$, $z = 0.08\lambda$.
Plate defined by: $-\lambda/2 < x, y < \lambda/2$, $z = 0$.

7.3.2 Input impedance of printed dipole

As a test of the capability of treating dielectric material the centre fed microstrip dipole in Fig. 7.16 was considered. The length of the dipole was varied and the input impedance at the feed point was calculated.

The following parameters were used:

- Frequency 3 GHz ($\lambda_0 = 100$ mm)
- Width of dipole, $W = 1$ mm
- Length of dipole, $L = 20 - 80$ mm (varied)
- Thickness of dielectric region, $d = 7.96$ mm
- Relative dielectric constant, $\epsilon_r = 3.25$
- Number of current elements 9 and 19, respectively

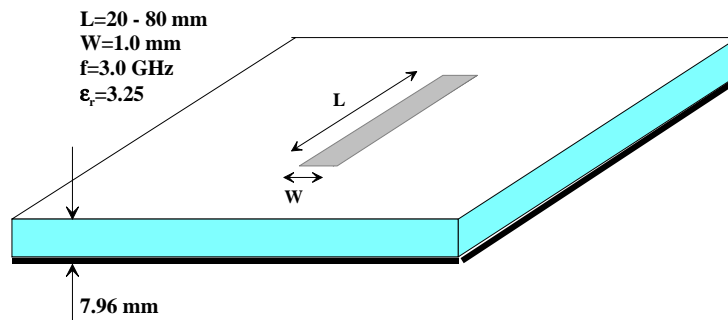


Fig. 7.16. Centre fed microstrip dipole.

The impedance was computed as $Z = U/I$, where U is the excitation voltage and I is the current in the current element where the voltage source is placed.

Fig. 7:17 shows the impedance, real-part and imaginary part, computed by the PCB-MoM program. The agreement is found to be very good with results reported in [5]. It can also be noted that the half and full wavelength resonances are predicted accurately.

Fig. 7:18 shows the convergence of the input impedance as the number of current elements is varied. It can be seen that already for 9 current elements the agreement is good, although the frequency is slightly shifted. Especially, it can be noted that the full wavelength resonance is shifted more than the half wavelength resonance. This is natural since the longer the dipole is in terms of the wavelength, the more elements we need in order to obtain good results.

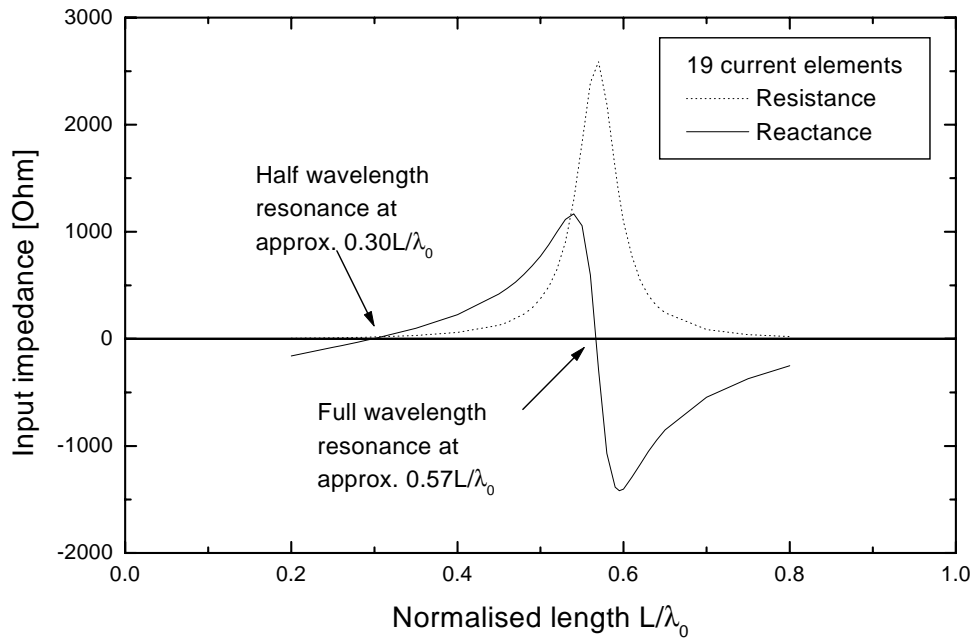


Fig. 7:17. Computed input impedance for the dipole in Fig. 7:16.

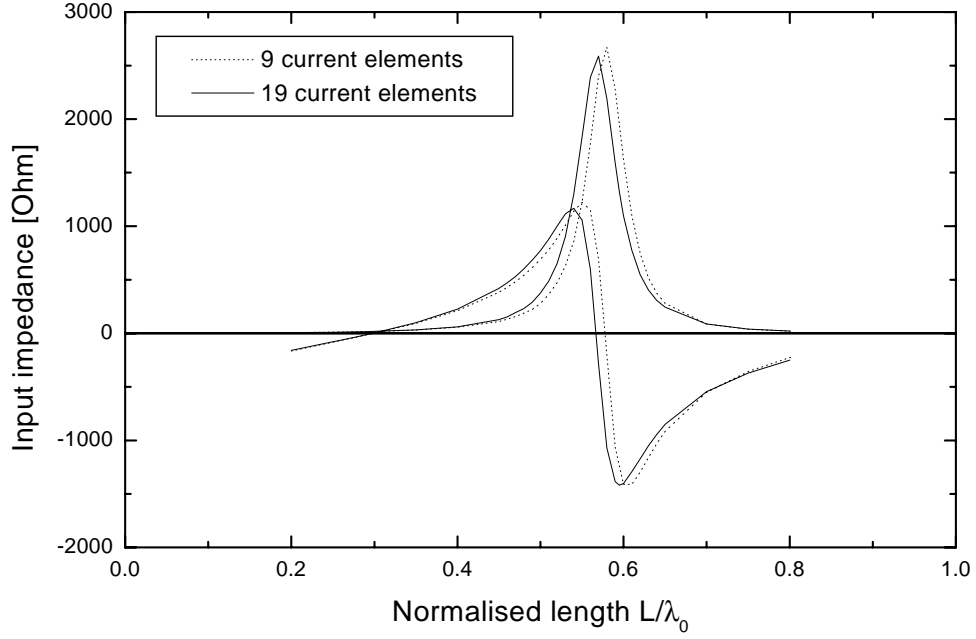


Fig. 7:18. Convergence of the input impedance for the dipole in Fig. 7:16. Number of current elements is 9 and 19, respectively.

7.3.3 Radiation from patch antenna

As a test of the capability of computing the radiation pattern when a dielectric material is present the patch antenna in Fig. 7:19 was considered.

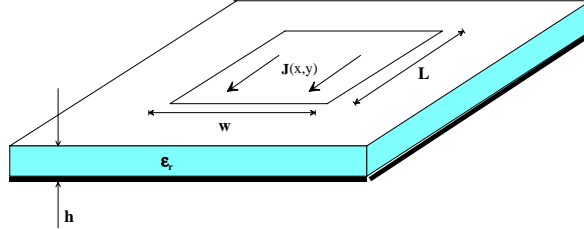


Fig. 7:19. Patch antenna with current only in one direction.

For the computations the length of the patch was chosen according to:

$$L = \frac{\lambda_0}{2\sqrt{\epsilon_{eff}}}$$

$$\text{where } \epsilon_{eff} = \frac{\epsilon_r + 1}{2} + \frac{\epsilon_r - 1}{2\sqrt{1 + \frac{10h}{w}}}$$

and λ_0 is the free space wavelength.

The computed quantity was the normalised power radiation pattern for different dielectric constants and geometries. All results compare very well with results published in [6].

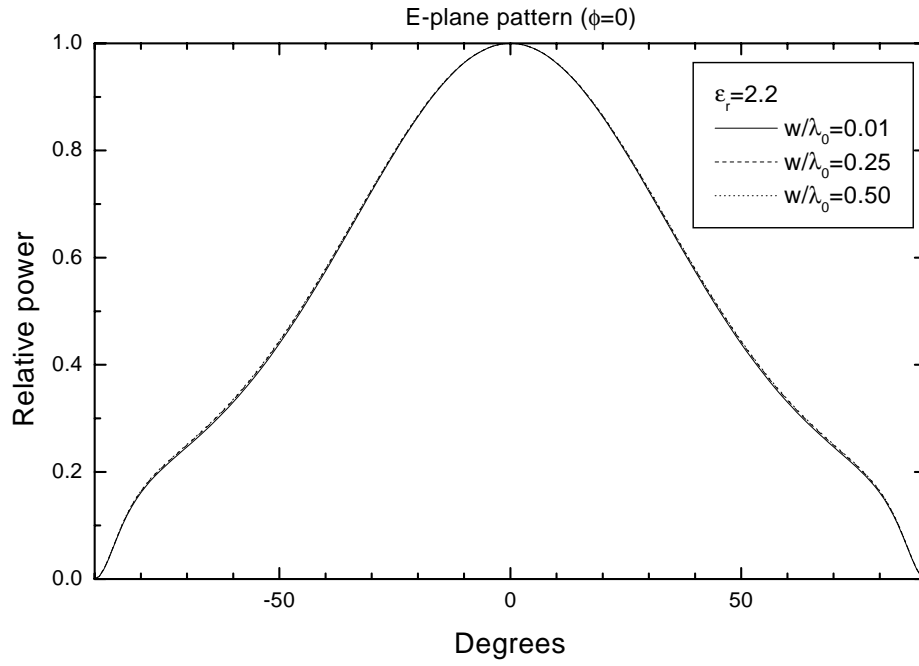


Fig. 7.20. Normalised power radiation pattern in E-plane for three different patch widths. $\epsilon_r = 2.2$. $h = \frac{0.05\lambda_0}{\sqrt{\epsilon_r}}$.

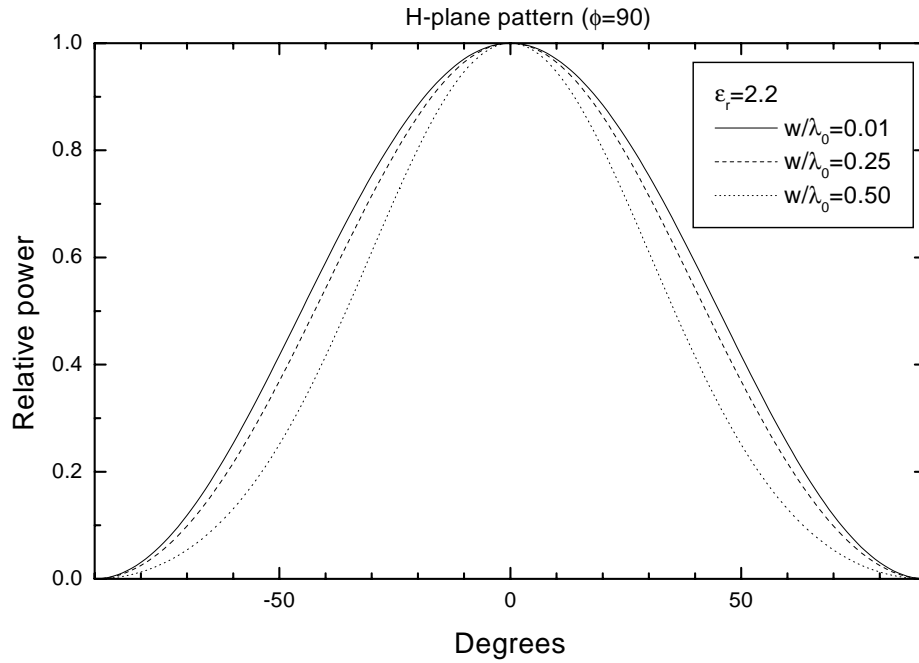


Fig. 7.21. Normalised power radiation pattern in H-plane for three different patch widths. $\epsilon_r = 2.2$. $h = \frac{0.05\lambda_0}{\sqrt{\epsilon_r}}$.

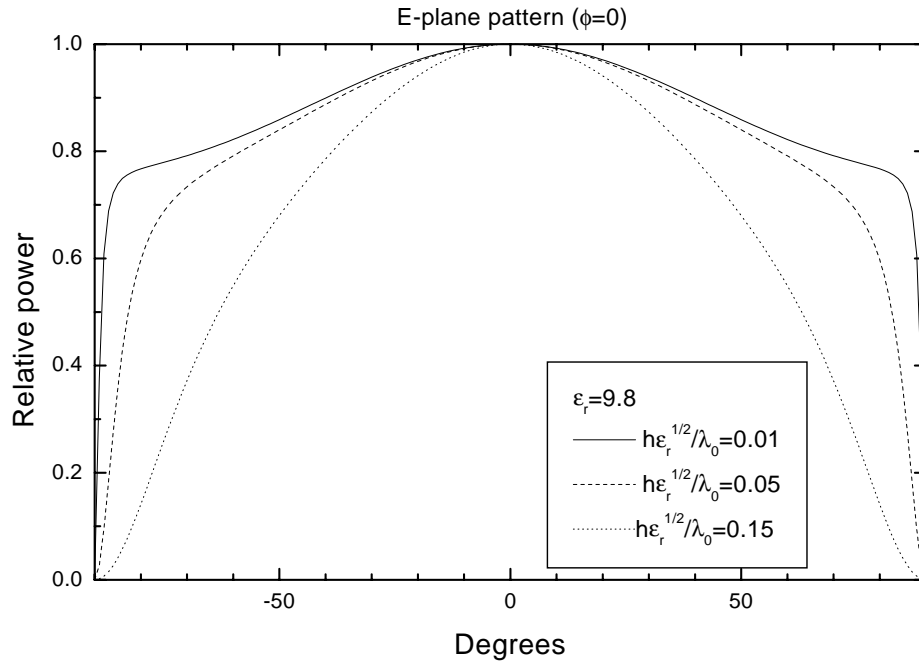


Fig. 7:22. Normalised power radiation pattern in E-plane for three different thickness of the dielectric. $\epsilon_r = 9.8$. $w = 0.4\lambda_0$.

8 Theory

In this chapter the theoretical basis for the PCB-MoM program is explained. We start by formulating the integral equation for the current distribution on a planar conducting structure in free space. After that the integral equation is solved by using the method of moments. We follow the method presented by Glisson & Wilton [1] although the integral equation is slightly different as we treat structures with a finite conductivity instead of perfectly conducting. By letting the finite conductivity be represented by a surface impedance and allowing it to be different at different locations on the structure we are able to model lumped impedance elements. These elements can then serve as models for discrete resistors, inductors and capacitors placed at arbitrary locations. When we have got the solution to the integral equation we start to generalise the formulation so that we also can treat structures above a ground plane, including structures that are connected to the ground plane. In the last step we introduce a dielectric material in-between the ground plane and the structure. This is treated in a different way by Fourier transforming the problem in two orthogonal directions so that we obtain a spectrum of one-dimensional problems instead of one three-dimensional. Thus, we can solve a spectrum of simple one-dimensional problems in the spectral domain and then perform an inverse Fourier transform to obtain the wanted solution for the three-dimensional problem in the spatial domain. We show that the asymptotic part of the inverse Fourier integrals are equal to the elements in the method of moments (MoM) matrix computed in the spatial domain. This fact is then used so that the asymptotic part of the inverse Fourier integrals are computed as the MoM matrix elements in the spatial domain. The main advantage of using this technique is that the only thing we have to do to include a dielectric material is to modify the elements in the MoM matrix, computed in the spatial domain, with a correction factor. The correction factor, which is an inverse Fourier integral, converge fast since the asymptotic part is extracted.

8.1 Current distribution on a planar conducting structure in free space - Integral equation

Consider the case where we have a conducting structure which we subject to an incident electromagnetic field, Fig. 8:1.

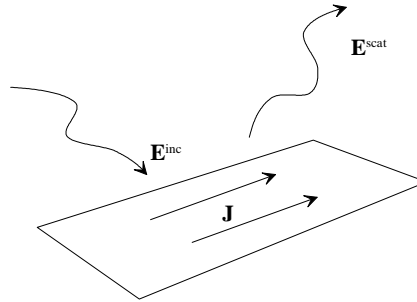


Fig. 8:1. Planar conducting structure subject to an incident electromagnetic field.

Due to the incident field a current will be induced on the surface of the structure and this current will in turn produce a field which we call the scattered field. We denote the incident field as \mathbf{E}^{inc} and the scattered field as \mathbf{E}^{scat} . If the structure is assumed to be a perfect conductor, we know that the tangential component of the electric field at the surface of the structure must vanish. Thus, the following equation follows:

$$(\mathbf{E}^{inc} + \mathbf{E}^{scat})_{\tan} = 0, \text{ at the surface of the structure}$$

If, instead, we assume that the structure is not a perfect conductor, we can then assume that the finite conductivity can be represented with a surface impedance. In this case the above formula has to be modified according to:

$$(\mathbf{E}^{inc} + \mathbf{E}^{scat})_{\tan} = Z_s \mathbf{J}, \text{ at the surface of the structure} \quad (8:1)$$

where Z_s is the surface impedance (in ohms) and \mathbf{J} is the induced surface current density (in A/m) on the structure.

For the case of thin planar conducting structures, we can assume the conducting sheet to be infinitesimal thin and that the current only can flow in two orthogonal directions. Without loss of generality, we can assume the conducting sheet to be placed in the xy-plane and the two orthogonal current directions to be in the x- and y-directions. For this case equation (8:1) can be written as two scalar equations (8:2).

$$\begin{cases} E_x^{inc} + E_x^{scat} = Z_s J_x \\ E_y^{inc} + E_y^{scat} = Z_s J_y \end{cases}, \text{ at the surface of the sheet} \quad (8:2)$$

From any standard text book on electromagnetics, e.g. [7], we can find expressions for the scattered field from a surface current density expressed in terms of a vector and a scalar potential, (8:3).

$$E_x^{scat} = -j\omega A_x - \frac{\partial \Phi}{\partial x}, \quad E_y^{scat} = -j\omega A_y - \frac{\partial \Phi}{\partial y} \quad (8:3)$$

where

$$\begin{cases} A_{x,y} = \frac{\mu}{4\pi} \iint_S J_{x,y} \frac{e^{-jkr}}{r} ds \\ \Phi = \frac{1}{4\pi\epsilon} \iint_S \sigma \frac{e^{-jkr}}{r} ds, \quad \sigma = \frac{j}{\omega} \left(\frac{\partial J_x}{\partial x} + \frac{\partial J_y}{\partial y} \right) \end{cases} \quad (8:4)$$

A is the vector potential, Φ is the scalar potential and σ is the charge density which is related to the current density through the continuity equation. r is the distance between the source point (the current) and the field point. For field points on the surface of the structure r is given by: $r = \sqrt{(x - x')^2 + (y - y')^2}$, where the source point is defined by (x', y') and the field point by (x, y) .

Summing up the expressions, we have the following two coupled (through the continuity equation) integral equations for the current densities:

$$\begin{cases} E_x^{inc} = \frac{j\omega\mu}{4\pi} \iint_S J_x \frac{e^{-jkr}}{r} ds + \frac{\partial}{\partial x} \left[\frac{1}{4\pi\epsilon} \iint_S \sigma \frac{e^{-jkr}}{r} ds \right] + Z_s J_x \\ E_y^{inc} = \frac{j\omega\mu}{4\pi} \iint_S J_y \frac{e^{-jkr}}{r} ds + \frac{\partial}{\partial y} \left[\frac{1}{4\pi\epsilon} \iint_S \sigma \frac{e^{-jkr}}{r} ds \right] + Z_s J_y \end{cases} \quad (8:5)$$

8.2 Solution by the method of moments

In order to solve the coupled integral equations (8:5) we use the method of moments [8] and the same type of basis and test functions as were introduced by Glisson & Wilton [1]. The first step in using the method of moments is to expand the unknowns in series of known basis functions with unknown coefficients. The choice here is to use so called pulse sub-domain basis functions. These functions are unity over a rectangular area and zero elsewhere. Thus, we express the current densities and charge density in the following way:

$$J_x = \sum_{n=1}^N J_{xn} \Pi, \quad J_y = \sum_{m=1}^M J_{ym} \Pi, \quad \sigma = \sum_{i=1}^I \sigma_i \Pi \quad (8:6)$$

where Π represents the two-dimensional pulse function. J_{xn} , J_{ym} and σ_i are the coefficients for the current and charge densities, respectively. The locations of the pulse functions for the current and charge elements are shown in Fig. 8:2.

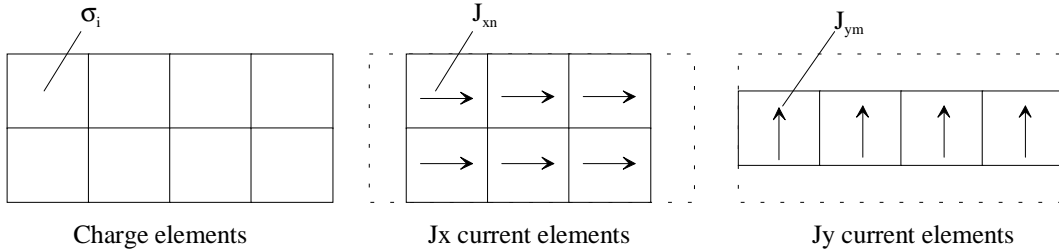


Fig. 8:2. Definition of current and charge elements.

Note in Fig. 8:2 that current elements do not extend all the way out to the edges of the structure. This is because J_x current must be zero at the vertical edges and J_y must be zero at the horizontal edges.

Also note that the charge density can be expressed in terms of the current densities through the continuity equation, (8:4), so the only unknowns are really the current densities. However, we expand the charge density as well in this first step and can later on drop the expansion for the charge density and treat only the current densities, the details follow.

Insertion of the expansions (8:6) in the integral equation (8:5) gives:

$$E_x^{inc}(x, y) = \frac{j\omega\mu}{4\pi} \sum_{n=1}^N J_{xn} F(S_{xn}, r) + \frac{\partial}{\partial x} \left[\frac{1}{4\pi\epsilon} \sum_{i=1}^I \sigma_i F(S_{ci}, r) \right] + Z_s(x, y) J_x(x, y) \quad (8:7)$$

$$E_y^{inc}(x, y) = \frac{j\omega\mu}{4\pi} \sum_{m=1}^M J_{ym} F(S_{ym}, r) + \frac{\partial}{\partial y} \left[\frac{1}{4\pi\epsilon} \sum_{i=1}^I \sigma_i F(S_{ci}, r) \right] + Z_s(x, y) J_y(x, y) \quad (8:8)$$

where $F(S, r) = \iint_S \frac{e^{-jkr}}{r} ds$, S_{xn} represents the area of J_x current element number n , S_{ym} the area of J_y current element number m and S_{ci} the area of charge element number i .

The next step is to define two sets of testing functions, one for equation (8:7) and one for equation (8:8). The choice here is to use functions that are constants along a line in x and y-directions, respectively, Fig. 8:3.

$$T_p = \begin{cases} 1, & \bar{p} \leq x \leq p^+, y = y_p, p = 1 \dots N \\ 0, & \text{elsewhere} \end{cases} \quad (8:9)$$

$$T_q = \begin{cases} 1, & x = x_q, \bar{q} \leq y \leq q^+, q = 1 \dots M \\ 0, & \text{elsewhere} \end{cases} \quad (8:10)$$

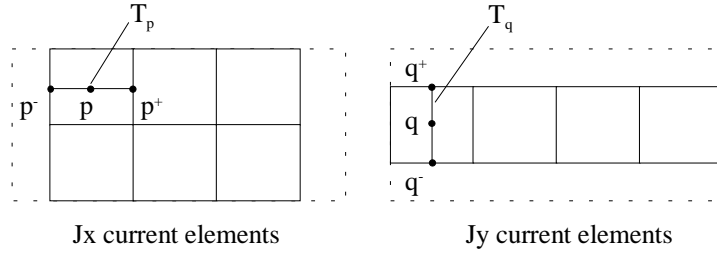


Fig. 8:3. Definition of the test functions T_p and T_q .

The starting point of the test function T_p is denoted by \bar{p} , the centre point by p and the end point by p^+ , see Fig. 8:3. Similar definitions also apply for the test function T_q .

Multiplying equation (8:7) with the test functions (8:9) and integrating over each test function gives:

$$\begin{aligned} \sum_{p=1}^N \int_{\bar{p}}^{p^+} E_x^{inc} T_p dx &= \frac{j\omega\mu}{4\pi} \sum_{p=1}^N \int_{\bar{p}}^{p^+} \sum_{n=1}^N J_{xn} F(S_{xn}, r) T_p dx + \sum_{p=1}^N \int_{\bar{p}}^{p^+} Z_s(x, y) J_x(x, y) T_p dx + \\ &+ \sum_{p=1}^N \int_{\bar{p}}^{p^+} \frac{\partial}{\partial x} \left[\frac{1}{4\pi\epsilon} \sum_{i=1}^I \sigma_i F(S_{ci}, r) \right] T_p dx \end{aligned} \quad (8:11)$$

Multiplying equation (8:8) with the test functions (8:10) and integrating over each test function gives:

$$\begin{aligned} \sum_{q=1}^M \int_{\bar{q}}^{q^+} E_y^{inc} T_q dy &= \frac{j\omega\mu}{4\pi} \sum_{q=1}^M \int_{\bar{q}}^{q^+} \sum_{m=1}^M J_{ym} F(S_{ym}, r) T_q dy + \sum_{q=1}^M \int_{\bar{q}}^{q^+} Z_s(x, y) J_y(x, y) T_q dy + \\ &+ \sum_{q=1}^M \int_{\bar{q}}^{q^+} \frac{\partial}{\partial y} \left[\frac{1}{4\pi\epsilon} \sum_{i=1}^I \sigma_i F(S_{ci}, r) \right] T_q dy \end{aligned} \quad (8:12)$$

Approximating the integration over the test functions by assuming the integrand to be constant over the integration interval gives, for equation (8:11):

$$\begin{aligned} \sum_{p=1}^N \Delta p E_x^{inc}(p) &= \frac{j\omega\mu}{4\pi} \sum_{p=1}^N \Delta p \sum_{n=1}^N J_{xn} F(S_{xn}, r_p) + \sum_{p=1}^N \Delta_{yp} Z_{sp} J_{xp} + \\ &+ \frac{1}{4\pi\epsilon} \sum_{p=1}^N \sum_{i=1}^I \sigma_i \left[F(S_{ci}, r_p^+) - F(S_{ci}, r_p^-) \right] \end{aligned} \quad (8:13)$$

where Δp is the length of the test function T_p given by $\Delta p = p^+ - p^-$, r_p is the distance from the source point (in the element) to the point p and $E_x^{inc}(p)$ means the value of the incident field in the point p . The second term in (8:13) involving the surface impedance can be understood if it is realised that the integration from p^- to p^+ over the impedance term is equal to the voltage drop over the distance from p^- to p^+ ($=\Delta p$). In the expression Z_{sp} is the total impedance in current element p and Δ_{yp} is the transverse dimension (width) of the current element p .

The same approximation for equation (8:12) gives:

$$\begin{aligned} \sum_{q=1}^M \Delta q E_y^{inc}(q) &= \frac{j\omega\mu}{4\pi} \sum_{q=1}^M \Delta q \sum_{m=1}^M J_{ym} F(S_{ym}, r_q) + \sum_{q=1}^M \Delta_{xq} Z_{sq} J_{yq} + \\ &+ \frac{1}{4\pi\epsilon} \sum_{q=1}^M \sum_{i=1}^I \sigma_i \left[F(S_{ci}, r_q^+) - F(S_{ci}, r_q^-) \right] \end{aligned} \quad (8:14)$$

The charge densities are given by the continuity equation (see (8:4)) and can be approximated as:

$$\sigma_i = \frac{j}{\omega} \left(\frac{\partial J_{xi}}{\partial x} + \frac{\partial J_{yi}}{\partial y} \right) \approx \frac{j}{\omega \Delta_{xi}} \left(J_{xi}^+ - J_{xi}^- \right) + \frac{j}{\omega \Delta_{yi}} \left(J_{yi}^+ - J_{yi}^- \right) \quad (8:15)$$

where Δ_{xi} and Δ_{yi} are the lengths of the charge element in x- and y-directions, respectively. J_{xi}^+ and J_{xi}^- are the current coefficients associated with the current elements on the right and the left part of the charge element i , respectively, see Fig. 8:2. J_{yi}^+ and J_{yi}^- are the current coefficients associated with the current elements on the top and the bottom part of the charge element i , respectively. Note that for charge elements at the edge of the structure one or two of the current coefficients are equal to zero.

Insertion of equation (8:15) in (8:13) gives:

$$\begin{aligned} \sum_{p=1}^N \Delta p E_x^{inc}(p) &= \frac{j\omega\mu}{4\pi} \sum_{p=1}^N \Delta p \sum_{n=1}^N J_{xn} F(S_{xn}, r_p) + \sum_{p=1}^N \Delta_{yp} Z_{sp} J_{xp} + \\ &+ \frac{j}{4\pi\omega\epsilon} \sum_{p=1}^N \sum_{i=1}^I \frac{1}{\Delta_{xi}} \left(J_{xi}^+ - J_{xi}^- \right) \left[F(S_{ci}, r_p^+) - F(S_{ci}, r_p^-) \right] + \\ &+ \frac{j}{4\pi\omega\epsilon} \sum_{p=1}^N \sum_{i=1}^I \frac{1}{\Delta_{yi}} \left(J_{yi}^+ - J_{yi}^- \right) \left[F(S_{ci}, r_p^+) - F(S_{ci}, r_p^-) \right] \end{aligned} \quad (8:16)$$

and insertion of equation (8:15) in (8:14):

$$\begin{aligned}
 \sum_{q=1}^M \Delta q E_y^{inc}(q) &= \frac{j\omega\mu}{4\pi} \sum_{q=1}^M \Delta q \sum_{m=1}^M J_{ym} F(S_{ym}, r_q) + \sum_{q=1}^M \Delta_{xq} Z_{sq} J_{yq} + \\
 &+ \frac{j}{4\pi\omega\epsilon} \sum_{q=1}^M \sum_{i=1}^I \frac{1}{\Delta_{xi}} \left(J_{xi}^+ - J_{xi}^- \right) \left[F(S_{ci}, r_q^+) - F(S_{ci}, r_q^-) \right] + \\
 &+ \frac{j}{4\pi\omega\epsilon} \sum_{q=1}^M \sum_{i=1}^I \frac{1}{\Delta_{yi}} \left(J_{yi}^+ - J_{yi}^- \right) \left[F(S_{ci}, r_q^+) - F(S_{ci}, r_q^-) \right]
 \end{aligned} \tag{8:17}$$

The last parts of equations (8:16) and (8:17) contain summations over the index i (i.e. summation over the charge elements). Since the J_{xn} and J_{ym} only are non-zero for indexes $n = 1 \dots N$ and $m = 1 \dots M$, respectively we only have to sum over these ranges. Thus, to get rid of the summations over the index i we change the index to n and m , respectively and also the notation for the surface over which the integration has to be done (i.e. $F(S_{ci}, r)$). It is important to realise that even though the summations can be done over the current elements instead of the charge elements the integrations still have to be done over the surfaces defined by the charge elements. The new notations are, see Fig. 8:4:

Δ_{xcn}^- is the length in the x-direction of the charge element associated with the left part of the current element J_{xn} .

Δ_{xcn}^+ is the length in the x-direction of the charge element associated with the right part of the current element J_{xn} .

S_{cn}^- is the surface of the charge element associated with the left part of the current element J_{xn} .

S_{cn}^+ is the surface of the charge element associated with the right part of the current element J_{xn} .

Similar notations apply for the y-directed currents J_{ym} .

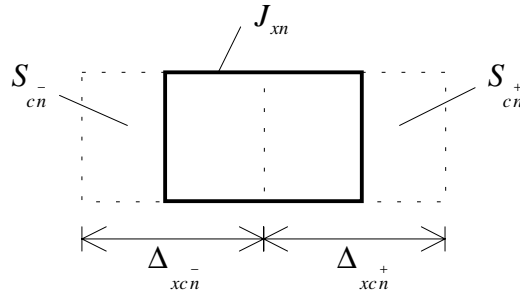


Fig. 8:4. Current elements (J_{xn}) and associated charge elements.

With the change of index and the use of the new notation equations (8:16) and (8:17) can be written as:

$$\begin{aligned}
\sum_{p=1}^N \Delta p E_x^{inc}(p) &= \frac{j\omega\mu}{4\pi} \sum_{p=1}^N \Delta p \sum_{n=1}^N J_{xn} F(S_{xn}, r_p) + \sum_{p=1}^N \Delta_{yp} Z_{sp} J_{xp} + \\
&+ \frac{j}{4\pi\omega\epsilon} \sum_{p=1}^N \sum_{n=1}^N J_{xn} \left\{ \frac{1}{\Delta_{-}^{xcn}} \left[F(S_{cn}^-, r_p^+) - F(S_{cn}^-, r_p^-) \right] - \frac{1}{\Delta_{+}^{xcn}} \left[F(S_{cn}^+, r_p^+) - F(S_{cn}^+, r_p^-) \right] \right\} + \\
&+ \frac{j}{4\pi\omega\epsilon} \sum_{p=1}^N \sum_{m=1}^M J_{ym} \left\{ \frac{1}{\Delta_{-}^{ycm}} \left[F(S_{cm}^-, r_p^+) - F(S_{cm}^-, r_p^-) \right] - \frac{1}{\Delta_{+}^{ycm}} \left[F(S_{cm}^+, r_p^+) - F(S_{cm}^+, r_p^-) \right] \right\}
\end{aligned} \tag{8:18}$$

$$\begin{aligned}
\sum_{q=1}^M \Delta q E_y^{inc}(q) &= \frac{j\omega\mu}{4\pi} \sum_{q=1}^M \Delta q \sum_{m=1}^M J_{ym} F(S_{ym}, r_q) + \sum_{q=1}^M \Delta_{xq} Z_{sq} J_{yq} + \\
&+ \frac{j}{4\pi\omega\epsilon} \sum_{q=1}^M \sum_{n=1}^N J_{xn} \left\{ \frac{1}{\Delta_{-}^{xcn}} \left[F(S_{cn}^-, r_q^+) - F(S_{cn}^-, r_q^-) \right] - \frac{1}{\Delta_{+}^{xcn}} \left[F(S_{cn}^+, r_q^+) - F(S_{cn}^+, r_q^-) \right] \right\} + \\
&+ \frac{j}{4\pi\omega\epsilon} \sum_{q=1}^M \sum_{m=1}^M J_{ym} \left\{ \frac{1}{\Delta_{-}^{ycm}} \left[F(S_{cm}^-, r_q^+) - F(S_{cm}^-, r_q^-) \right] - \frac{1}{\Delta_{+}^{ycm}} \left[F(S_{cm}^+, r_q^+) - F(S_{cm}^+, r_q^-) \right] \right\}
\end{aligned} \tag{8:19}$$

In order to simplify the notation equations (8:18) and (8:19) can be written in matrix form as:

$$\begin{bmatrix} E_x^{inc} \\ E_y^{inc} \end{bmatrix} = \begin{bmatrix} Z_{xx} & Z_{xy} \\ Z_{yx} & Z_{yy} \end{bmatrix} \begin{bmatrix} J_x \\ J_y \end{bmatrix} \tag{8:20}$$

where the matrices are defined by:

$[E_x^{inc}]$ is a column vector with dimension N and the elements: $(E_x^{inc})_p = \Delta p E_x^{inc}(p)$

$[E_y^{inc}]$ is a column vector with dimension M and the elements: $(E_y^{inc})_q = \Delta q E_y^{inc}(q)$

$[J_x]$ is a column vector with dimension N and the elements: $(J_x)_n = J_{xn}$

$[J_y]$ is a column vector with dimension M and the elements: $(J_y)_m = J_{ym}$

$[Z_{xx}]$ is a matrix with dimension N by N and the elements:

$$(Z_{xx})_{pn} = \frac{j\omega\mu}{4\pi} \Delta p F(S_{xn}, r_p) + \Delta_{yp} Z_{sp} + \\ + \frac{j}{4\pi\omega\epsilon} \left\{ \frac{1}{\Delta_{xcn}^-} \left[F(S_{cn}^-, r_p^+) - F(S_{cn}^-, r_p^-) \right] - \frac{1}{\Delta_{xcn}^+} \left[F(S_{cn}^+, r_p^+) - F(S_{cn}^+, r_p^-) \right] \right\}$$

$[Z_{xy}]$ is a matrix with dimension N by M and the elements:

$$(Z_{xy})_{pm} = \frac{j}{4\pi\omega\epsilon} \left\{ \frac{1}{\Delta_{ycm}^-} \left[F(S_{cm}^-, r_p^+) - F(S_{cm}^-, r_p^-) \right] - \frac{1}{\Delta_{ycm}^+} \left[F(S_{cm}^+, r_p^+) - F(S_{cm}^+, r_p^-) \right] \right\}$$

$[Z_{yx}]$ is a matrix with dimension M by N and the elements:

$$(Z_{yx})_{qn} = \frac{j}{4\pi\omega\epsilon} \left\{ \frac{1}{\Delta_{xcn}^-} \left[F(S_{cn}^-, r_q^+) - F(S_{cn}^-, r_q^-) \right] - \frac{1}{\Delta_{xcn}^+} \left[F(S_{cn}^+, r_q^+) - F(S_{cn}^+, r_q^-) \right] \right\}$$

$[Z_{yy}]$ is a matrix with dimension M by M and the elements:

$$(Z_{yy})_{qm} = \frac{j\omega\mu}{4\pi} \Delta q F(S_{ym}, r_q) + \Delta_{xq} Z_{sq} + \\ + \frac{j}{4\pi\omega\epsilon} \left\{ \frac{1}{\Delta_{ycm}^-} \left[F(S_{cm}^-, r_q^+) - F(S_{cm}^-, r_q^-) \right] - \frac{1}{\Delta_{ycm}^+} \left[F(S_{cm}^+, r_q^+) - F(S_{cm}^+, r_q^-) \right] \right\}$$

Note that in the above expressions Z_{sp} and Z_{sq} are non-zero only for $n = p$ and $m = q$, respectively. Thus, the surface impedance effects only the diagonal elements in the matrices.

Now, when all matrices are defined the current density on the structure can be found by inverting the impedance matrix in (8:20).

8.2.1 Integration over self-terms

In order to fill the impedance matrix in (8:20) we have to compute the matrix elements and especially we have to perform the integrations $F(S, r)$. For the case when the observation point, defined by r , is not within the source rectangle, defined by S , the integration can be done numerically without any difficulties. When the observation point is within the source rectangle the integrand becomes infinity (since r in the denominator becomes zero) and special care must be taken. Fortunately, the singularity is integrable and can be treated in the following way.

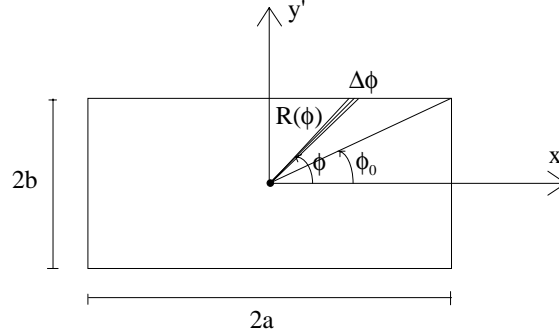


Fig. 8:5. Integration over source rectangle when the observation point is located at the centre of the source rectangle.

The integral $F(S, r)$ for the case shown in Fig. 8:5 is given by:

$$F(S, r) = \int_{-b-a}^b \int_{-a}^a \frac{e^{-jk\sqrt{x'^2+y'^2}}}{\sqrt{x'^2+y'^2}} dx' dy' = 4 \int_0^b \int_0^a \frac{e^{-jk\sqrt{x'^2+y'^2}}}{\sqrt{x'^2+y'^2}} dx' dy'$$

changing to polar coordinates gives:

$$F(S, r) = 4 \int_0^b \int_0^a \frac{e^{-jk\sqrt{x'^2+y'^2}}}{\sqrt{x'^2+y'^2}} dx' dy' = \left\{ \begin{array}{l} r = \sqrt{x'^2+y'^2} \\ dx' dy' = r dr d\phi \end{array} \right\} = 4 \int_0^{\pi/2} \int_0^{R(\phi)} e^{-jkr} dr d\phi \quad (8:21)$$

$$\text{where: } R(\phi) = \begin{cases} \frac{a}{\cos \phi} & , \quad 0 \leq \phi \leq \phi_0 \\ \frac{b}{\sin \phi} & , \quad \phi_0 \leq \phi \leq \pi/2 \end{cases} \quad \text{and } \phi_0 = \arctan\left(\frac{b}{a}\right) \quad (8:22)$$

Approximating the integral (8:21) by a summation over ϕ angles gives:

$$\begin{aligned} F(S, r) &= 4 \int_0^{\pi/2} \int_0^{R(\phi)} e^{-jkr} dr d\phi \approx 4 \sum_{\phi} \Delta\phi \int_0^{R(\phi)} e^{-jkr} dr = 4 \sum_{\phi} \Delta\phi \frac{j}{k} [e^{-jkR(\phi)} - 1] = \\ &= \frac{4}{k} \sum_{\phi} \Delta\phi \left\{ \sin(kR(\phi)) + j[\cos(kR(\phi)) - 1] \right\} \end{aligned} \quad (8:23)$$

The integral given by (8:23) with the definitions given by (8:22) is simple to implement in a computer code.

8.2.2 Excitation with incident plane wave and voltage sources

In order to fill the excitation vectors $[E_x^{inc}]$ and $[E_y^{inc}]$ we have to know the incident electric field in points on the conducting sheet. Assume the conducting sheet to be planar and placed in the xy-plane (same assumption as before) and that the excitation is done by an incident uniform plane wave as shown in Fig. 8:6.

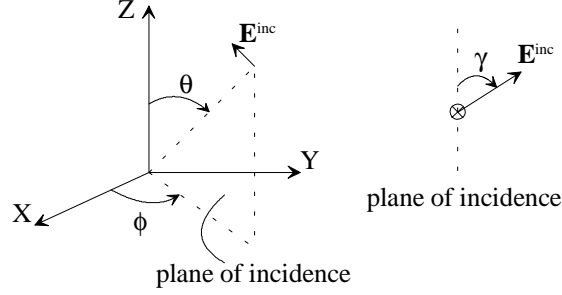


Fig. 8:6. Excitation by an incident uniform plane wave.

The incident uniform plane wave is given by: $\mathbf{E}^{inc}(\mathbf{r}) = \mathbf{E}_0 e^{-j\mathbf{k} \cdot \mathbf{r}}$, where \mathbf{k} is defined by the direction of propagation: $\mathbf{k} = -k(\hat{x} \sin \theta \cos \phi + \hat{y} \sin \theta \sin \phi + \hat{z} \cos \theta)$ and \mathbf{r} is the radius-vector for the evaluation point, $\mathbf{r} = \hat{x}x + \hat{y}y$ ($z = 0$ on the surface of the conducting sheet). Thus, $\mathbf{E}^{inc}(\mathbf{r}) = \mathbf{E}_0 e^{jk \sin \theta (x \cos \phi + y \sin \phi)}$.

The amplitude factor, \mathbf{E}_0 , can be divided into one vertical and one horizontal (with respect to the plane of incidence) component as:
$$\begin{cases} E_v = E_0 \cos \gamma \\ E_h = E_0 \sin \gamma \end{cases}$$

Projecting these components into the xy-plane gives:
$$\begin{cases} -E_v \cos \theta (\hat{x} \cos \phi + \hat{y} \sin \phi) \\ -E_h (\hat{x} \sin \phi - \hat{y} \cos \phi) \end{cases}$$

Summing-up the expressions, the incident electric field in a point (x, y) due to an incident uniform plane wave with polarisation angle γ can be written as:

$$E_0 e^{jk \sin \theta (x \cos \phi + y \sin \phi)} \left[-\hat{x} (\cos \gamma \cos \theta \cos \phi + \sin \gamma \sin \phi) + \hat{y} (\sin \gamma \cos \phi - \cos \gamma \cos \theta \sin \phi) \right]$$

If the excitation is done by a voltage generator instead of an incident field, the component of the excitation matrix is simply equal to the voltage of the generator.

8.2.3 Determination of far-field radiation

In the preceding chapters we have derived expressions for computing the currents on the conductors due to either an incident field or voltage generators placed on the conductors. Another quantity of interest is the field radiated from the structure, i.e. the scattered field. This is especially of interest if the structure is fed by voltage sources in which case the problem simulates e.g. a printed circuit board. The scattered field, both in the near- and the far-field, can be computed with equation (8:3) which involves complicated integrations. If we only are interested in the far-field the computation can be simplified considerably, as is shown in this chapter.

For the case when we have a planar conducting body situated in the xy-plane the far-field radiation can be written as, [7]:

$$\begin{cases} E_r = 0 \\ E_\theta = -\frac{jk\eta}{4\pi} \frac{e^{-jkr}}{r} N_\theta \\ E_\phi = -\frac{jk\eta}{4\pi} \frac{e^{-jkr}}{r} N_\phi \end{cases} \quad (8:24)$$

in V/m at a distance of r from the structure (assumed to be large). To get rid of the distance we normalise the expressions:

$$\begin{cases} E_r^{nor} = 0 \\ E_\theta^{nor} = -\frac{jk\eta}{4\pi} N_\theta \\ E_\phi^{nor} = -\frac{jk\eta}{4\pi} N_\phi \end{cases} \quad (8:25)$$

in Volts, where η is the free-space impedance (120π Ohm) and

$$\begin{cases} N_\theta = \iint_S (J_x \cos\theta \cos\phi + J_y \cos\theta \sin\phi) e^{jkr' \cos\psi} ds \\ N_\phi = \iint_S (-J_x \sin\phi + J_y \cos\phi) e^{jkr' \cos\psi} ds \\ r' \cos\psi = x' \sin\theta \cos\phi + y' \sin\theta \sin\phi \end{cases} \quad (8:26)$$

Insertion of the series expansion for the current densities (8:6) in (8:26) and approximating the integrations gives:

$$\begin{aligned} N_\theta &= \sum_{n=1}^N J_{x_n} \cos\theta \cos\phi \Delta x_n \Delta y_n e^{jk(x_n \sin\theta \cos\phi + y_n \sin\theta \sin\phi)} + \\ &+ \sum_{m=1}^M J_{y_m} \cos\theta \sin\phi \Delta x_m \Delta y_m e^{jk(x_m \sin\theta \cos\phi + y_m \sin\theta \sin\phi)} \end{aligned} \quad (8:27)$$

$$\begin{aligned}
N_\phi = & - \sum_{n=1}^N J_{xn} \sin \phi \Delta x_n \Delta y_n e^{jk(x_n \sin \theta \cos \phi + y_n \sin \theta \sin \phi)} + \\
& + \sum_{m=1}^M J_{ym} \cos \phi \Delta x_m \Delta y_m e^{jk(x_m \sin \theta \cos \phi + y_m \sin \theta \sin \phi)}
\end{aligned} \tag{8:28}$$

where

$x_{n,m}, y_{n,m}$ denotes the centre of J_{xn} and J_{ym} current elements, respectively and $\Delta x_{n,m}, \Delta y_{n,m}$ are the lengths of current elements in x - and y -directions.

So, for every direction, given by θ, ϕ , for which we are interested in the scattered field we have to perform the summations given by (8:27) and (8:28).

8.3 Extension to include a ground plane

In many cases the structure that we want to analyse is placed over a ground plane. If we assume the ground plane to be infinitely large and perfectly conducting we can use image theory to solve the problem. The situation when the structure is placed at a constant height over the ground plane (i.e. the ground plane is placed in the xy-plane) is shown in Fig. 8:7.

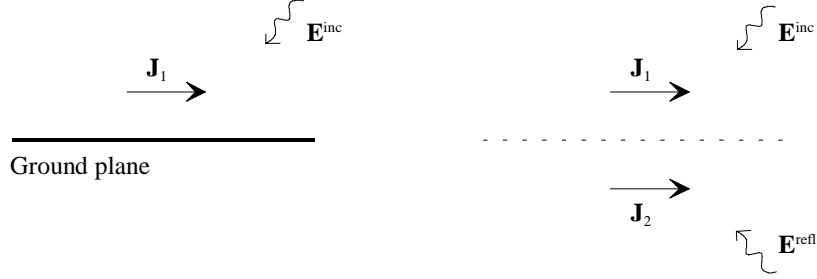


Fig. 8:7. Structure placed over a perfect ground and the equivalent image problem.

Following the same procedure as in the preceding chapters we can directly write down the matrix equation for the equivalent image problem (note that the equivalent problem is only equivalent for the region above the ground plane). The matrix equation becomes:

$$\begin{bmatrix} E_x^{inc} + E_x^{refl} \\ E_y^{inc} + E_y^{refl} \\ E_x^{inc} + E_x^{refl} \\ E_y^{inc} + E_y^{refl} \end{bmatrix} = \begin{bmatrix} [Z_{11}] & [Z_{12}] & [Z_{13}] & [Z_{14}] \\ [Z_{21}] & [Z_{22}] & [Z_{23}] & [Z_{24}] \\ [Z_{31}] & [Z_{32}] & [Z_{33}] & [Z_{34}] \\ [Z_{41}] & [Z_{42}] & [Z_{43}] & [Z_{44}] \end{bmatrix} \begin{bmatrix} J_{x1} \\ J_{y1} \\ J_{x2} \\ J_{y2} \end{bmatrix} \quad (8:29)$$

Where the first row in the matrix equation is associated with testing in x-direction on the currents above the ground plane, the second row with testing in y-direction on the currents above the ground plane, the third row with testing in x-direction on the currents below the ground plane and the fourth row with testing in y-direction on the currents below the ground plane.

Inspecting equation (8:29) it seems like we have four unknown currents but this is not really the case since the following equalities follow from image theory:

$[J_{x2}] = -[J_{x1}]$, $[J_{y2}] = -[J_{y1}]$ and also the excitation on the first row equals the negative of the excitation on the third row and the same is true for the second and fourth row. This means that equation (8:29) can be simplified to:

$$\begin{bmatrix} E_x^{inc} + E_x^{refl} \\ E_y^{inc} + E_y^{refl} \end{bmatrix} = \begin{bmatrix} [Z_{xx} - Z_{xx}^{im}] & [Z_{xy} - Z_{xy}^{im}] \\ [Z_{yx} - Z_{yx}^{im}] & [Z_{yy} - Z_{yy}^{im}] \end{bmatrix} \begin{bmatrix} J_x \\ J_y \end{bmatrix} \quad (8:30)$$

Where the matrices without superscript are the same as before and the matrices with superscript "im" should be computed in the same way as the corresponding matrix without superscript but with the distance changed from $\sqrt{(x-x')^2 + (y-y')^2}$ to

$\sqrt{(x-x')^2 + (y-y')^2 + (2h)^2}$ when evaluating the integrals over the free space Green's function (h is the height of the layout over the ground plane)

In conclusion, what we have to do to take a ground plane into account is to modify the excitation vectors in order to also include the reflected field and modify the MoM-matrix as described above. With this technique the matrix filling time will be approximately doubled and the matrix inversion time will remain the same as for the case without a ground plane.

In order to modify the excitation vectors the following equation is used:

$$E_{x,y}^{inc} + E_{x,y}^{refl} = E_{x,y}^{inc} \left(1 - e^{-j2kh\cos\theta}\right)$$

Also when the far-field is evaluated we have to take the ground plane into account. Since the currents are parallel with the ground plane all we have to do is to multiply with a simple correction factor (the same as for the incident field):

$$CF = 1 - e^{-j2kh\cos\theta}$$

With this correction factor the phase-centre is located on the conducting structure above the ground plane.

8.4 Extension to include connections to the ground plane

Often we have connections between the structure and the ground plane in various points. In order to treat also this problem we consider the equivalent image problem of the preceding chapter. The equivalent image problem of a simple structure connected to the ground plane is shown in Fig. 8:8.

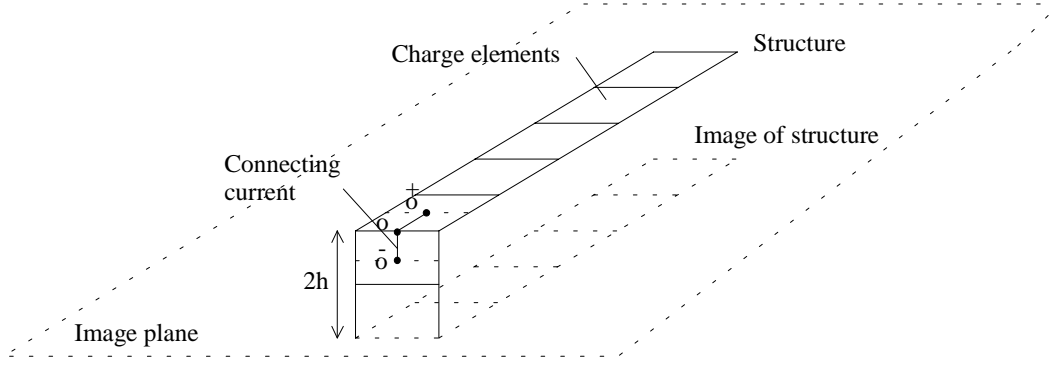


Fig. 8:8. Connection between a simple structure and the ground plane, equivalent image problem. Distance between structure and ground plane is h .

If we assume the distance between the structure and the ground plane to be small, compared to the wavelength, it is sufficient to model the connecting current with only one element as shown in Fig. 8:8 (i.e. we assume the current to be constant). The connecting current flows over the corner, shown in the figure, and can be divided into one z -directed component and one x - or y -directed component, depending on how the connection is done. From image theory it is realised that the z -directed component of the image connecting current (i.e. the current from the image structure to the point \bar{o} in Fig 8:8) is equal to the z -directed component of the connecting current shown in Fig. 8:8 (equal sign as opposed to the x and y -directed components). Therefore, when constructing the equations, as shown below, it is only necessary to take the connecting current (and not the image connecting current) into account and to match in the points \bar{o} , o and o^+ (same as was done when the ground plane was introduced in the preceding chapter). It should also be noted that since the z -directed currents are connected to either x - or y -directed currents a positive reference direction will be either in the positive or the negative z -direction depending on where the ground connection is made. Referring to Fig. 8:8 the shown connecting current will have a reference direction in the positive z -direction. A ground connection in the other end of the strip will support a z -directed current with the reference direction in the negative z -direction.

In order to take a z -directed current connecting the structure to the ground plane into account we have to modify equation (8:30). First we simplify the notation in equation (8:30) so that it becomes:

$$\begin{bmatrix} E_x^{inc,GP} \\ E_y^{inc,GP} \end{bmatrix} = \begin{bmatrix} Z_{xx}^{GP} & Z_{xy}^{GP} \\ Z_{yx}^{GP} & Z_{yy}^{GP} \end{bmatrix} \begin{bmatrix} J_x \\ J_y \end{bmatrix} \quad (8:31)$$

Following the same procedure as in the preceding chapters it is realised that equation (8:31) should be modified to the form in (8:32) in order to take the z-directed currents into account.

$$\begin{bmatrix} E_x^{inc,GP} \\ E_y^{inc,GP} \\ E_z^{inc,GP} \end{bmatrix} = \begin{bmatrix} Z_{xx}^{GP} & Z_{xy}^{GP} & Z_{xz}^{GP} \\ Z_{yx}^{GP} & Z_{yy}^{GP} & Z_{yz}^{GP} \\ Z_{zx}^{GP} & Z_{zy}^{GP} & Z_{zz}^{GP} \end{bmatrix} \begin{bmatrix} J_x \\ J_y \\ J_z \end{bmatrix} \quad (8:32)$$

where the new sub-matrices are defined as, if a total number of O ground connections is assumed:

$[E_z^{inc,GP}]$ is a column vector with dimension O and elements:

$$(E_z^{inc,GP})_u = \Delta_x E_x^{inc,GP}(u) + h E_z^{inc,GP}(u) \text{ and / or } \Delta_y E_y^{inc,GP}(u) + h E_z^{inc,GP}(u)$$

where Δ_x, Δ_y is the length of the connecting current in x and y-direction, respectively

$[J_z]$ is a column vector with dimension O and elements: $(J_z)_o = J_{zxo}$ and / or J_{zyo}

$[Z_{xz}^{GP}]$ is a matrix with dimension N by O and elements:

$$\begin{aligned} (Z_{xz}^{GP})_{po} &= \frac{j\omega\mu}{4\pi} \Delta p \left[F(S_{xo,yo}, r_p) - F(S_{xo,yo}^{im}, r_p) \right] + \\ &+ \frac{j}{4\pi\omega\epsilon} \left\{ \frac{1}{\Delta_{co}^-} \left[F(S_{co}^-, r_p^+) - F(S_{co}^-, r_p^-) - F(S_{co}^{im}, r_p^+) + F(S_{co}^{im}, r_p^-) \right] - \right. \\ &\left. - \frac{1}{\Delta_{co}^+} \left[F(S_{co}^+, r_p^+) - F(S_{co}^+, r_p^-) - F(S_{co}^{im}, r_p^+) + F(S_{co}^{im}, r_p^-) \right] \right\} \end{aligned}$$

where $S_{xo,yo}$ is the area of the x or y-directed component of the current and S_c is the area of the charge elements associated with the current. "im" means integration over the image element, i.e. at the z-coordinate $-2h$.

$[Z_{yz}^{GP}]$ is a matrix with dimension M by O and elements:

$$\begin{aligned} (Z_{yz}^{GP})_{qo} &= \frac{j\omega\mu}{4\pi} \Delta q \left[F(S_{xo,yo}, r_q) - F(S_{xo,yo}^{im}, r_q) \right] + \\ &+ \frac{j}{4\pi\omega\epsilon} \left\{ \frac{1}{\Delta_{co}^-} \left[F(S_{co}^-, r_q^+) - F(S_{co}^-, r_q^-) - F(S_{co}^{im}, r_q^+) + F(S_{co}^{im}, r_q^-) \right] - \right. \\ &\left. - \frac{1}{\Delta_{co}^+} \left[F(S_{co}^+, r_q^+) - F(S_{co}^+, r_q^-) - F(S_{co}^{im}, r_q^+) + F(S_{co}^{im}, r_q^-) \right] \right\} \end{aligned}$$

$[Z_{zx}^{GP}]$ is a matrix with dimension O by N and elements:

$$\begin{aligned}
(Z_{zx}^{GP})_{um} &= \frac{j\omega\mu}{4\pi} \Delta_{x,y} \left[F(S_{xn}, r_u) - F(S_{xn}^{im}, r_u) \right] + \\
&\frac{j}{4\pi\omega\epsilon} \left\{ \frac{1}{\Delta_{xcn}^-} \left[F(S_{cn}^-, r_u^+) - F(S_{cn}^-, r_u^-) - F(S_{cn}^{im}, r_u^+) + F(S_{cn}^{im}, r_u^-) \right] - \right. \\
&\left. - \frac{1}{\Delta_{xcn}^+} \left[F(S_{cn}^+, r_u^+) - F(S_{cn}^+, r_u^-) - F(S_{cn}^{im}, r_u^+) + F(S_{cn}^{im}, r_u^-) \right] \right\}
\end{aligned}$$

$[Z_{zy}^{GP}]$ is a matrix with dimension O by M and elements:

$$\begin{aligned}
(Z_{zy}^{GP})_{um} &= \frac{j\omega\mu}{4\pi} \Delta_{x,y} \left[F(S_{ym}, r_u) - F(S_{ym}^{im}, r_u) \right] + \\
&\frac{j}{4\pi\omega\epsilon} \left\{ \frac{1}{\Delta_{ycm}^-} \left[F(S_{cm}^-, r_u^+) - F(S_{cm}^-, r_u^-) - F(S_{cm}^{im}, r_u^+) + F(S_{cm}^{im}, r_u^-) \right] - \right. \\
&\left. - \frac{1}{\Delta_{ycm}^+} \left[F(S_{cm}^+, r_u^+) - F(S_{cm}^+, r_u^-) - F(S_{cm}^{im}, r_u^+) + F(S_{cm}^{im}, r_u^-) \right] \right\}
\end{aligned}$$

$[Z_{zz}^{GP}]$ is a matrix with dimension O by O and elements:

$$\begin{aligned}
(Z_{zz}^{GP})_{uo} &= \frac{j\omega\mu}{4\pi} \Delta_{x,y} \left[F(S_{xo,yo}, r_u) - F(S_{xo,yo}^{im}, r_u) \right] + \frac{j\omega\mu}{4\pi} h \left[F(S_{zo}, r_u) + F(S_{zo}^{im}, r_u) \right] + \\
&+ \frac{j}{4\pi\omega\epsilon} \left\{ \frac{1}{\Delta_{co}^-} \left[F(S_{co}^-, r_u^+) - F(S_{co}^-, r_u^-) - F(S_{co}^{im}, r_u^+) + F(S_{co}^{im}, r_u^-) \right] - \right. \\
&\left. - \frac{1}{\Delta_{co}^+} \left[F(S_{co}^+, r_u^+) - F(S_{co}^+, r_u^-) - F(S_{co}^{im}, r_u^+) + F(S_{co}^{im}, r_u^-) \right] \right\}
\end{aligned}$$

Note the plus-sign in the second term of $(Z_{zz}^{GP})_{uo}$ which is due to the fact that the image connecting current in the z-direction is of the same sign as the connecting current in the z-direction.

In order to complete the solution also for the case when we have connections to the ground plane we have to compute the z-directed incident field with the presence of a ground plane (for incident field excitation) and also take the z-directed currents into account when we are computing the radiated field in the far-field. Both these tasks are straight forward following the same procedures as described in the preceding chapters.

8.5 Extension to include dielectric material

There exist several different approaches to extend the formulation to include also a dielectric material between the structure and the ground plane. Perhaps, the most natural way is to exchange the free space Green's function (in eq. 8:5) to the Green's function for a grounded dielectric slab. However, this approach requires that slowly converging integrals of Sommerfeld type have to be evaluated. Another approach is to perform a Fourier transform of the structure along the two uniform directions. This will give a spectrum of 1D field problems instead of one 3D field problem. This approach will also result in slowly converging integrals, but as is shown in this chapter the convergence can be speeded up by using the fact that the solution in the preceding chapters (in the spatial domain) is equal to the asymptotic part of these integrals.

The extension presented in this chapter is valid for structures placed on a grounded dielectric substrate. Connections from the structure to the ground plane are not considered.

8.5.1 Strategy

What we would like to do is to modify the elements in the method of moments matrix (the impedance matrix) (8:30) so that a dielectric material between the structure and the ground plane is taken into account. Inspecting the expressions in the preceding chapters that lead to the impedance matrix (8:30), it is realised that the elements can be written as:

$$(Z)_{mn} = - \iint_S \mathbf{E}(\mathbf{J}_n^{ex}) \cdot \mathbf{T}_m dS \quad (8:33)$$

where $\mathbf{E}(\mathbf{J}_n^{ex})$ is the electric field produced by the current element number n , \mathbf{T}_m is the test function number m and S represents the area of the test function (reduced to a line integral for the chosen test functions). Now, by performing a Fourier transformation the impedance elements can be written as:

$$(Z)_{mn} = - \frac{1}{4\pi^2} \int_{-\infty-\infty}^{\infty} \int_{-\infty-\infty}^{\infty} \mathbf{E}(\mathbf{J}_n^{ex}) \cdot \mathbf{T}_m^* dk_x dk_y \quad (8:34)$$

where $\tilde{f}(k_x, k_y) = \iint_S f(x, y) e^{jk_x x} e^{jk_y y} dx dy$ and $*$ denotes complex conjugate. Since we

only have current elements in two orthogonal directions the impedance elements can be written as integrals over scalar functions.

$$(Z_{xx})_{pn} = - \frac{1}{4\pi^2} \int_{-\infty-\infty}^{\infty} \int_{-\infty-\infty}^{\infty} E_x(\mathcal{J}_{xn}^{ex}) \mathcal{T}_{xp}^* dk_x dk_y \quad (8:35a)$$

$$(Z_{xy})_{pm} = - \frac{1}{4\pi^2} \int_{-\infty-\infty}^{\infty} \int_{-\infty-\infty}^{\infty} E_x(\mathcal{J}_{ym}^{ex}) \mathcal{T}_{xp}^* dk_x dk_y \quad (8:35b)$$

$$(Z_{yx})_{qn} = - \frac{1}{4\pi^2} \int_{-\infty-\infty}^{\infty} \int_{-\infty-\infty}^{\infty} E_y(\mathcal{J}_{xn}^{ex}) \mathcal{T}_{yq}^* dk_x dk_y \quad (8:35c)$$

$$(Z_{yy})_{qm} = - \frac{1}{4\pi^2} \int_{-\infty-\infty}^{\infty} \int_{-\infty-\infty}^{\infty} E_y(\mathcal{J}_{ym}^{ex}) \mathcal{T}_{yq}^* dk_x dk_y \quad (8:35d)$$

where \mathbf{T}_{xp} is the x directed test function number p , \mathbf{J}_{xm}^{ex} is the x directed current element number m and similar for the other functions.

We denote the E-field generated by the current element when the grounded dielectric substrate is present as $\mathbf{E}^{diel}(\mathbf{J}_n^{ex})$. This means that we have to determine $\mathbf{E}^{diel}(\mathbf{J}_n^{ex})$ in order to be able to compute the impedance elements (8:35) for the grounded dielectric substrate.

8.5.2 Formulation in the spectral domain

We start by considering a single current element placed on a grounded dielectric substrate, Fig. 8:9.

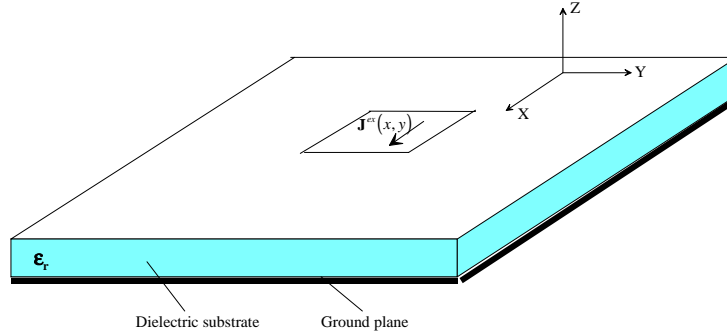


Fig. 8:9. Current element on a grounded dielectric substrate.

If we assume the substrate and the ground plane to be infinite in extent in the x and y directions it is only the current that is not constant in these directions. By expressing the current as a Fourier transform in the k_x, k_y -plane we can view the current as a spectrum of current sheets. These current sheets will have an infinite extent in the x and y directions and a harmonic variation in these directions. Thus, by Fourier transforming the current we have got a spectrum of harmonic 1D field problems instead of the original 3D field problem [9].

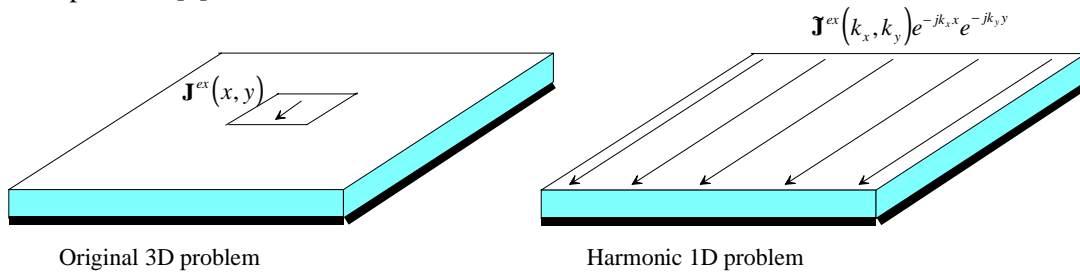


Fig. 8:10. Fourier transform of the original 3D problem to obtain a spectrum of 1D problems.

The current in the spectral domain is expressed as:

$$\mathbf{J}^{ex}(k_x, k_y) = \int_{-\infty-\infty}^{\infty} \int_{-\infty-\infty}^{\infty} \mathbf{J}^{ex}(x, y) e^{jk_x x} e^{jk_y y} dx dy \quad (8:36)$$

This means that

$$\mathbf{J}^{ex}(x, y) = \left(\frac{1}{2\pi} \right)^2 \int_{-\infty}^{\infty} \int_{-\infty}^{\infty} \mathbf{J}^{ex}(k_x, k_y) e^{-jk_x x} e^{-jk_y y} dk_x dk_y \quad (8:37)$$

By approximating the latter Fourier integral we can view it as a superposition of a spectrum of differential currents of the form

$$\Delta \mathbf{J}^{ex}(x, y) = \left(\frac{1}{2\pi} \right)^2 \mathbf{J}^{ex}(k_x, k_y) e^{-jk_x x} e^{-jk_y y} \Delta k_x \Delta k_y \quad (8:38)$$

which are currents in the spatial x,y,z domain with an infinite extent in the x and y directions and a harmonic variation in these directions.

By using the equivalence principle [10, Sec. 3-5] the obtained spectrum of harmonic 1D field problems can be further divided into field problems for homogenous regions. The problem of a current over a grounded dielectric substrate, Fig. 8:10, can be divided into three different homogenous regions: free space, the dielectric region and the ground plane (field equal to zero), Fig. 8:11.

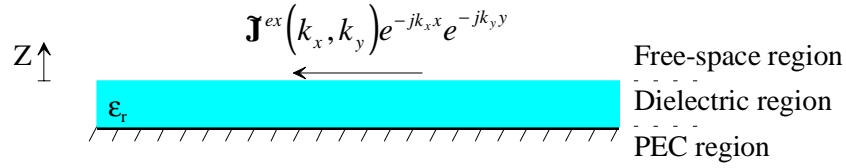


Fig. 8:11. The three-region 1D harmonic field problem.

8.5.3 Solution of the harmonic 1D field problem

Now, when we have the spectrum of harmonic 1D field problems we have to solve these problems in order to be able to compute the elements in the method of moments matrix. We start by determining the solution to the asymptotic problem, i.e. for large $k_x^2 + k_y^2$.

8.5.3.1 Asymptotic solution

In the following we concentrate on the $(Z_{xx})_{pn}$ elements as defined in (8:35a), the other elements can be treated in the same way. This means that we have to determine $\mathbf{E}_x^{diel}(\mathbf{J}_{xn}^{ex})$ in order to be able to compute the impedance elements (8:35a) for the grounded dielectric substrate.

It can be argued that the fields in all layers must have the same harmonic x and y variations as the currents in order to satisfy the boundary conditions at the boundaries of each layer. As stated earlier the three-region problem can be divided into problems for homogenous regions. In doing this equivalent electric and magnetic current sheets are placed at locations where the boundaries between the layers were before. Each current sheet excites two plane waves, one propagating upwards away from the sheet and one downwards away from it. Since we have a multilayer structure we will have a number of transmitted and reflected waves in each layer with propagation constants equal to

k_x, k_y, k_{zn} in the x, y and z directions, respectively. $k_{zn} = \sqrt{k_n^2 - k_x^2 - k_y^2}$ when $k_x^2 + k_y^2 < k_n^2$ and $k_{zn} = -j\sqrt{k_x^2 + k_y^2 - k_n^2}$ when $k_x^2 + k_y^2 > k_n^2$, n denotes the n th layer, $k_n = k_0\sqrt{\epsilon_m\mu_m}$ is the wave number of the n th layer, ϵ_m and μ_m are the relative permittivity and permeability of the n th layer and k_0 is the free-space wave number. Note that the propagation constant in the x and y directions is equal for all layers, which is a consequence of the boundary conditions.

For large $k_x^2 + k_y^2$ the propagation constant in the z direction, k_{zn} , becomes imaginary which means that the fields are strongly evanescent. Thus, the fields decay rapidly in the z direction and this also means that the ground plane under the dielectric cannot be seen. Therefore, it is a reasonable assumption that we for large $k_x^2 + k_y^2$ can approximate the three-region problem by a two-region problem, Fig. 8:12.

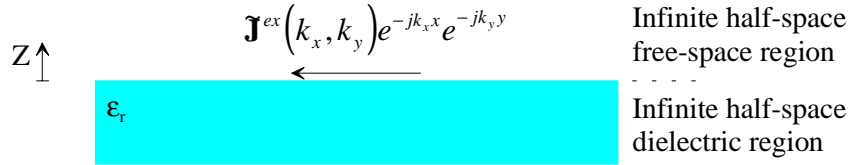


Fig. 8:12. The two-region problem for large $k_x^2 + k_y^2$.

By using the equivalence principle [10, Sec. 3-5] we can obtain equivalent problems for the two-region problem in Fig. 8:12. Since we are aiming at expressions for the impedance elements in (8:35a) we consider the case when $\mathbf{J}^{ex}(x, y) = \hat{x}J_x^{ex}(x, y)$ which means that $\mathbf{J}^{ex}(k_x, k_y) = \hat{x}J_x^{ex}(k_x, k_y)$. We are also only interested in the electric field in the x direction generated by this current.

Equivalent problem for the free-space region, region 0

$$\overleftarrow{\mathbf{J}^{ex}} \quad \overleftarrow{\mathbf{J}} \quad \overleftarrow{\mathbf{M}} \quad \epsilon_0, \mu_0 \text{ in whole space}$$

where $\mathbf{J} = \hat{z} \times \mathbf{H}$ and $\mathbf{M} = \mathbf{E} \times \hat{z}$ are equivalent currents.

Equivalent problem for the dielectric region, region 1

$$\overleftarrow{-\mathbf{J}} \quad \overleftarrow{-\mathbf{M}} \quad \epsilon_r, \mu_r \text{ in whole space}$$

Matching of fields at the boundary between the two regions

The boundary condition at the boundary between the two regions is that the tangential fields (both electric and magnetic) have to be continuous, thus

$$\begin{cases} \mathbf{E}_{x,y}^{0+}(\mathbf{M}) + \mathbf{E}_{x,y}^{0+}(\mathbf{J}) - \mathbf{E}_{x,y}^{1-}(-\mathbf{M}) - \mathbf{E}_{x,y}^{1-}(-\mathbf{J}) = -\mathbf{E}_{x,y}^{0-}(\mathbf{J}^{ex}) \\ \mathbf{H}_{x,y}^{0+}(\mathbf{M}) + \mathbf{H}_{x,y}^{0+}(\mathbf{J}) - \mathbf{H}_{x,y}^{1-}(-\mathbf{M}) - \mathbf{H}_{x,y}^{1-}(-\mathbf{J}) = -\mathbf{H}_{x,y}^{0-}(\mathbf{J}^{ex}) \end{cases} \quad (8:39)$$

where the plus sign in the superscript means that the field is evaluated just above the current sheet and the minus sign just below it. It should be noted that the field from the

current element (excitation current, \mathbf{J}^{ex}) is evaluated just below the current sheet since the current is considered to be placed just above the boundary.

Next we need the field expressions for electric and magnetic current sheets acting in a homogenous region. The field expressions for a harmonic electric current sheet, \mathbf{J} , can be found in [9]. Since we here only are interested in the field just above or just below the current sheet the expressions can be simplified to:

$$\mathbf{E}^\pm(\mathbf{J}) = \frac{-\eta k}{2k_z} [\mathbf{J} - (\mathbf{J} \cdot \hat{k}^\pm) \hat{k}^\pm], \quad \mathbf{H}^\pm(\mathbf{J}) = \frac{k}{2k_z} (\mathbf{J} \times \hat{k}^\pm) \quad (8:40a)$$

and by using duality [10, Sec. 3-2] we have the following expressions for the fields generated by magnetic currents:

$$\mathbf{H}^\pm(\mathbf{M}) = \frac{-k}{2\eta k_z} [\mathbf{M} - (\mathbf{M} \cdot \hat{k}^\pm) \hat{k}^\pm], \quad \mathbf{E}^\pm(\mathbf{M}) = \frac{k}{2k_z} (\mathbf{M} \times \hat{k}^\pm) \quad (8:40b)$$

where $\hat{k}^\pm = (k_x \hat{x} + k_y \hat{y} \pm k_z \hat{z})/k$, $k = k_0 \sqrt{\epsilon_r \mu_r}$, $\eta = \eta_0 \sqrt{\mu_r / \epsilon_r}$ with k_0 and η_0 the wave number and wave impedance of free space, respectively. The plus sign means that the field is evaluated just above the current sheet and the minus sign just below it.

By inserting the field expressions (8:40) in the field matching equations (8:39) we obtain the following system of equations for the equivalent currents:

$$\begin{cases} \mathcal{J}_x \left[k_x^2 \left(1 + \frac{k_{z0}}{\epsilon_r k_{z1}} \right) - k_0^2 \left(1 + \frac{k_{z0}}{k_{z1}} \right) \right] + \mathcal{J}_y k_x k_y \left(1 + \frac{k_{z0}}{\epsilon_r k_{z1}} \right) = -\mathcal{J}_x^{ex} (k_x^2 - k_0^2) \\ \mathcal{J}_x k_x k_y \left(1 + \frac{k_{z0}}{\epsilon_r k_{z1}} \right) + \mathcal{J}_y \left[k_y^2 \left(1 + \frac{k_{z0}}{\epsilon_r k_{z1}} \right) - k_0^2 \left(1 + \frac{k_{z0}}{k_{z1}} \right) \right] = -\mathcal{J}_y^{ex} k_x k_y \\ \mathcal{M}_x \left[k_x^2 \left(1 + \frac{k_{z0}}{k_{z1}} \right) - k_0^2 \left(1 + \epsilon_r \frac{k_{z0}}{k_{z1}} \right) \right] + \mathcal{M}_y k_x k_y \left(1 + \frac{k_{z0}}{k_{z1}} \right) = 0 \\ \mathcal{M}_x k_x k_y \left(1 + \frac{k_{z0}}{k_{z1}} \right) + \mathcal{M}_y \left[k_y^2 \left(1 + \frac{k_{z0}}{k_{z1}} \right) - k_0^2 \left(1 + \epsilon_r \frac{k_{z0}}{k_{z1}} \right) \right] = -k_{z0} \eta_0 k_0 \mathcal{J}_x^{ex} \end{cases}$$

where we have used the fact that $\frac{\eta_1 k_1}{\eta_0 k_0} = 1$ if μ_r is assumed to be unity in both regions.

Since the asymptotic problem was constructed under the assumption that $k_x^2 + k_y^2$ is large we now use this fact and notice that $k_{z0}/k_{z1} \approx 1$, since $k_{z0} = -j\sqrt{k_x^2 + k_y^2 - k_0^2}$ and $k_{z1} = -j\sqrt{k_x^2 + k_y^2 - \epsilon_r k_0^2}$. We also introduce an effective permittivity, $\epsilon_{eff} = \frac{1 + \epsilon_r}{2}$, which leads to the following system of equations:

$$\begin{cases}
\mathcal{J}_x \left[\varepsilon_{eff} k_x^2 - \varepsilon_r k_0^2 \right] + \mathcal{J}_y \varepsilon_{eff} k_x k_y = -\mathcal{J}_x^{ex} \frac{\varepsilon_r}{2} (k_x^2 - k_0^2) \\
\mathcal{J}_x \varepsilon_{eff} k_x k_y + \mathcal{J}_y \left[\varepsilon_{eff} k_y^2 - \varepsilon_r k_0^2 \right] = -\mathcal{J}_x^{ex} \frac{\varepsilon_r}{2} k_x k_y \\
\tilde{\mathcal{M}}_x \left[k_x^2 - \varepsilon_{eff} k_0^2 \right] + \tilde{\mathcal{M}}_y k_x k_y = 0 \\
\tilde{\mathcal{M}}_x k_x k_y + \tilde{\mathcal{M}}_y \left[k_y^2 - \varepsilon_{eff} k_0^2 \right] = -\frac{1}{2} k_{z0} \eta_0 k_0 \mathcal{J}_x^{ex}
\end{cases} \quad (8:41)$$

Solving the system of equations (8:41) gives:

$$\begin{cases}
\mathcal{J}_x = \mathcal{J}_x^{ex} \frac{\varepsilon_r k_x^2 + \varepsilon_{eff} k_y^2 - \varepsilon_r k_0^2}{2(\varepsilon_r k_0^2 - \varepsilon_{eff} k_x^2 - \varepsilon_{eff} k_y^2)} \\
\mathcal{J}_y = \mathcal{J}_x^{ex} \frac{(\varepsilon_r - \varepsilon_{eff}) k_x k_y}{2(\varepsilon_r k_0^2 - \varepsilon_{eff} k_x^2 - \varepsilon_{eff} k_y^2)} \\
\tilde{\mathcal{M}}_x = \mathcal{J}_x^{ex} \frac{\eta_0 k_{z0} k_x k_y}{2\varepsilon_{eff} k_0 (\varepsilon_{eff} k_0^2 - k_x^2 - k_y^2)} \\
\tilde{\mathcal{M}}_y = -\mathcal{J}_x^{ex} \frac{\eta_0 k_{z0} (k_x^2 - \varepsilon_{eff} k_0^2)}{2\varepsilon_{eff} k_0 (\varepsilon_{eff} k_0^2 - k_x^2 - k_y^2)}
\end{cases} \quad (8:42)$$

Once again using that $k_x^2 + k_y^2$ is large and letting $k_x = k_r \cos \phi$ and $k_y = k_r \sin \phi$ the expressions (8:42) can be simplified to:

$$\begin{cases}
\mathcal{J}_x = -\mathcal{J}_x^{ex} \frac{1}{2\varepsilon_{eff}} (\varepsilon_r \cos^2 \phi + \varepsilon_{eff} \sin^2 \phi) \\
\mathcal{J}_y = -\mathcal{J}_x^{ex} \frac{1}{2\varepsilon_{eff}} (\varepsilon_r - \varepsilon_{eff}) \cos \phi \sin \phi \\
\tilde{\mathcal{M}}_x = -\mathcal{J}_x^{ex} \frac{\eta_0 k_{z0}}{2\varepsilon_{eff} k_0} \cos \phi \sin \phi \\
\tilde{\mathcal{M}}_y = \mathcal{J}_x^{ex} \frac{\eta_0 k_{z0}}{2\varepsilon_{eff} k_0 k_r^2} (k_r^2 \cos^2 \phi - \varepsilon_{eff} k_0^2)
\end{cases} \quad (8:43)$$

Now, by using (8:40) we can determine $\tilde{\mathbf{E}}_x^{diel,as}(\mathcal{J}_x^{ex})$ (where the superscript ‘as’ means asymptotic field expression):

$$\begin{aligned}
E_x^{diel,as}(\mathcal{J}_x^{ex}) &= \frac{\eta_0 k_0}{2k_{z0}} \left[(\mathcal{J}_x^{ex} + \mathcal{J}_x) \left(\frac{k_x^2}{k_0^2} - 1 \right) + \mathcal{J}_y \frac{k_x k_y}{k_0^2} \right] - \frac{1}{2} M_y = \\
&= \left\{ (8:43) \text{ and } k_x = k_r \cos \phi, k_y = k_r \sin \phi \right\} = \\
&= \mathcal{J}_x^{ex} \frac{\eta_0}{4\epsilon_{eff} k_0 k_{z0}} \left[(2\epsilon_{eff} - \epsilon_r \cos^2 \phi - \epsilon_{eff} \sin^2 \phi) (k_r^2 \cos^2 \phi - k_0^2) - \right. \\
&\quad \left. - k_r^2 (\epsilon_r - \epsilon_{eff}) \cos^2 \phi \sin^2 \phi - \frac{k_{z0}^2}{k_r^2} (k_r^2 \cos^2 \phi - \epsilon_{eff} k_0^2) \right] = \left\{ \frac{k_{z0}^2}{k_r^2} \approx -1 \right\} = \\
&= \mathcal{J}_x^{ex} \frac{\eta_0}{4\epsilon_{eff} k_0 k_{z0}} \left[(2k_r^2 + k_0^2 (\epsilon_r - \epsilon_{eff})) \cos^2 \phi - 2\epsilon_{eff} k_0^2 \right] = \{k_r \gg k_0\} = \\
&= \mathcal{J}_x^{ex} \frac{\eta_0}{2\epsilon_{eff} k_0 k_{z0}} (k_r^2 \cos^2 \phi - \epsilon_{eff} k_0^2) = \mathcal{J}_x^{ex} \frac{\eta_0}{2\epsilon_{eff} k_0 k_{z0}} (k_x^2 - \epsilon_{eff} k_0^2)
\end{aligned} \tag{8:44}$$

Since $k_{z0} \approx k_{zeff} = -j\sqrt{k_x^2 + k_y^2 - \epsilon_{eff} k_0^2}$ for large $k_x^2 + k_y^2$ (8:44) can be written as:

$$E_x^{diel,as}(\mathcal{J}_x^{ex}) = \mathcal{J}_x^{ex} \frac{\eta_0}{2\epsilon_{eff} k_0 k_{zeff}} (k_x^2 - \epsilon_{eff} k_0^2) \tag{8:45}$$

The expression (8:45) for the electric field generated by the current sheet, \mathcal{J}_x^{ex} , with the dielectric substrate present is exactly the same as the field generated by an electric current sheet acting in a homogenous region with the permittivity ϵ_{eff} . Thus, the asymptotic problem for the three-region problem in Fig. 8:11 can in fact be expressed as a field problem for a homogenous region with a permittivity $\epsilon_{eff} = (1 + \epsilon_r)/2$. In other words, the original three-region problem is reduced to a one-region problem for large $k_x^2 + k_y^2$.

It should be noted that the derived asymptotic field expression (8:45) is valid also when we do not have a ground plane under the dielectric. It can even be used for grounded or ungrounded multilayer structures. For such cases the effective permittivity should be defined by using the permittivity of the uppermost layer (i.e. the layer closest to the current element).

Since we here only are interested in problems having a single layer of dielectric material it is realised that the asymptotic expression (8:45) can be improved for $k_x^2 + k_y^2$ that is not very large by inserting the ground plane again, now in the homogenous region. Especially, in the limit when the permittivity is approaching unity it is realised that by inserting a ground plane the asymptotic expression becomes equal to the exact expression. The effect of the ground plane inserted in the homogenous region can easily be taken into account by using image theory.

It can be argued that the asymptotic problems for the other field components needed in (8:35) (i.e. $E_x^{diel,as}(\mathcal{J}_y^{ex})$, $E_y^{diel,as}(\mathcal{J}_x^{ex})$, $E_y^{diel,as}(\mathcal{J}_y^{ex})$) also can be expressed as field problems for a homogenous region. Thus, we have the following asymptotic field expressions where we have taken the ground plane into account by using image theory:

$$\mathbf{E}_x^{diel,as}(\mathcal{J}_x^{ex}) = \mathcal{J}_x^{ex} \frac{\eta_0}{2\varepsilon_{eff} k_0 k_{zeff}} (k_x^2 - \varepsilon_{eff} k_0^2) (1 - e^{-j2hk_{zeff}}) = \mathbf{E}_{xx}^{diel,as} \mathcal{J}_x^{ex} \quad (8:46a)$$

$$\mathbf{E}_x^{diel,as}(\mathcal{J}_y^{ex}) = \mathcal{J}_y^{ex} \frac{\eta_0}{2\varepsilon_{eff} k_0 k_{zeff}} k_x k_y (1 - e^{-j2hk_{zeff}}) = \mathbf{E}_{xy}^{diel,as} \mathcal{J}_y^{ex} \quad (8:46b)$$

$$\mathbf{E}_y^{diel,as}(\mathcal{J}_x^{ex}) = \mathcal{J}_x^{ex} \frac{\eta_0}{2\varepsilon_{eff} k_0 k_{zeff}} k_x k_y (1 - e^{-j2hk_{zeff}}) = \mathbf{E}_{yx}^{diel,as} \mathcal{J}_x^{ex} \quad (8:46c)$$

$$\mathbf{E}_y^{diel,as}(\mathcal{J}_y^{ex}) = \mathcal{J}_y^{ex} \frac{\eta_0}{2\varepsilon_{eff} k_0 k_{zeff}} (k_y^2 - \varepsilon_{eff} k_0^2) (1 - e^{-j2hk_{zeff}}) = \mathbf{E}_{yy}^{diel,as} \mathcal{J}_y^{ex} \quad (8:46d)$$

where h is the thickness of the dielectric substrate.

The asymptotic expression (8:46a) is the same as used by Pozar [11]. However, we have derived the expression in a different way by using a physical reasoning.

8.5.3.2 Exact solution

In order to complete the solution of the harmonic 1D field problem we need field expressions that are valid for all $k_x^2 + k_y^2$, not just for large values. Such field expressions can be obtained by using the computer routine G1DMULT [12]. This routine is general in the sense that it can be used for multilayer structures, i.e. when we have several layers of dielectric materials. Unfortunately this capability makes the routine relatively slow and since we here only are interested in the case of one layer of dielectric material we use another approach.

Field expressions for a current sheet on a grounded dielectric substrate can be found in the literature, e.g. in [13], and are as follows.

$$\begin{aligned} \mathbf{E}_x^{diel}(\mathcal{J}_x^{ex}) &= -\mathcal{J}_x^{ex} j\eta_0 \sin(k_{ze} h) \frac{(\varepsilon_r k_0^2 - k_x^2) k_{z0} \cos(k_{ze} h) + jk_{ze} (k_0^2 - k_x^2) \sin(k_{ze} h)}{k_0 T_e T_m} = \\ &= \mathbf{E}_{xx}^{diel} \mathcal{J}_x^{ex} \end{aligned} \quad (8:47a)$$

$$\mathbf{E}_x^{diel}(\mathcal{J}_y^{ex}) = \mathcal{J}_y^{ex} \frac{j\eta_0 k_x k_y \sin(k_{ze} h) [k_{z0} \cos(k_{ze} h) + jk_{ze} \sin(k_{ze} h)]}{k_0 T_e T_m} = \mathbf{E}_{xy}^{diel} \mathcal{J}_y^{ex} \quad (8:47b)$$

$$\mathbf{E}_y^{diel}(\mathcal{J}_x^{ex}) = \mathcal{J}_x^{ex} \frac{j\eta_0 k_x k_y \sin(k_{ze} h) [k_{z0} \cos(k_{ze} h) + jk_{ze} \sin(k_{ze} h)]}{k_0 T_e T_m} = \mathbf{E}_{yx}^{diel} \mathcal{J}_x^{ex} \quad (8:47c)$$

$$\begin{aligned} \mathbf{E}_y^{diel}(\mathcal{J}_y^{ex}) &= -\mathcal{J}_y^{ex} j\eta_0 \sin(k_{ze} h) \frac{(\varepsilon_r k_0^2 - k_y^2) k_{z0} \cos(k_{ze} h) + jk_{ze} (k_0^2 - k_y^2) \sin(k_{ze} h)}{k_0 T_e T_m} = \\ &= \mathbf{E}_{yy}^{diel} \mathcal{J}_y^{ex} \end{aligned} \quad (8:47d)$$

where:

$$\begin{aligned}
T_e &= k_{z\varepsilon} \cos(k_{z\varepsilon} h) + jk_{z0} \sin(k_{z\varepsilon} h) \\
T_m &= \varepsilon_r k_{z0} \cos(k_{z\varepsilon} h) + jk_{z\varepsilon} \sin(k_{z\varepsilon} h) \\
k_{z\varepsilon} &= \sqrt{\varepsilon_r k_0^2 - k_x^2 - k_y^2} \text{ when } k_x^2 + k_y^2 < \varepsilon_r k_0^2 \\
k_{z\varepsilon} &= -j\sqrt{k_x^2 + k_y^2 - \varepsilon_r k_0^2} \text{ when } k_x^2 + k_y^2 > \varepsilon_r k_0^2
\end{aligned}$$

8.5.4 Modification of the method of moments matrix

The elements in the method of moments matrix can be written, in the spectral domain, as (8:34):

$$(Z)_{mn}^{diel} = -\frac{1}{4\pi^2} \int_{-\infty}^{\infty} \int_{-\infty}^{\infty} \mathbf{E}^{diel}(\mathbf{J}_n^{ex}) \cdot \mathbf{T}_m^* dk_x dk_y$$

where $\mathbf{E}^{diel}(\mathbf{J}_n^{ex})$ is the electric field produced by the current element number n with the grounded dielectric substrate present. \mathbf{T}_m^* is the test function number m . By using the asymptotic field expressions derived in the preceding chapter the impedance elements can be expressed as:

$$\begin{aligned}
(Z)_{mn}^{diel} &= -\frac{1}{4\pi^2} \int_{-\infty}^{\infty} \int_{-\infty}^{\infty} \mathbf{E}^{diel,as} \cdot \mathbf{T}_m^* dk_x dk_y - \frac{1}{4\pi^2} \int_{-\infty}^{\infty} \int_{-\infty}^{\infty} (\mathbf{E}^{diel} - \mathbf{E}^{diel,as}) \cdot \mathbf{T}_m^* dk_x dk_y = \\
&= (Z)_{mn}^{as} + (Z)_{mn}^{diel-as}
\end{aligned} \tag{8:48}$$

where $\mathbf{E}^{diel,as}$ are the asymptotic field expressions, i.e. expressions (8:46), and \mathbf{E}^{diel} are the exact field expressions, i.e. expressions (8:47).

It was shown in chapter 8.5.3.1 that the asymptotic field expressions (8:46) are equal to the fields generated by a current sheet over a ground plane in a homogeneous region with the permittivity $\varepsilon_{eff} = (1 + \varepsilon_r)/2$. The corresponding problem in the spatial domain is equal to a single current element over a ground plane in a homogeneous region with the same permittivity. This means that the impedance elements $(Z)_{mn}^{as}$ just as well can be computed in the spatial domain and in fact are equal to the impedance elements derived in chapter 8.3. The only difference is that the impedance elements have to be computed with a permittivity equal to $\varepsilon_{eff} = (1 + \varepsilon_r)/2$. Thus, in order to take the grounded dielectric substrate into account we only have to add a correction factor to the impedance elements already computed (using the permittivity $\varepsilon_{eff} = (1 + \varepsilon_r)/2$). The correction factors for the impedance elements are:

$$(Z_{xx})_{pn}^{diel-as} = -\frac{1}{4\pi^2} \int_{-\infty}^{\infty} \int_{-\infty}^{\infty} (\mathbf{E}_{xx}^{diel} - \mathbf{E}_{xx}^{diel,as}) \mathcal{J}_{xn} \mathbf{T}_{xp}^* dk_x dk_y \tag{8:49a}$$

$$(Z_{xy})_{pm}^{diel-as} = -\frac{1}{4\pi^2} \int_{-\infty}^{\infty} \int_{-\infty}^{\infty} (\mathbf{E}_{xy}^{diel} - \mathbf{E}_{xy}^{diel,as}) \mathcal{J}_{ym} \mathbf{T}_{xp}^* dk_x dk_y \tag{8:49b}$$

$$(Z_{yx})_{qn}^{diel-as} = -\frac{1}{4\pi^2} \int_{-\infty-\infty}^{\infty} \int_{-\infty-\infty}^{\infty} (E_{yx}^{diel} - E_{yx}^{diel,as}) \mathcal{J}_{xn} \mathcal{T}_{yq}^* dk_x dk_y \quad (8:49c)$$

$$(Z_{yy})_{qm}^{diel-as} = -\frac{1}{4\pi^2} \int_{-\infty-\infty}^{\infty} \int_{-\infty-\infty}^{\infty} (E_{yy}^{diel} - E_{yy}^{diel,as}) \mathcal{J}_{ym} \mathcal{T}_{yq}^* dk_x dk_y \quad (8:49d)$$

These integrals converge fast since the asymptotic field expressions approach the exact field expressions for large $k_x^2 + k_y^2$.

8.5.5 Computational details

8.5.5.1 Fourier transform of the current basis and test functions

In order to compute the correction factors in (8:49) we must first have the Fourier transforms of the current basis and test functions.

Current basis function

Current basis function is defined, in the spatial domain, as:

$$J(x, y) = \begin{cases} 1, & (x_c - a) < x < (x_c + a), (y_c - b) < y < (y_c + b) \\ 0, & \text{elsewhere} \end{cases}$$

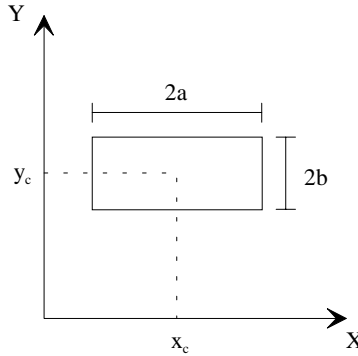


Fig. 8:13. Current basis function.

In the spectral domain the current basis function can be written as:

$$\mathcal{J}(k_x, k_y) = \frac{4}{k_x k_y} \sin(ak_x) \sin(bk_y) e^{j(x_c k_x + y_c k_y)}$$

Test functions

Test functions are defined, in the spatial domain, as:

$$\text{In the } x \text{ direction: } T_x(x, y) = \begin{cases} 1, & (x_t - a) < x < (x_t + a), \quad y = y_t \\ 0, & \text{elsewhere} \end{cases}$$

$$\text{and in the } y \text{ direction: } T_y(x, y) = \begin{cases} 1, & x = x_t, \quad (y_t - b) < y < (y_t + b) \\ 0, & \text{elsewhere} \end{cases}$$

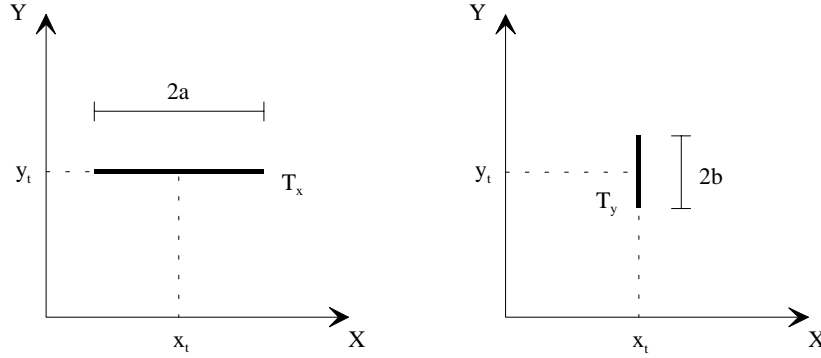


Fig. 8:14. Test functions.

Corresponding expressions in the spectral domain:

$$\mathcal{T}_x(k_x, k_y) = \frac{2}{k_x} \sin(ak_x) e^{j(x_t k_x + y_t k_y)}$$

$$\mathcal{T}_y(k_x, k_y) = \frac{2}{k_y} \sin(bk_y) e^{j(x_t k_x + y_t k_y)}$$

8.5.5.2 Performing the integration

The integration is performed by first changing to polar coordinates, so that:

$$\begin{cases} k_x = k_r \cos \phi \\ k_y = k_r \sin \phi \end{cases} \text{ where } \begin{cases} 0 \leq k_r \rightarrow \infty \\ 0 \leq \phi < 2\pi \end{cases}$$

This means that the integrals (8:49) are converted according to:

$$\int_{-\infty}^{\infty} \int_{-\infty}^{\infty} f(k_x, k_y) dk_x dk_y = \int_0^{\infty} \int_0^{2\pi} f(k_r, \phi) k_r dk_r d\phi$$

Unfortunately, the exact field expressions (8:48) have poles somewhere along the real k_r axis (the poles are located below the axis for a lossy dielectric) which we must avoid. For a lossless dielectric the poles are located in the interval : $k_0 \leq k_r < \sqrt{\epsilon_r} k_0$ [13]. In order to avoid the poles we deform the integration path according to Fig. 8:15.

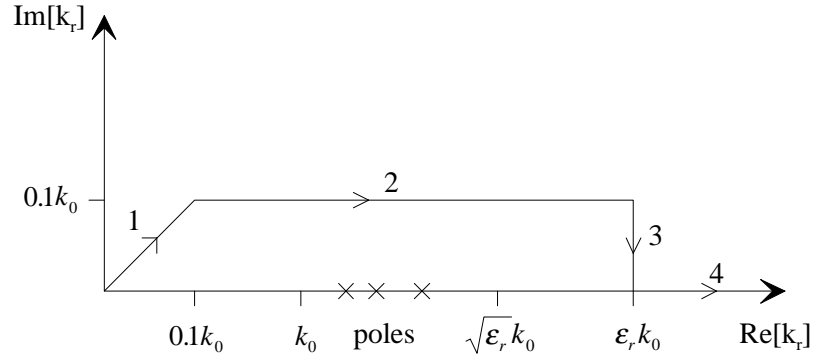


Fig. 8:15. Integration path in the complex k_r plane.

The four paths are described as:

Path 1

$$k_r = 0.1k_0(1+j)t, \quad 0 \leq t \leq 1$$

$$\Rightarrow k_r dk_r = j0.02k_0^2 t dt$$

Path 2

$$k_r = 0.1k_0(1+j) + (\epsilon_r - 0.1)k_0 t, \quad 0 \leq t \leq 1$$

$$\Rightarrow k_r dk_r = (\epsilon_r - 0.1)k_0^2 [0.1(1+j) + (\epsilon_r - 0.1)t] dt$$

Path 3

$$k_r = \epsilon_r k_0 + j0.1k_0(1-t), \quad 0 \leq t \leq 1$$

$$\Rightarrow k_r dk_r = 0.1k_0^2 [0.1(1-t) - j\epsilon_r] dt$$

Path 4

$$k_r, \quad \epsilon_r k_0 \leq k_r \rightarrow \infty$$

8.5.5.3 Symmetry of the integrand

By studying the integrands in (8:49) we find that they have a symmetry in the ϕ angle which we can use to reduce the integration interval in ϕ for path 4. The symmetries for the integrands are shown in Fig. 8:16 and 8:17.

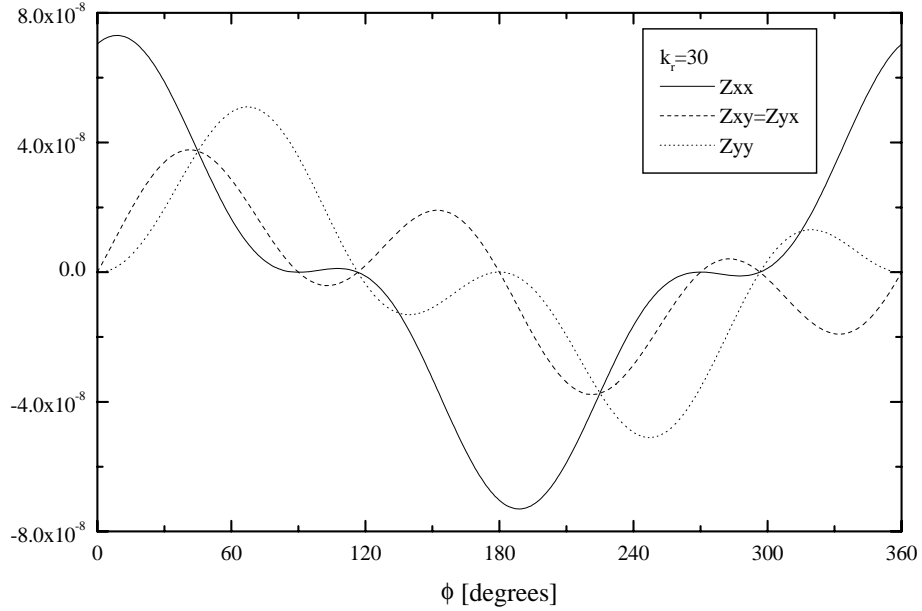


Fig. 8:16. Symmetry of real-part of integrands in ϕ . Square current element 5 x 5 mm. Length of test function 5 mm. Distance between current and test functions: $r_x = 10$, $r_y = 5$ mm. $\epsilon_r = 4$, $h = 2$ mm, $f = 300$ MHz.

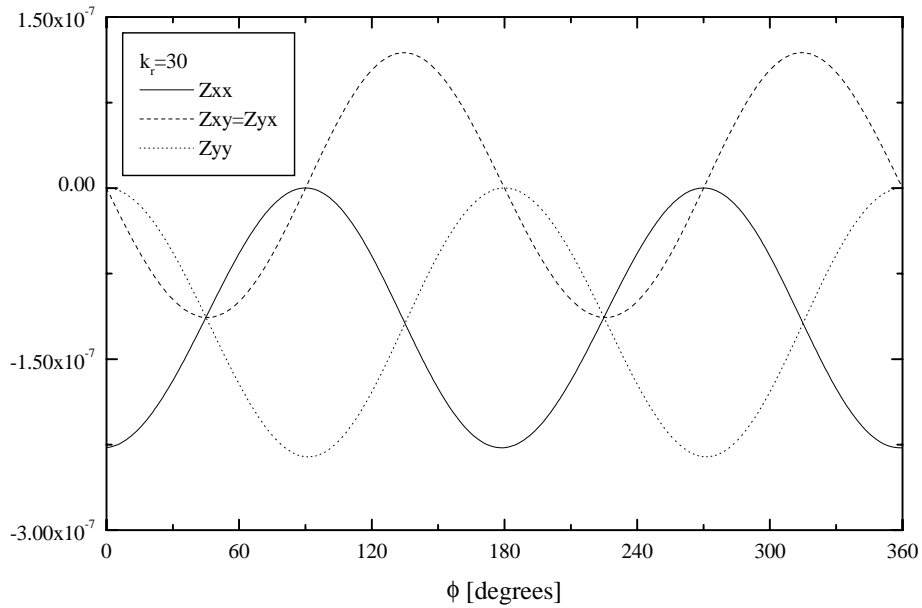


Fig. 8:17. Symmetry of imaginary-part of integrands in ϕ . Square current element 5 x 5 mm. Length of test function 5 mm. Distance between current and test functions: $r_x = 10$, $r_y = 5$ mm. $\epsilon_r = 4$, $h = 2$ mm, $f = 300$ MHz.

Based upon the above observations the integrals along path 4 can be written as:

$$\int_0^{2\pi} \int_{\varepsilon_r k_0}^{\infty} f(k_r, \phi) k_r dk_r d\phi = j2 \int_0^{\pi} \int_{\varepsilon_r k_0}^{\infty} \text{Im}[f(k_r, \phi)] k_r dk_r d\phi$$

and the real-part is equal to zero.

8.5.5.4 Oscillation of the integrand

All integrands in (8:49) contain the product of the current basis and test functions. The phase factor of this product is:

$e^{j[k_x(x_c - x_t) + k_y(y_c - y_t)]} = e^{j(k_x r_x + k_y r_y)}$ where $r = \sqrt{r_x^2 + r_y^2}$ is the distance between the centre of the current element and the test function. The phase factor can be written as $e^{jk_r(r_x \cos \phi + r_y \sin \phi)}$ from which it is clear that the integrand will oscillate along the k_r axis with a period given by:

$$\text{Period} = \frac{2\pi}{r_x \cos \phi + r_y \sin \phi}$$

In performing the integration it is important to have enough sampling points in order to resolve the variations in the integrand. It is noted that the period will be smaller the longer the distance between the current element and the test function. Thus, more sampling points are needed when the distance is large.

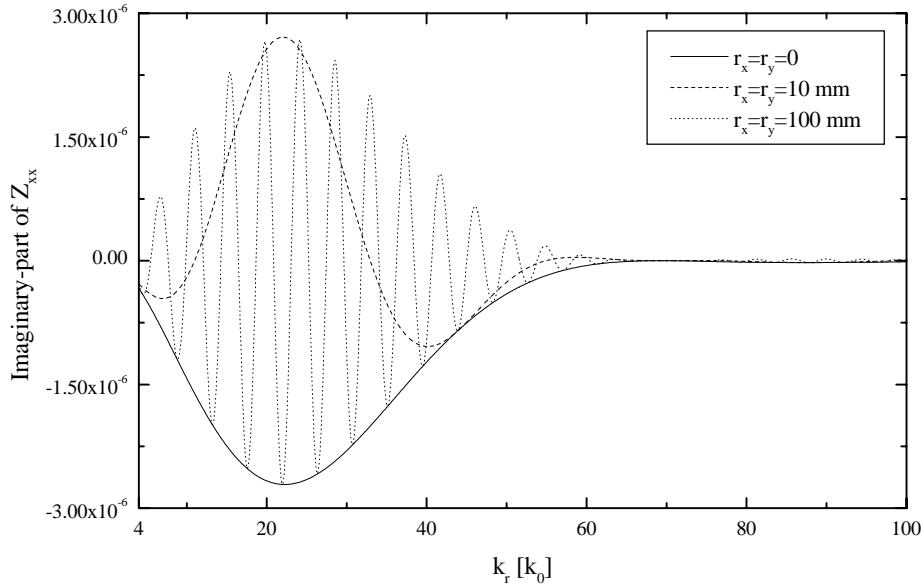


Fig. 8:18. Imaginary-part of integrand (Z_{xx}) for different distances between current and test functions. Frequency 500 MHz. Square current element 5 x 5 mm. Length of test function 5 mm. $\varepsilon_r = 4$, $h = 2$ mm, $\phi = \pi/6$.

8.5.5.5 Upper limit for integration

The upper integration limit for k_r along path 4 is infinity. Fortunately, the integrands decay rapidly so that we can terminate the integration for some (large) k_r . However, as can be seen in Fig. 8:19-21 the value of k_r when the integration can be terminated will depend on several parameters (permittivity, frequency, thickness of dielectric etc.). Thus, we need a way to determine the value of k_r when we can terminate the integration. Studying the behaviour of the absolute value of the integrands as a function of k_r it is noted that the first maximum of the integrand of $(Z_{xx})_{11}$ (i.e. the self-term) always is the largest. The following maxima are decreasing in amplitude. It is also noted that the first maximum can not always be found in path 4. For these cases the first value (i.e. for $k_r = \epsilon_r k_0$) is the largest (see e.g. Fig. 8:19 for 4 GHz).

The strategy for determining the upper limit will therefore be as follows:

- Search for the first maximum of $Abs[(Z_{xx})_{11}] = A_0$
- Search for following maxima A_n and determine upper limit $k_{r,max}$ when $\frac{A_n}{A_0} = factor$

The PCB-MoM program follows this strategy and searches for the first maximum and then for subsequent maxima until the quotient A_n/A_0 is less than a user specified value.

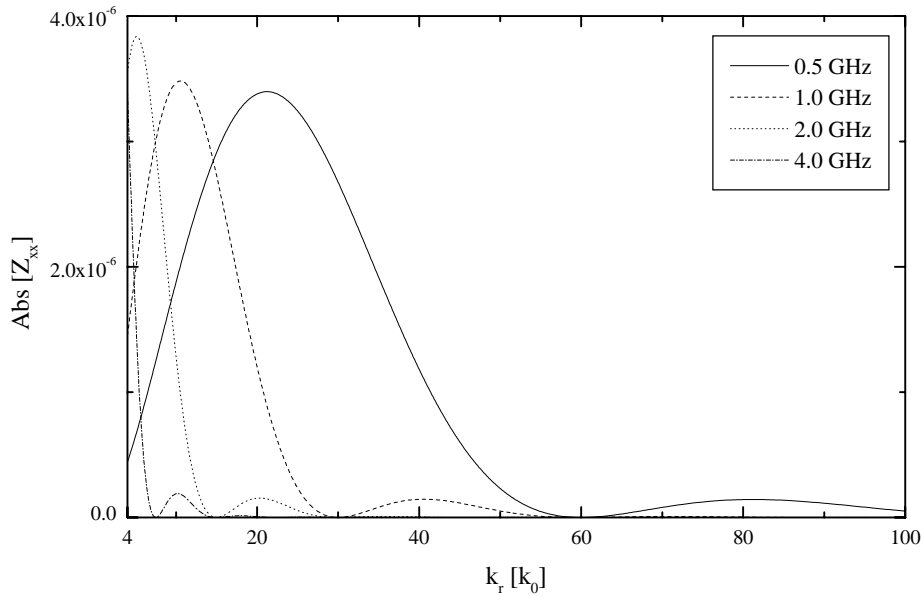


Fig. 8:19. Behaviour of the integrand for the self-terms in Z_{xx} for large k_r as a function of frequency. Square current element 5 x 5 mm.
 $\epsilon_r = 4$, $h = 2$ mm, $\phi = 0$.

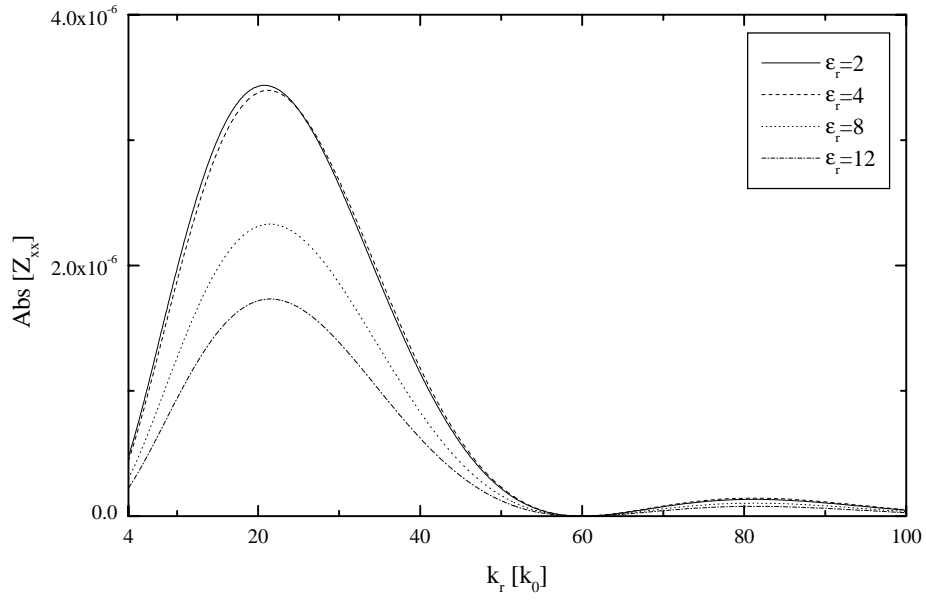


Fig. 8:20. Behaviour of the integrand for the self-terms in Z_{xx} for large k_r as a function of the permittivity. Square current element 5 x 5 mm. $h = 2$ mm, $f = 500$ MHz, $\phi = 0$.

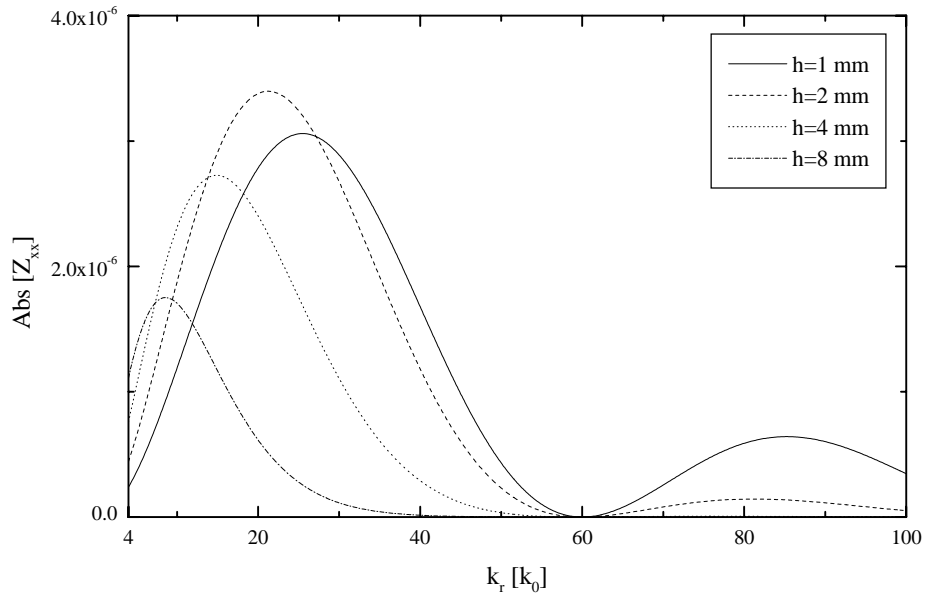


Fig. 8:21. Behaviour of the integrand for the self-terms in Z_{xx} for large k_r as a function of the thickness of the dielectric. Square current element 5 x 5 mm. $\epsilon_r = 4$, $f = 500$ MHz, $\phi = 0$.

8.5.5.6 Determination of far-field radiation

The radiation field for the grounded dielectric substrate can directly be obtained from the spectral domain solution as [14]:

$$E_{\theta}^{nor}(\theta, \phi) = \frac{jk_0}{2\pi} \left(\tilde{E}_x(k_x, k_y) \cos \phi + \tilde{E}_y(k_x, k_y) \sin \phi \right)$$

$$E_{\phi}^{nor}(\theta, \phi) = \frac{jk_0}{2\pi} \left(-\tilde{E}_x(k_x, k_y) \cos \theta \sin \phi + \tilde{E}_y(k_x, k_y) \cos \theta \cos \phi \right)$$

where $\begin{cases} \frac{1}{r} e^{-jk_0 r} \text{ has been suppressed} \\ k_x = k_0 \sin \theta \cos \phi \\ k_y = k_0 \sin \theta \sin \phi \end{cases}$

and

- \tilde{E}_x due to \mathcal{J}_x is computed by (8:47a)
- \tilde{E}_x due to \mathcal{J}_y is computed by (8:47b)
- \tilde{E}_y due to \mathcal{J}_x is computed by (8:47c)
- \tilde{E}_y due to \mathcal{J}_y is computed by (8:47d)

8.5.5.7 Excitation with incident plane wave

In order to fill the excitation vector for the case of a grounded dielectric substrate we must be able to compute the E_x and E_y on the surface of the dielectric. By using reciprocity [10, Sec. 3-8] this can be done by using the formulation for the radiation field (8.5.5.6) as is described in the following.

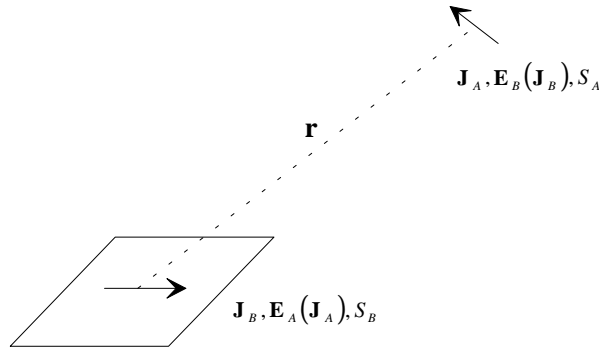


Fig. 8:22. Illustration of reciprocity.

The reciprocity relation is:
$$\iint_{S_B} \mathbf{E}_A(\mathbf{J}_A) \cdot \mathbf{J}_B dS = \iint_{S_A} \mathbf{E}_B(\mathbf{J}_B) \cdot \mathbf{J}_A dS$$

By letting $r \rightarrow \infty$ \mathbf{E}_A and \mathbf{E}_B will be plane waves, i.e. we can think of \mathbf{E}_A as the wanted excitation by the incident plane wave. Also, \mathbf{E}_B can be computed as the radiation

field. The term $\iint_{S_B} \mathbf{E}_A(\mathbf{J}_A) \cdot \mathbf{J}_B dS$ is equal to the elements in the excitation vectors if the current \mathbf{J}_A is adjusted to produce the wanted incident plane wave. \mathbf{J}_B corresponds to the test function.

Now, we let \mathbf{J}_A be a short current element with the dipole moment $I\mathbf{l}$ aligned perpendicular to the direction of the incident field θ, ϕ . If this short dipole should produce a plane wave (far away from the source) with the amplitude E_0 the dipole moment must be [10, Sec. 2-9]: $I\mathbf{l} = -E_0 \frac{4\pi}{j\mu_0\omega} \frac{r}{e^{-jk_0r}}$ (the minus sign comes from the direction of radiation, i.e. $\theta + \pi$). Insertion in the right-hand side of the reciprocity relation gives:

$$\iint_{S_A} \mathbf{E}_B(\mathbf{J}_B) \cdot \mathbf{J}_A dS = -\frac{4\pi}{j\mu_0\omega} \mathbf{E}_B^{nor}(\mathbf{J}_B) \cdot \mathbf{E}_0$$

By also taking the polarisation angle, γ , (see Fig. 8:6) into consideration the elements in the excitation vectors can be written as:

$$(E_x^{inc})_p = \frac{4\pi}{j\mu_0\omega} E_0 \left(E_\theta^{nor}(\theta, \phi, T_{xp}) \cos \gamma - E_\phi^{nor}(\theta, \phi, T_{xp}) \sin \gamma \right) e^{jk_0 \sin \theta (x_i \cos \phi + y_i \sin \phi)}$$

$$(E_y^{inc})_q = \frac{4\pi}{j\mu_0\omega} E_0 \left(E_\theta^{nor}(\theta, \phi, T_{yq}) \cos \gamma - E_\phi^{nor}(\theta, \phi, T_{yq}) \sin \gamma \right) e^{jk_0 \sin \theta (x_i \cos \phi + y_i \sin \phi)}$$

where

T_{xp} is test function in x direction number p , T_{yq} is test function in y direction number q , θ, ϕ, γ are the direction and polarisation angles of the incident field, respectively and E_0 is the amplitude of the incident field.

8.5.5.8 Symmetric matrix fill

By analysing the sizes of the current elements we can use symmetries in the impedance matrices in order to reduce the fill time. The symmetries are, of course, independent of whether the elements are computed in the spatial or the spectral domain. We can find three different levels of symmetries:

- All J_x current elements have the same size. For this case the Z_{xx} matrix is symmetrical and only the elements on the diagonal and above have to be computed.
- All J_y current elements have the same size. For this case the Z_{yy} matrix is symmetrical and only the elements on the diagonal and above have to be computed.
- All current elements have the same size and are square. For this case both the Z_{xx} and the Z_{yy} matrices are symmetrical and the matrix Z_{yx} is equal to the transpose of the Z_{xy} matrix.

For the symmetrical matrices the elements are only a function of the distance between the current element and the test function, so that in many cases only a few elements have to be computed. Although, for the case when all elements have the same size and are square the matrices Z_{xy} and Z_{yx} are not symmetrical but the elements are only a function of the distance between the current element and the test function.

When one of the above symmetries are found the program stores the impedance values together with the distance between current element and test function in a table so that impedances do not have to be computed more than once. This is only done for the case when a dielectric material is present since the computation for this case takes a longer time than if no dielectric material is present.

9 References

- [1] A. W. Glisson and D. R. Wilton, "Simple and efficient numerical methods for problems of electromagnetic radiation and scattering from surfaces," *IEEE Trans. Antennas Propagat.*, vol. AP-28, pp. 593-603, Sep. 1980.
- [2] J. Carlsson, "Computer code LC-Calc," (also in *J. Carlsson, Crosstalk on printed circuit boards, SP report 1994:14*).
- [3] J. Carlsson, "Computer code BMTL - A FDTD program for computing responses on branched multi-conductor transmission lines," .
- [4] R. Paknys and L. R. Raschkowan, "Moment method surface patch and wire grid accuracy in the computation of near fields," *Applied Computational Electromagnetics Society Journal*, vol. 12, pp. 16-25, Nov 1997.
- [5] M. Marin, S. Barkeshli, and P. H. Pathak, "Efficient analysis of planar microstrip geometries using a closed-form asymptotic representation of the grounded dielectric slab Green's function," *IEEE Trans. Microwave Theory and Tech.*, vol. 37, pp. 669-679, 1989.
- [6] P. Perlmutter, S. Shtrikman, and D. Treves, "Electric surface current model for the analysis of microstrip antennas with application to rectangular elements," *IEEE Trans. Antennas Propagat.*, vol. AP-33, pp. 301-311, March 1985.
- [7] C. A. Balanis, *Advanced Engineering Electromagnetics*: John Wiley & Sons inc., 1989.
- [8] R. F. Harrington, *Field Computation by Moment Methods*. New York: Macmillan, 1968.
- [9] Z. Sipus, P.-S. Kildal, R. Leijon, and M. Johansson, "An algorithm for calculating Green's functions for planar, circular cylindrical and spherical multilayer substrates," Accepted for publication in *Applied Computational Electromagnetics Society Journal*.
- [10] R. F. Harrington, *Time-harmonic electromagnetic fields*. New York: McGraw-Hill, 1961.
- [11] D. M. Pozar, "Improved computational efficiency for the moment method solution of printed dipoles and patches," *Electromagnetics*, vol. 3, pp. 299-309, Jul-Dec 1983.
- [12] P.-S. Kildal, Z. Sipus, and M. Johansson, "A numerical algorithm G1DMULT for computing Green's functions of multilayer objects," Proc. ACES Symposium, Monterey, 1997.
- [13] D. M. Pozar, "Input impedance and mutual coupling of rectangular microstrip antennas," *IEEE Trans. Antennas Propagat.*, vol. AP-30, pp. 1191-1196, Nov. 1982.
- [14] E. H. Newman and D. Forrai, "Scattering from a microstrip patch," *IEEE Trans. Antennas Propagat.*, vol. AP-35, pp. 245-251, March 1987.

Appendix File formats

When a project is saved the PCB-MoM program will save several files in order to keep track of all details. These files will get the name the user gives to the project but with a unique extension that reflects the contents in the file. All files are ASCII files.

The file types used by the program are:

- *.PRO Project file containing a short summary about the project
- *.SEG Segment file containing geometrical data for segments
- *.CHE Charge element file containing geometrical data for charge elements
- *.JXE Jx-current element file containing geometrical data for Jx-current elements except the connecting Jx-current elements
- *.JXC Jx-current element file containing geometrical data for connecting Jx-current elements (this file is created when segments are connected)
- *.JYE Jy-current element file containing geometrical data for Jy-current elements except the connecting Jy-current elements
- *.JYC Jy-current element file containing geometrical data for connecting Jy-current elements (this file is created when segments are connected)
- *.GEN Voltage source file containing data for voltage sources
- *.IMP Impedance element file containing data for impedances
- *.GPC Ground point file containing data for connections between the layout and the ground plane
- *.XXX Current file containing computed Jx-currents
- *.YYY Current file containing computed Jy-currents
- *.ZZX Current file containing computed Jz-currents connected to Jx-current elements
- *.ZZY Current file containing computed Jz-currents connected to Jy-current elements
- *.NFE Near field file containing computed electric field in near field points
- *.NFH Near field file containing computed magnetic field in near field points
- *.RAD Radiation pattern file containing computed far fields
- *.TXT File containing any notes written by the user in the show project file dialog

The format for the different files are as follows:

*.PRO

Project file containing a short summary about the project.

Format:

- Date and time of last saving of project
- Length of PCB in mm
- Width of PCB in mm
- Total number of segments in layout
- Total number of charge elements in layout
- Ground plane distance, if not present 0
- Resistivity in Ohm, if not specified 0
- Grid size in mm
- Number of charges per grid cell in x-direction
- Number of charges per grid cell in y-direction
- Number of voltage sources in layout
- Number of impedance elements in layout
- Number of ground points in layout
- Relative dielectric constant for region between structure and ground plane

*.SEG

Segment file containing geometrical data for segments.

Format:

First row:

PCB length in mm, PCB width in mm, Grid size in mm, Number of charges in x-direction per grid, Number of charges in y-direction per grid

Succeeding rows:

Centre x-coordinate in mm for segment, Centre y-coordinate in mm for segment, Length of segment in x-direction in mm, Length of segment in y-direction in mm, Number of charges in x-direction contained in segment, Number of charges in y-direction contained in segment

*.CHE

Charge element file containing geometrical data for charge elements.

Format:

Centre x-coordinate in mm for charge element, Centre y-coordinate in mm for charge element, Length of charge element in x-direction in mm, Length of charge element in y-direction in mm

*.JXE

Jx-current element file containing geometrical data for Jx-current elements except the connecting Jx-current elements.

Format:

Centre x-coordinate in mm for current element, Centre y-coordinate in mm for current element, Length of current element in x-direction in mm, Length of current element in y-direction in mm, Index number for adjacent charge element on the left, Index number for adjacent charge element on the right

*.JXC

Jx-current element file containing geometrical data for connecting Jx-current elements.

Format:

Centre x-coordinate in mm for current element, Centre y-coordinate in mm for current element, Length of current element in x-direction in mm, Length of current element in y-direction in mm, Index number for adjacent charge element on the left, Index number for adjacent charge element on the right

*.JYE

Jy-current element file containing geometrical data for Jy-current elements except the connecting Jy-current elements.

Format:

Centre x-coordinate in mm for current element, Centre y-coordinate in mm for current element, Length of current element in x-direction in mm, Length of current element in y-direction in mm, Index number for adjacent charge element below, Index number for adjacent charge element on top

*.JYC

Jy-current element file containing geometrical data for connecting Jy-current elements.

Format:

Centre x-coordinate in mm for current element, Centre y-coordinate in mm for current element, Length of current element in x-direction in mm, Length of current element in y-direction in mm, Index number for adjacent charge element below, Index number for adjacent charge element on top

*.GEN

Voltage source file containing data for voltage sources.

Format:

Centre x-coordinate in mm for source element, Centre y-coordinate in mm for source element, Length of source element in x-direction in mm, Length of source element in y-direction in mm, Real-part of voltage, Imaginary-part of voltage, 1: if placed in Jx-element 0: if placed in Jy-element, Index number for current element in which source is placed in

*.IMP

Impedance element file containing data for impedances.

Format:

Centre x-coordinate in mm for impedance element, Centre y-coordinate in mm for impedance element, Length of impedance element in x-direction in mm, Length of impedance element in y-direction in mm, Resistance in ohms, If>0 inductance in Henry if<0 capacitance in Farad, 1: if placed in Jx-element 0: if placed in Jy-element, Index number for current element in which impedance is placed in

*.GPC

Ground connection file containing data for connections between layout and ground plane.

Format:

Index number for charge element in which connection is placed in, 1: placed on left edge 2: right edge 3: bottom edge 4: top edge, Size (only used for plotting), Centre x-coordinate in mm for connection, Centre y-coordinate in mm for connection

*.XXX

Current file containing computed Jx-currents.

Format:

First row:

Frequency in MHz, Number of current elements

Succeeding rows:

Centre x-coordinate in mm for current element, Centre y-coordinate in mm for current element, Length of current element in x-direction in mm, Length of current element in y-direction in mm, Real-part of current, Imaginary-part of current

For swept frequency mode the current file will contain data for several frequencies. For each frequency data according to the format given above will be appended to the file.

*.YYY

Current file containing computed Jy-currents.

Format:

First row:

Frequency in MHz, Number of current elements

Succeeding rows:

Centre x-coordinate in mm for current element, Centre y-coordinate in mm for current element, Length of current element in x-direction in mm, Length of current element in y-direction in mm, Real-part of current, Imaginary-part of current

For swept frequency mode the current file will contain data for several frequencies. For each frequency data according to the format given above will be appended to the file.

*.ZZX

Current file containing computed Jz-currents, x-directed part.

Format:

First row:

Frequency in MHz, Number of current elements

Succeeding rows:

Centre x-coordinate in mm for current element, Centre y-coordinate in mm for current element, Length of current element in x-direction in mm, Length of current element in y-direction in mm, Length of current element in z-direction in mm (height over ground plane), Real-part of current, Imaginary-part of current

For swept frequency mode the current file will contain data for several frequencies. For each frequency data according to the format given above will be appended to the file.

Note that the length of the current element in the x-direction could be negative which implies that the z-directed current is negative (flows from the layout towards the ground plane).

*.ZZY

Current file containing computed Jz-currents, y-directed part.

Format:

First row:

Frequency in MHz, Number of current elements

Succeeding rows:

Centre x-coordinate in mm for current element, Centre y-coordinate in mm for current element, Length of current element in x-direction in mm, Length of current element in y-direction in mm, Length of current element in z-direction in mm (height over ground plane), Real-part of current, Imaginary-part of current

For swept frequency mode the current file will contain data for several frequencies. For each frequency data according to the format given above will be appended to the file.

Note that the length of the current element in the y-direction could be negative which implies that the z-directed current is negative (flows from the layout towards the ground plane).

*.NFE

Near field file containing computed electric field in near-field points.

Format:

First row:

Frequency in MHz, Number of field points

Succeeding rows:

x, y and z-coordinates for field point (separate row)
Real-part of Ex, Imaginary-part of Ex (separate row)
Real-part of Ey, Imaginary-part of Ey (separate row)
Real-part of Ez, Imaginary-part of Ez (separate row)

For swept frequency mode the near-field file will contain data for several frequencies. For each frequency data according to the format given above will be appended to the file.

*.NFH

Near field file containing computed magnetic field in near-field points.

Format:

First row:

Frequency in MHz, Number of field points

Succeeding rows:

x, y and z-coordinates for field point (separate row)
Real-part of Hx, Imaginary-part of Hx (separate row)
Real-part of Hy, Imaginary-part of Hy (separate row)
Real-part of Hz, Imaginary-part of Hz (separate row)

For swept frequency mode the near-field file will contain data for several frequencies. For each frequency data according to the format given above will be appended to the file.

*.RAD

Radiation pattern file containing computed far-fields.

Format:

First row:

Frequency in MHz, Number of directions for which computation was performed

Succeeding rows:

Theta angle in degrees, Phi angle in degrees, Normalised ETheta component in Volt,
Normalised EPhi component in Volt

For swept frequency mode the radiation pattern file will contain data for several frequencies. For each frequency data according to the format given above will be appended to the file.